

UCSF

UC San Francisco Electronic Theses and Dissertations

Title

Architecture and Assembly of Chlamydomonas Flagella

Permalink

<https://escholarship.org/uc/item/41v540tt>

Author

Wemmer, Kimberly A.

Publication Date

2011

Peer reviewed|Thesis/dissertation

Architecture and Assembly of Chlamydomonas Flagella

by

Kimberly A. Wemmer

DISSERTATION

Submitted in partial satisfaction of the requirements for the degree of

DOCTOR OF PHILOSOPHY

in

Cell Biology

in the

GRADUATE DIVISION

of the

UNIVERSITY OF CALIFORNIA, SAN FRANCISCO

Copyright 2011

by

Kimberly A. Wemmer

Acknowledgements

First of all, I would of course like to thank Wallace Marshall for his support, mentorship and patience with me. It's really nice to have a great person who will always have your back as a boss! His endless and unfailing enthusiasm for science makes it easy to explore any question in his lab, and has resulted in a wonderful and diverse group of people gathering together.

So many of those people around me in lab have generously and graciously supported me I almost don't know where to begin - but really there are two people who must be acknowledged first. This thesis would not have been anything without the help of Will Ludington and Juliette Azimzadeh. They are two of the smartest and most generous scientists I know, and I hope that they continue to excel in their chosen fields, cause we need them to be in science, helping and teaching others. I consider Juliette as my vice-P.I. and Will as my mentor in absolutely everything I know nothing about - and he's patient enough to put up with me! I owe them both an inexpressible debt, and quite literally couldn't have done this without them.

I also am grateful to Prachee Crofts and Susanne Rafelski for showing me what it is to be fearless in science, and to Jessica Feldman for being a mentor without even meaning to be - I have learned so much from her, just by hanging around her. Mark Chan sits directly to my back, and I'm so grateful for his calm around my craziness, I'd be a mess with anyone else there. I have to thank Hiro Ishikawa and Mark Slabodnick for being stalwart supports whenever I need them. Finally, I have to thank Elisa Kannegaard and Lani Keller - they are so much

more than labmates, and without their friendship, support, and unique brilliance, I would have been lost. Lani's unflagging positive attitude was essential to ensuring my sanity, and Elisa was with me right there to the end, I couldn't have survived this process without her being there with me through it.

Outside of my lab, I have many people to thank. My classmates Genevieve (and by extension Martin), Oliver, Chris, and Bill have been there through it all, and have always provided help when needed and a welcome distraction when desired. I wouldn't have wanted to be stuck in grad school with anyone else! The people in the labs next to me have had exceptional tolerance to my unending dropping in on them - Holly, Lynn, Eric, and Paolo in the Cox lab have all been especially supportive and helpful, and always put up with my siphoning of their extensive knowledge while being fantastic friends at the same time. Holly especially was ever encouraging. In the Madhani Lab, I was lucky enough to spend time with Emma, Terry, and Smita who, along with Bill and Oliver, let me crash their social outings whenever I felt like it. They are so much fun and I'm grateful to have their friendship way, way beyond lab.

Outside of lab entirely, I am grateful for the friendship of James and Mary, Martha and Nate, Eunice, and Ayse and Pete. They have made the non-lab part of my life much better at a time when I really needed it.

And speaking of making my life better, I have to thank Bill Hwang in particular. I am so lucky to have him as my ever patient sanity and support, and I benefit from his kindness every single day. Finding him has made this all worth it, and I genuinely don't know what I would do without him.

I need to thank my family - especially my mom & pops, Joanne and Dave, and my sisters Megan and Sarah - they are the BEST! They have always been there with me every step of the way, and their unquestioning love and support is endlessly reassuring. I am so lucky to have such wonderful people as my family. They really have been the greatest.

Finally, I would like to thank Radiolab and This American Life, Lady Gaga, Adele, Mumford & Sons, OK Go, and Sleigh Bells for their help in the microscope room, the Field and Radiohead for getting me through my reading, and finally BMRC, Franz, Bruce, Block Party, the National and the Killers for always being there for me.

Acknowledgement of Published Materials

Chapter 2 and Figure 1 of Chapter 3 of this dissertation is a reprint of material as it appears in "Flagellar Length Control in *Chlamydomonas* -- A Paradigm for Organelle Size Regulation." Kimberly A. Wemmer and Wallace F. Marshall, *International Review of Cytology*. 2007. **260**: 175-212. Figure 1 in Chapters 1 and 5 is modified from "Flagellar Motility: All Pull Together." Kimberly A. Wemmer and Wallace F. Marshall, *Current Biology*. 2004. **14**: R992-993.

Architecture and Assembly of *Chlamydomonas* Flagella

Kimberly A. Wemmer

Abstract

Eukaryotic cilia and flagella play crucial roles in development, signaling, and motility, and their proper function is essential to many organisms, including all vertebrates. Cilia and flagella are microtubule based, membrane bound structures that protrude from the surface of the cell, and they possess a highly stereotyped, precise internal geometry. This internal structure must be correctly built and maintained for the proper functioning of these organelles, and perturbations to the structure can result in altered functionality and disease states in humans.

Their extension out away from the cell body and tendency to vary in only a single dimension - their length - also make cilia and flagella ideal model organelles for the study of organelle size control. Proper size is crucial to the functioning of a cellular organelle, however, very little is understood about size control is achieved. These structures are uniquely situated to teach us more about the mechanisms cells use to regulate the size of their organelles.

This dissertation seeks to further elucidate how the structure of cilia and flagella is established and maintained using the green alga *Chlamydomonas*. *Chlamydomonas* has served as an excellent model organism for the study of flagella in the past and is amenable to a wide range of genetic and biochemical experiments. Their flagella make ideal structures to use as models as they are essentially identical to those found in vertebrates, have an highly precise

geometry, and mutants strains with altered internal structure and length are readily available.

In this work, I first review the state of knowledge about length control of flagella in *Chlamydomonas*. I use *Chlamydomonas* mutant strains with altered flagellar length to investigate the mechanisms that result in this phenotype, and to examine how both intrinsic and extrinsic biological noise may affect these cellular structures. Finally, I identify new components of the *Chlamydomonas* central pair structure. Collectively, this work furthers our understanding of flagellar architecture and motility.

Table of Contents

CHAPTER 1

Introduction 1

CHAPTER 2

Flagellar Length Control in *Chlamydomonas* -
a Paradigm for Organelle Size Regulation 16

CHAPTER 3

Quantitative Analysis of Intraflagellar Transport
in *Chlamydomonas* Long-flagella Mutants 86

CHAPTER 4

Biological Noise in an Organelle Size Control System 139

CHAPTER 5

Identification of New Protein Components of the
Chlamydomonas Central Pair 177

List of Tables

CHAPTER 3

Table 1. <i>Chlamydomonas</i> strains used in this work	131
Table 2. <i>Chlamydomonas</i> strains created for this work	132
Table 3. Primers used in strain verification	133
Table 4. Summary of flagellar phenotypes of <i>If Chlamydomonas</i> strains	134

CHAPTER 4

Table 1. Results of noise calculations	174
--	-----

CHAPTER 5

Table 1. List of central pair candidates.....	206
Supplementary Table 1. Complete list of proteins identified by 2D-DIGE	211
Supplementary Table 2. Data for FAP21 RNAi in Planaria	213

List of Figures

CHAPTER 1

Figure 1. The structure of a flagellum..... 12

CHAPTER 2

Figure 1. Diagram of flagellum showing components involved in
length control..... 76

Figure 2. Length-Independent Regulation of Intraflagellar Transport –
the Elevator Model. 77

CHAPTER 3

Figure 1. Diagram of flagellum showing components involved in
length control..... 120

Figure 2. Example kymographs from control and *If* cells..... 121

Figure 3. IFT content in flagella is increased of some *If* mutants. 123

Figure 4. Analysis of IFT Parameters in *If* mutants. 124

Figure 5. Altered dependence of IFT injection rate on length. 125

Figure 6. Examples of KAP-GFP fluorescence in *If* strains. 126

Figure 7. Accumulation of KAP-GFP at the basal bodies of *If* strains. 128

Figure 8. A wild type cell undergoes the long-zero response..... 129

Figure 9. Some *If* strains have altered long-zero responses. 130

CHAPTER 4

Figure 1. Measuring intrinsic and extrinsic noise in a flagellar length control system.	168
Figure 2. Noise affects fitness.	170
Figure 3. Noise analysis of a length control system model.	171
Figure 4. Identification of genes that participate in flagellar length noise suppression.	173

CHAPTER 5

Figure 1. The structure of a flagellum.....	202
Figure 2. Overview of mid-scale flagellar preparation.	203
Figure 3. Gel images from 2D-DIGE experiment.	204
Figure 4. FAP 21 and FAP161 are present only in organisms which have motile cilia with central pairs.	207
Figure 5. Knock-down of FAP21 with RNAi impairs swimming of Planaria.	209
Figure 6. Constructs created to express FAP161 and FAP21 in <i>Chlamydomonas</i>	210

Chapter 1

Introduction

Introduction

It is a truth universally acknowledged, that for an organelle to perform its function properly, it must be correctly constructed. This includes not only accurately assembling all of the organelle's constituent components, but also ensuring that organelle has achieved the appropriate size, number, shape, and position within the cell (Rafelski and Marshall, 2008). Only when the proper structure and organization of an organelle is achieved can it correctly perform the biochemical or mechanical functions required of it.

But while the importance of organelle size to its proper function is a phenomena that has been observed many times, the mechanisms behind size control are far from understood. The size of an organelle may dynamically adapt to changing cellular conditions, such as when the accumulation of unfolded proteins triggers the unfolded protein response (UPR), resulting in the expansion of the endoplasmic reticulum (ER) (Bernales et al., 2006). Alternately, the size of an organelle may be crucial to the identity of a cell. This is true in cells with a high secretory load, including pancreatic β -cells, which produce insulin, and plasma B cells, which secrete high levels of antibodies; both these cells types are characterized by highly developed ER and Golgi structures. In other examples, organelle size scales with cell size. Wühr et al. (2008) demonstrated that larger cells tend to form larger mitotic spindles. Additionally, as discussed in Chapter 3, larger *Chlamydomonas* cells tend to have longer flagella. However, in no case are the detailed mechanisms that generate such scaling fully understood (Chan and Marshall, 2010).

While the problem of how cells regulate the size of their organelles is an intriguing one, it is also technically challenging to address. The complex three-dimensional shapes of organelles render them difficult to measure, and also create questions as to which measurements constitute the relevant parameters - for example, should the size of the ER be determined by its total volume, by its surface area, or by the fraction of cytoplasm it encompasses? Due to such challenges, the mechanisms controlling the size of most organelles have yet to be elucidated.

In contrast to the difficulties in measuring and defining complicated three-dimensional organelles, the problem of size control is much more easily approached through study of linear structures for which only one dimension must be quantified: length. Cilia and flagella are particularly tractable organelles for studying organelle size control, as they are fairly large structures that protrude out from the surface of the cell body. This allows for easy observation and quantification of their length, and permits us to achieve high accuracy and precision in our measurements.

Cilia are important organelles with diverse functions

Cilia and flagella are highly conserved throughout nature, appearing in nearly identical forms in vertebrates, invertebrates, algae, lower plants, and protists. In eukaryotes, distinctions between these two different names, cilia and flagella, are historical and, as they describe essentially the same structure, they

will be used interchangeably herein. I will refer to each structure by the name that is conventionally used in each particular context.

Apart from their utility as model organelles for the study of size control, eukaryotic cilia and flagella are, in and of themselves, fascinating cellular structures with a diverse array of functions that include motility, mechanosensation, and signaling. These organelles have a complex internal structure, discussed below, and any perturbation of the ciliary structure can negatively impact their functioning (Ocbina et al., 2011).

One crucial role of cilia is to generate motility. In the case of single cells, the beating of cilia can propel the cell through the environment. This mobility can be effectively generated by a single flagellum, as in sperm; two flagella, as in *Chlamydomonas*; or by a multitude of cilia, as in organisms of the phylum *Ciliophora* like *Tetrahymena*. In the context of a stationary tissue, ciliary motility can generate fluid flow. This production of flow is important for circulation of cerebrospinal fluid in the brain and mucus flow in the respiratory system.

Additionally, cilia play a key role in intercellular signaling and have been demonstrated to be instrumental in regulating signaling through the Hedgehog pathway (Huangfu et al., 2003). They have also been implicated in properly modulating Notch and non-canonical Wnt-planar cell polarity signaling (for review, see: Eggenchwiler and Anderson, 2007; Hildebrandt et al., 2011; Lopes et al., 2010). Furthermore, cilia have been demonstrated to play an essential role in the left-right patterning of vertebrate embryos (Nonaka et al., 2002). This occurs via the generation of fluid flow within structures like the mouse node,

resulting in the first left-right asymmetrical signaling within the developing embryo.

The ubiquity of cilia is indicative of their importance in development and disease; nearly all vertebrate cells can produce cilia, and defects in cilia can give rise to a broad spectrum of pathologies termed ciliopathies. This list includes polycystic kidney disease, nephronophthisis, Joubert's syndrome, Meckel's syndrome, Kartagener's syndrome, and primary ciliary dyskinesia. Because cilia are so widespread throughout the body, mutations impairing their function affect a variety of tissues and organ systems, leading to symptoms including cystic kidneys, polydactyly, obesity, retinal degeneration, chronic airway ailments, and *situs inversus* (Hildebrandt et al., 2011; Lee, 2011).

Ciliary structure and assembly

Cilia themselves are elegant structures with a precise internal geometry (Figure 1) that must be correctly assembled to achieve the full functionality of the organelle. They are microtubule based, membrane bound organelles that project from the surface of the cell, and are nucleated by a modified centriole called a basal body. The structure of the cilium consists of over 360 polypeptides that make up organelle, which range from proteins attached to the core microtubules, to proteins associated with the ciliary membrane (Pazour et al., 2005). Although the ciliary membrane is contiguous with the plasma membrane, analysis of protein diffusion indicated that there is a septin-mediated diffusion barrier at the base of the cilium (Hu et al., 2010).

Motile cilia, the subject of this thesis, have a '9+2' structure, with nine outer microtubule doublets (consisting of an A and a B tubule, attached along their length), running from the base to the tip of a cilium. These surround a structure called the central pair, which consists of two more individual microtubules named the C1 and C2 tubules and their accessory proteins. All these microtubules, along with their accessory proteins, make up the backbone of the cilia and are collectively referred to as the axoneme. It is known that the A tubules of the outer doublets have several large protein projections which are used to generate ciliary motility. These structures include the inner and outer dynein arms, which interact with the B tubule of the adjacent doublet, and the radial spoke, which interacts with the central pair. The central pair is also decorated with proteins along the length of its microtubules, many of which have yet to be identified, a topic addressed in Chapter 5. These projections are one of the few structures within the cilium that are not radially symmetrical; this asymmetry is very important to generating the correct waveform during ciliary beating. Briefly, the proteins on the central pair are thought to regulate the activity of the dynein arms, through interactions with the radial spoke. Active dynein arms pull on the adjacent doublet microtubule, generating a sliding force. If the microtubules were unattached, this would cause them to slide apart from each other, but as they are fixed at the base, this force creates a bend in the cilium, resulting in a ciliary stroke.

Primary cilia have a '9+0' structure that retain the 9 pairs of outer doublets running the length of the axoneme; however, they lack the central pair, radial

spokes, and often some or all of the dynein arms. Typically, there is one primary cilium per cell and they are rarely motile, whereas motile cilia are typically present in large numbers per cell and are highly dynamic.

Interestingly, the construction of these very complex structures occurs exclusively at the distal tip of cilia, away from the cell body (Johnson and Rosenbaum, 1992; Marshall et al., 2005; Marshall and Rosenbaum, 2001; Stephens, 1999). Therefore, the ciliary components must be brought out to the distal tip, by way of an active process called intraflagellar transport or IFT (Kozminski et al., 1993). Only after they are brought out to the tip of the cilia may these components then be assembled onto the axoneme. IFT is the process by which two large protein complexes carrying ciliary subunits are moved from the cell body to the tip by a kinesin motor (anterograde transport), and used subunits are then returned to the cell body by a cytoplasmic dynein (retrograde transport) (reviewed by: Cole, 2003; Scholey, 2003; Sloboda, 2002). These two complexes are referred to as IFT complex A and complex B, and seem to serve as adaptors between the IFT motors and their cargo (Qin et al., 2005; Qin et al., 2004). The entire assembly of motors, A and B complexes, and cargoes are assembled into linear arrays that are collectively referred to as IFT trains. Remarkably, these complexes are constructed in a way such that the dynein complex is inactivated while the kinesin is functioning to move the IFT particles to the distal tip. At the tip a rearrangement occurs that results in the activation of the dynein, allowing all the IFT components and cargo to be brought back to the cell body (Pedersen et al., 2006). The process of IFT can be broken down into

four distinct phases: (i) initiation of movement from the base, (ii) movement out to the distal tip, (iii) rearrangement of IFT complexes and reversal of direction at the distal tip, and finally (iv) movement back to the base. These four phases can be measured in kymographic analyses and mutants which differentially affect the various phases exist (Iomini et al., 2001). The molecular mechanisms behind these shifts in phase are still not known. This process of IFT is as conserved as the presence of cilia themselves, and involves the same set of molecules across all the organisms that have cilia, from algae to humans.

Importantly, IFT is not a process that stops once the cilium is constructed, but continues even after the organelle has reached its steady state length (Marshall and Rosenbaum, 2001; Song and Dentler, 2001; Stephens, 1999). This is due to the fact that there is a continuous basal rate of disassembly occurring at the distal tip of cilia, which must be matched by constant assembly if the length of a cilium is to be maintained. If for some reason the anterograde transport of components is ceased, the cilia gradually but immediately begin to resorb, a process that will continue until they are completely absent, unless IFT function is restored. Interestingly, a new, shorter steady state length may be achieved by only partially impairing IFT out to the distal tip, indicating that the length of cilia is indeed responsive to levels of IFT within the cilia (Marshall and Rosenbaum, 2001).

The length of motile cilia and flagella is directly related to their function, since the length determines the hydrodynamic interactions between the flagellum and the surrounding media during swimming or flow generation. This direct link

between size and fitness, combined with the dynamic nature of the organelle and the ease with its size may be measured, makes it an ideal system in which to study the more general problem of organelle size control. Moreover, the fact that length can be easily measured in living cells makes it relatively convenient for measuring fluctuations and variation in length, allowing flagella to serve as a model system for studying biological noise at the level of organelle structure.

Flagellar length control in Chlamydomonas

Given the intricacies of the eukaryotic cilium, studying the structure in a highly tractable organism is to be desired. Therefore, these studies have been conducted in *Chlamydomonas reinhardtii*, a unicellular chlorophyte green algae. *Chlamydomonas* makes an excellent model organism in which to study cilia for numerous reasons. Sometimes referred to as 'green yeast,' it is a single celled organism that has many of the same practical advantages as working with yeast. *Chlamydomonas* has a rapid life cycle, grows in both liquid and solid media as either haploid or diploid cells, has a sequenced genome, and is amenable to genetic studies, molecular biology techniques, and biochemical experimentation. However, unlike yeast, *Chlamydomonas* cells possess two highly stereotypic flagella on every cell; flagella that are virtually indistinguishable from the cilia found on animal cells. These flagella confer motility to the cell; they form a breast-stroke like waveform that pushes cells through media. Additionally, the flagella perform sensory functions, which allows the cells to interact with each

other, as well as with their environment, so cells may alter their behaviors appropriately.

Chlamydomonas flagella are an excellent model organelle to use in the study of size control. The flagella are built with incredible precision; on individual wild type cells there are always two flagella of the same length, and within a population all fully grown flagella are always found within a tight range of lengths. Typically the majority of flagella fall within 10-14 μm in rich media, while in minimal media they are often a few microns longer; the average length also depends on time of day and cell cycle progression (Tuxhorn et al., 1998). It is incredibly easy to isolate flagella from *Chlamydomonas*, as there are several techniques which will cause the cells to sever their flagella at the base, just above the transition zone that marks the delineation of the basal body from the ciliary axoneme. The cells will also re-grow their flagella after severing one or both of their flagella, making the study of flagellar growth dynamics possible. Furthermore, *Chlamydomonas* flagella have been studied for decades, providing a rich legacy of useful mutants, many of which affect flagellar assembly and length. These include *lf* mutants, which assemble abnormally long flagella (Asleson and Lefebvre, 1998; Barsel et al., 1988; McVittie, 1972); *shf* mutants, which have short flagella (Kuchka and Jarvik, 1987); *fla* mutants, which cannot assemble or maintain flagella at restrictive temperature (Adams et al., 1982); and *pf* mutants, which have immotile cilia (reviewed in Silflow and Lefebvre, 2001). The extensive work performed in this system has provided a wealth of information from which to begin my studies.

Summary

In this work, I attempt to add to our understanding of how organelles are constructed by the cell, using *Chlamydomonas* flagella as a model. The current state of knowledge about length control of flagella in *Chlamydomonas* is reviewed in Chapter 2. In Chapter 3, I explore the mechanistic basis of *Chlamydomonas* mutations that increase flagellar length, illustrating how this model system can be used to study organelle size control. Chapter 4 addresses how biological noise may affect cellular structures, examining the effect both intrinsic and extrinsic noise on flagellar length. Finally in Chapter 5, new components of the *Chlamydomonas* central pair structure are identified, adding to our understanding of flagellar architecture and motility.

Figure 1

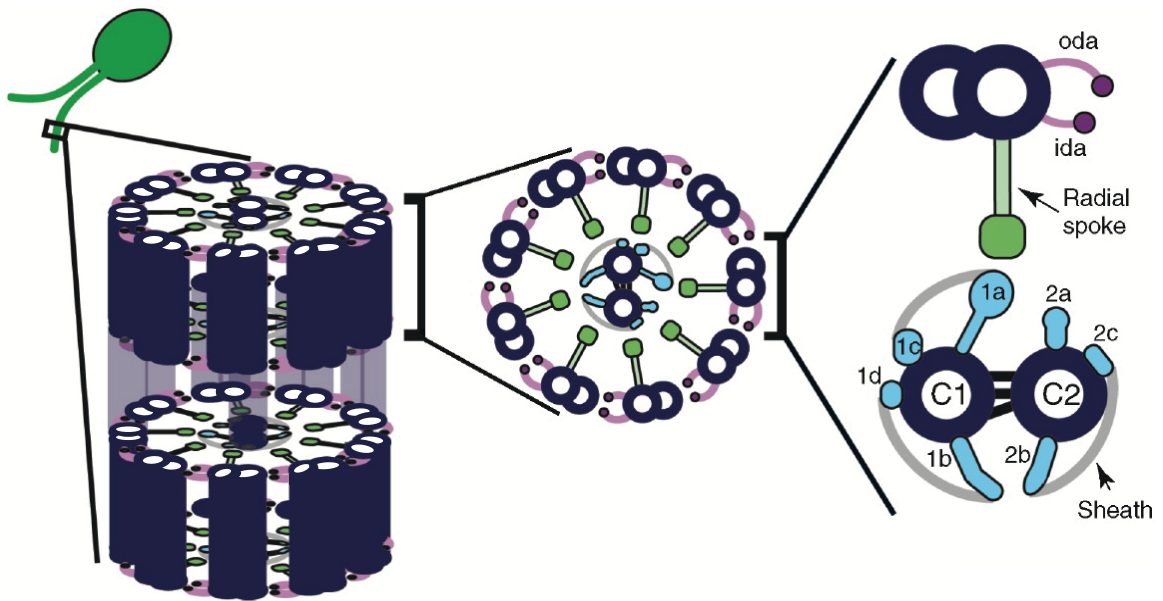


Figure 1. The structure of a flagellum.

This drawing depicts the structures within a flagellum. Microtubules (dark blue circles) make up the backbone of the structure. Middle: Cross section of a flagellum. Far right: the largest magnification, showing the central pair, consisting of the C1 and C2 tubules with their associated projections (1a-2c, light blue) and sheath (gray curves); and a single outer doublet with its radial spoke (green) and inner (ida) and outer (oda) dynein arms (pink).

References

- Adams, G.M., B. Huang, and D. Luck. 1982. Temperature-Sensitive, Assembly-Defective Flagella Mutants of *CHLAMYDOMONAS REINHARDTII*. *Genetics*. **100**:579-586.
- Asleson, C.M., and P.A. Lefebvre. 1998. Genetic analysis of flagellar length control in *Chlamydomonas reinhardtii*: a new long-flagella locus and extragenic suppressor mutations. *Genetics*. **148**:693-702.
- Barsel, S.E., D.E. Wexler, and P.A. Lefebvre. 1988. Genetic analysis of long-flagella mutants of *Chlamydomonas reinhardtii*. *Genetics*. **118**:637-648.
- Bernales, S., K.L. McDonald, and P. Walter. 2006. Autophagy counterbalances endoplasmic reticulum expansion during the unfolded protein response. *PLoS biology*. **4**:e423.
- Chan, Y.H., and W.F. Marshall. 2010. Scaling properties of cell and organelle size. *Organogenesis*. **6**:88-96.
- Cole, D.G. 2003. The intraflagellar transport machinery of *Chlamydomonas reinhardtii*. *Traffic*. **4**:435-442.
- Eggenchwiler, J.T., and K.V. Anderson. 2007. Cilia and developmental signaling. *Annu Rev Cell Dev Biol*. **23**:345-373.
- Hildebrandt, F., T. Benzing, and N. Katsanis. 2011. Ciliopathies. *N Engl J Med*. **364**:1533-1543.
- Hu, Q., L. Milenkovic, H. Jin, M.P. Scott, M.V. Nachury, E.T. Spiliotis, and W.J. Nelson. 2010. A septin diffusion barrier at the base of the primary cilium maintains ciliary membrane protein distribution. *Science*. **329**:436-439.
- Huangfu, D., A. Liu, A.S. Rakeman, N.S. Murcia, L. Niswander, and K.V. Anderson. 2003. Hedgehog signalling in the mouse requires intraflagellar transport proteins. *Nature*. **426**:83-87.
- Iomini, C., V. Babaev-Khaimov, M. Sassaroli, and G. Piperno. 2001. Protein particles in *Chlamydomonas* flagella undergo a transport cycle consisting of four phases. *J Cell Biol*. **153**:13-24.
- Johnson, K.A., and J.L. Rosenbaum. 1992. Polarity of flagellar assembly in *Chlamydomonas*. *J Cell Biol*. **119**:1605-1611.
- Kozminski, K.G., K.A. Johnson, P. Forscher, and J.L. Rosenbaum. 1993. A motility in the eukaryotic flagellum unrelated to flagellar beating. *Proc Natl Acad Sci USA*. **90**:5519-5523.

- Kuchka, M.R., and J.W. Jarvik. 1987. Short-Flagella Mutants of *Chlamydomonas reinhardtii*. *Genetics*. **115**:685-691.
- Lee, L. 2011. Mechanisms of mammalian ciliary motility: Insights from primary ciliary dyskinesia genetics. *Gene*. **473**:57-66.
- Lopes, S.S., R. Lourenço, L. Pacheco, N. Moreno, J. Kreiling, and L. Saúde. 2010. Notch signalling regulates left-right asymmetry through ciliary length control. *Development*.
- Marshall, W.F., H. Qin, M. Rodrigo Brenni, and J.L. Rosenbaum. 2005. Flagellar length control system: testing a simple model based on intraflagellar transport and turnover. *Mol Biol Cell*. **16**:270-278.
- Marshall, W.F., and J.L. Rosenbaum. 2001. Intraflagellar transport balances continuous turnover of outer doublet microtubules: implications for flagellar length control. *J Cell Biol*. **155**:405-414.
- McVittie, A. 1972. Flagellum mutants of *Chlamydomonas reinhardtii*. *J Gen Microbiol*. **71**:525-540.
- Nonaka, S., H. Shiratori, Y. Saijoh, and H. Hamada. 2002. Determination of left-right patterning of the mouse embryo by artificial nodal flow. *Nature*. **418**:96-99.
- Ocbina, P.J.R., J.T. Eggenschwiler, I. Moskowitz, and K.V. Anderson. 2011. Complex interactions between genes controlling trafficking in primary cilia. *Nat Genet*. **43**:547-553.
- Pazour, G.J., N. Agrin, J. Leszyk, and G.B. Witman. 2005. Proteomic analysis of a eukaryotic cilium. *J Cell Biol*. **170**:103-113.
- Pedersen, L.B., S. Geimer, and J.L. Rosenbaum. 2006. Dissecting the molecular mechanisms of intraflagellar transport in *Chlamydomonas*. *Curr Biol*. **16**:450-459.
- Qin, H., D.T. Burnette, Y.K. Bae, P. Forscher, M.M. Barr, and J.L. Rosenbaum. 2005. Intraflagellar transport is required for the vectorial movement of TRPV channels in the ciliary membrane. *Curr Biol*. **15**:1695-1699.
- Qin, H., D.R. Diener, S. Geimer, D.G. Cole, and J.L. Rosenbaum. 2004. Intraflagellar transport (IFT) cargo: IFT transports flagellar precursors to the tip and turnover products to the cell body. *The Journal of cell biology*. **164**:255-266.
- Rafelski, S.M., and W.F. Marshall. 2008. Building the cell: design principles of cellular architecture. *Nat Rev Mol Cell Biol*. **9**:593-602.
- Scholey, J.M. 2003. Intraflagellar transport. *Annual review of cell and developmental biology*. **19**:423-443.

Silflow, C.D., and P.A. Lefebvre. 2001. Assembly and motility of eukaryotic cilia and flagella. Lessons from *Chlamydomonas reinhardtii*. *Plant physiology*. **127**:1500-1507.

Sloboda, R.D. 2002. A healthy understanding of intraflagellar transport. *Cell motility and the cytoskeleton*. **52**:1-8.

Song, L., and W.L. Dentler. 2001. Flagellar protein dynamics in *Chlamydomonas*. *The Journal of biological chemistry*. **276**:29754-29763.

Stephens, R.E. 1999. Turnover of tubulin in ciliary outer doublet microtubules. *Cell structure and function*. **24**:413-418.

Tuxhorn, J., T. Daise, and W.L. Dentler. 1998. Regulation of flagellar length in *Chlamydomonas*. *Cell motility and the cytoskeleton*. **40**:133-146.

Wühr, M., Y. Chen, S. Dumont, A.C. Groen, D.J. Needleman, A. Salic, and T.J. Mitchison. 2008. Evidence for an upper limit to mitotic spindle length. *Curr Biol*. **18**:1256-1261.

Chapter 2

Flagellar Length Control in *Chlamydomonas* - a Paradigm for Organelle Size Regulation

Flagellar Length Control in *Chlamydomonas* - a Paradigm for Organelle Size Regulation

Kimberly A. Wemmer and Wallace F. Marshall

Dept. Biochemistry & Biophysics

University of California San Francisco

Running Title: Flagellar Length Control

Corresponding Author:

Wallace Marshall

GH-N372F Box 2200 Dept. Biochemistry

UCSF

600 16th St.

San Francisco, CA 94143

(415) 514-4304

wmarshall@biochem.ucsf.edu

Abstract

A fundamental unsolved question in cell biology is how the cell controls the size of its organelles. Cilia and flagella are an ideal test case to study the mechanism of organelle size control, because their size is easily measured and can be represented by a single number - Length. Moreover, the involvement of cilia in many developmental and physiological processes such as hedgehog signaling suggests that an understanding of their size control system is critical for understanding ciliary diseases, many of which (for example, autosomal recessive polycystic kidney disease) are known to involve abnormally short cilia. The flagella of the model organism *Chlamydomonas reinhardtii* provide the best genetic and cell-biological system to study length control of cilia. Studies in this organism using genetics, biochemistry, imaging, and mathematical modeling, have revealed many genes involved in length control of cilia and flagella, and have suggested several testable models for length regulation.

Table of Contents

I. Introduction

II. Size of Organelles

A. Size Control

1. Examples of Studies of Organelle Size Control
2. Flagella as A Model System for Size Control
3. Length control in *Chlamydomonas* - The Green Yeast

B. Flagella and Cilia

1. Structure and Function
2. Human Disease Involving Abnormal Flagellar Length Control
3. Intraflagellar Transport and Flagellar Assembly

C. Phenomenological Studies of Flagellar Length Control

1. Measurements of Length Variation
2. Flagellar Regeneration
3. Flagellar Length Equalization
4. Flagellar Length versus Number

D. Genetic Studies of Flagellar Length Control

1. Identifying Length Mutants in *Chlamydomonas* Genetic Screens
2. Phenotypic and Genetic Analysis of Long-Flagella Mutants
3. Intraflagellar Transport in Length Mutants
4. Length Control Proteins - Localization and Function

III. Models for Flagellar Length Control System

A. Molecular Ruler

B. Quantal Production of Limiting Precursor

C. Cumulative Strain Model

D. Feedback Control

E. Balance-Point Model

IV. Concluding Remarks: What We Have Learned from Flagellar Length Control

A. Length Control as Pharmacological Target for Ciliary Disease

B. Flagellar Length Control as Paradigm for General Organelles

C. Length Control in Nanotechnology

I. Introduction

Recently great leaps in understanding cell biology have been occurring, yet we have only begun to understand the importance of organelle size control for the optimal functioning of cells. The organelles of a cell must be the correct size to perform their required functions or the biology of the cell will break down. In addition, organelle size also plays an important role in cell differentiation and identity, with different cell types varying a great deal in their requirement for and use of organelles in order to perform their specific functions. The study of organelle size control will be crucial to a complete understanding of how cells function.

In addition to being able to regulate the overall size of the cell body (Morris, 2002; Umen, 2005), cells must have a way to control the "abundance" or quantity of each organelle within the cell. For most organelles, the abundance in a given cell will be a function of the number of individuals of each organelle present, and the size of each organelle. Depending on how function depends on size and number, the cell might be more interested in controlling the size of individuals, or alternatively it might be more important to control the total abundance regardless of how this material is apportioned among the multiple copies of the organelle found within one cell. Flagella and the centrioles that nucleate them provide a very convenient approach to the study of organelle abundance, because they separate the two factors of number and size. The number of flagella in the cell is determined entirely by the number of centrioles that become active as basal bodies, and so flagellar abundance can be

expressed strictly in terms of the size of the flagella. Conversely, centrioles are always the same size, and hence their abundance can be expressed strictly in terms of the number of centrioles present. Taken together, the centriole-flagella system allows the general problem of organelle abundance to be reduced into two distinct problems of size and number. It also turns out that flagella have special advantages as a system for the study of size, even apart from the fact that number need not be taken directly into consideration as it would for other organelles. To see these advantages, we first discuss an overview of organelle size control systems, before moving on to a summary of the specialized features of flagella that relate to size.

II. Size of organelles

A. Size control

A 1. Examples of Studies of Organelle Size Control

There are currently very few studies of the mechanisms that determine size in eukaryotic organelles. Size control has been studied for several viral and prokaryotic systems, especially bacteriophage tails and bacterial flagella and flagellar hook structures. In these cases, identification of mutants affecting length has played a key role in suggesting possible mechanisms for length control. For instance, in bacteriophage, mutants in specific proteins result in defined reductions in length proportional to the size of the deleted region, suggesting the gene products function as molecular rulers (Katsura, 1990). In bacteria, length control of hooks and flagellar filaments has been studied by both

genetic and math modeling (Keener, 2006) approaches, resulting in a fairly detailed understanding of size control. However, these structures are exceedingly small, and one can legitimately ask whether the types of control systems that have evolved to regulate such small sizes can also work in the much larger organelles of eukaryotes.

The majority of cellular organelles are membrane-bound compartments with potentially complex three-dimensional structures. The size of organelles tends to be consistent within a given cell type, and is moreover under a degree of cell-cycle dependent regulation (reviewed in Blank et al., 2006). The endoplasmic reticulum serves as an excellent example. While the structure is challenging to measure, an important insight has been gained, more or less fortuitously, from studies of the unfolded protein response (UPR), a molecular pathway that becomes activated when the ER is unable to properly fold proteins within its lumen. Activation of the UPR pathways causes induction of a large number of genes, some of which encode chaperones and other response proteins that directly cope with the unfolded proteins, but more interestingly, some of the UPR targets appear genes involved in ER biogenesis. Recent work has suggested that the UPR plays a normal role in controlling ER size, using folding of proteins effectively as a size sensor (Bernales et al., 2006). The idea is that, assuming secreted proteins are produced at a constant rate, then if the ER were to become too small to cope with these proteins, the UPR would trigger additional ER synthesis until the organelle became large enough to perform its task. This is an interesting system in which the organelle does not necessarily

attempt to reach a defined size, but just a defined level of functionality depending on the particular requirements of the cell. This model suggests that many other interesting surprises may await us as we probe more deeply into the mechanisms that control organelle size.

A 2. Flagella as a Model System for Size Control

However, this fascinating problem can be technically difficult to study, as determining the size of organelles is a very difficult problem. The organelles are complex 3-D structures contained within cell bodies and the simple act of measuring the dimensions of the organelles can be extremely challenging. Traditionally, measurement of size would require laborious serial-section electron microscopy, followed by stereometric techniques to infer size descriptors such as volume and surface area based on the edges of the structure observed in individual sections. Use of electron tomography can simplify the task of measuring volume by directly acquiring the entire organelle, and the ability of tomography to be automated (Fung et al., 1996) is gradually helping this approach to become more routine. However, it is still quite difficult, requiring substantial technical skills, and the thickness of sections that can be imaged puts a strong upper limit on the size of an individual organelle that can be imaged entirely in a single tomographic data set. The fact that organelles in general have complex three dimensional structures also creates a challenge for mathematical analysis - which number should one use to describe size? Surface area and volume are obvious measures, but other size descriptors may also be

necessary such as end-to-end distance or the volume of a convex hull containing the organelle. We thus see that the inherent three dimensionality of most organelles makes the study of size control extremely challenging, both from a technical point of view and from a mathematical point of view.

By focusing our attention on a single dimension, length, the problem of organelle size control can be vastly simplified. Although length control has been studied in a variety of structures, including bacteriophage tails and sarcomere spacing (reviewed in Marshall, 2004), we feel that flagella and cilia represent a particularly tractable situation for studying the mechanisms of biological length control because they protrude from the cell, away from the cell body, and thus are easy to image and observe. They are significantly larger than bacteriophage tails or bacterial hooks, obviating the need for electron microscopy - indeed it is easy to measure flagellar lengths even in living cells using the very simplest of light microscopes. They are also very easy to measure as their size changes in only one dimension, length, making this the only dimension in which measurements must be made to observe differences in total organelle size.

A 3. Studying Length Control in Chlamydomonas - the Green Yeast

This review will focus on studies of flagellar length control in the unicellular green alga *Chlamydomonas*, which is without question the most convenient model organism in which to study flagella. *Chlamydomonas* is sometimes referred to as “green yeast” because it has many of the same practical advantages for doing genetics as yeast, such as the ability to work with both

haploid and diploid cells, tetrad analysis, growth as colonies on plates, and a rapid life cycle. However unlike yeast, *Chlamydomonas* has flagella which are virtually indistinguishable from cilia and flagella in animal cells. This allows the powerful genetics of this organism to be brought to bear on questions of flagellar assembly and function, and for this reason most of what we know about flagellar assembly, including the polarity of assembly and the process of IFT, has been discovered in *Chlamydomonas* (see reviews by Dutcher, 1995; Silflow and Lefebvre 2001). Consequently, there is a rich legacy of pre-existing mutants in *Chlamydomonas* which affect flagellar assembly and length. These include *fla* mutants, which cannot assemble flagella at the restrictive temperature (Adams et al., 1982), *lf* (long-flagella) mutants, which have abnormally long flagella (McVittie et al., 1972; Barsel et al., 1988; Asleson et al., 1998), and *shf* (short-flagella) mutants which have abnormally short flagella (Jarvik et al., 1984; Kuchka and Jarvik, 1987). Most of these mutants are available from the NSF-sponsored *Chlamydomonas* Genetics Center stock collection. In addition to its genetic advantages, *Chlamydomonas* is also an excellent system for molecular biology, as it is easy to transform with DNA using simple methods (for example by electroporation), protein localization can be visualized using green fluorescent protein fusions, and gene expression profiles can be obtained using cDNA microarrays that have just become available. The recent completion of the *Chlamydomonas* genome, as well as the establishment of a large database of EST sequences, has solidified this organism's position as the premier model system for studying flagellar structure and function.

B. Flagella and Cilia

The terms "flagella" and "cilia" refer to essentially identical organelles, and we will use the two terms interchangeably. Historically, *Chlamydomonas* researchers have used the term "flagella" exclusively, so we will use this term in this review. However, we urge the reader to use the term "cilia" whenever possible, in order to avoid confusion with bacterial flagella, which bear no relation whatsoever to eukaryotic flagella.

B 1. Structure and Composition

Flagella and cilia are microtubule based structures consisting of nine doublet microtubules that are nucleated by modified centrioles known as basal bodies. The microtubule doublets extend from the cell, and are surrounded by an extension of the plasma membrane. These doublets are all oriented with the microtubule plus-ends located at the distal tip of the flagellum, and the minus-ends located at the basal body located at the cell surface (Figure 1). The term "axoneme" describes the microtubule doublets themselves along with the structural components that hold them together. Cilia and flagella are highly conserved throughout evolution, appearing in virtually identical forms in vertebrates, invertebrates, algae, lower plants, and protists.

Although flagella and cilia are generally thought of as motile structures, many cells contain immotile cilia that are likely to play a sensory role (reviewed in Marshall and Nonaka, 2006). For instance, a class of somatostatin receptors (Handel et al, 1999) is located on immotile cilia in the brain. Indeed, most

sensory input to an animal are provided via sensory cilia, including both olfaction and vision (rods and cones being, in essence, highly modified cilia).

B 2. Human Diseases Involving Length Control Defects

Given the near ubiquity of cilia and flagella in various tissues, it should not be surprising that many human diseases and their animal models appear to involve defects in cilia or flagella (reviewed in Pazour et al., 2002). Examples include polycystic kidney disease (Pazour et al., 2000; Haycraft et al., 2001), biliary cystogenesis (Masyuk et al., 2003), male infertility (Toyama et al., 1996; Chemes et al., 1990), situs inversus, chronic sinusitis (Toskala et al., 1995), nephronophthisis (Otto et al., 2003), and Bardet-Biedl syndrome (Ansley et al., 2003). In many cases, disease pathology involves the presence of abnormally long or short cilia and flagella (Chemes et al., 1990; Toskala et al., 1995; Toyama et al., 1996; Pazour et al., 2000; Ortug et al., 2003; Masyuk et al., 2003). This suggests that in order to understand, and possibly develop treatments for, such diseases, we will need to understand not only what functions these cilia and flagella provide in human physiology, but also the mechanisms that specify their assembly and length determination. Since human cilia are highly homologous to *Chlamydomonas* flagella, both at the level of ultrastructure as well as in terms of their molecular composition, it is to be expected that lessons learned from flagellar length control will be directly applicable to the study of human ciliary disease.

B 3. Intraflagellar Transport and Flagellar Assembly.

Flagellar assembly is a particularly fascinating biosynthetic process because it occurs in a highly polarized manner (Rosenbaum and Child, 1967; Johnson and Rosenbaum, 1992). When flagella assemble, addition of new subunits (tubulin, etc.) occurs exclusively at the tip. In contrast, all protein synthesis in occurs in the cell body, the flagellum being completely devoid of ribosomes. Therefore, flagellar precursor proteins must be transported out to the distal tip of the flagellum where they are assembled. This transport is achieved by a process called intraflagellar transport (IFT, see Figure 1) in which a pair of protein complexes (called IFT complex A and complex B) are moved from the cell body out to the tip by a kinesin motor and then returned to the cell body by cytoplasmic dynein (reviewed by Sloboda 2002; Cole 2003; Scholey 2003). The IFT protein complexes directly bind to flagellar precursor proteins in order to bring them to the tip (Qin et al., 2004; Qin et al., 2005). At the tip, the A and B subcomplexes undergo a rearrangement ultimately activating cytoplasmic dynein 1b, which then brings the IFT proteins back to the base of the flagellum (Pedersen et al., 2006). The process of IFT can be broken down into four distinct phases, i.e. initiation of movement from the base, movement out to the tip, reversal of direction at the tip (accompanied by rearrangement of complexes) and then movement back to the base. These four phases can be measured in kymograph analyses and it has been shown that mutants exist which differentially affect various phases (Iomini et al., 2001). The molecules that regulate the switching between these phases remain unknown.

Although IFT and its role in flagellar assembly were first discovered in the green alga *Chlamydomonas*, the process is highly conserved and involves the same set of molecules in all organisms that have cilia or flagella, including humans.

Flagellar assembly at the tip not only occurs when the flagellum first grows, but continues even after the flagellum has reached its final length (Stephens, 1999; Marshall and Rosenbaum, 2001; Song and Dentler, 2001). This steady-state assembly is necessary to balance a continuous removal of subunits from the tip of the flagellum that occurs even once the flagellum has reached its final length. The continuous assembly and disassembly at the flagellar tip result in continuous turnover at steady state. The teleological purpose of this turnover is unclear, but it may have first evolved as a mechanism to allow disassembly of cilia and flagella prior to cell division (Grimes and Gavin, 1987; Parker and Quarmby, 2003). Flagella are normally present in cells during the G1 growth phase, and are resorbed prior to mitosis. Resorption can also be triggered by various chemical agents, and the mechanisms that mediate this resorption are currently the object of intense study (Parker and Quarmby, 2003; Pan and Snell, 2005), but one possibility is that it involves an up-regulation of the underlying steady-state turnover rate. The steady-state assembly requires IFT to provide subunits for assembly (Adams et al., 1982; Piperno et al., 1996), and when IFT is turned off in full length flagella, the flagellum immediately begins to resorb. Another interesting question is the mechanism of turnover. Flagellar axonemal microtubules are completely stable when isolated, suggesting they

aren't simply disassembling via conventional microtubule depolymerization. Instead, it appears that tubulin turnover may involve exchange of tubulin at the junction between the two microtubules of the doublet (Stephens, 1999; Stephens, 2000), via an unknown mechanism. It would be of great interest to identify the proteins that catalyze axonemal microtubule turnover, but so far there is no information about their identity. Given that the turnover occurs at the tip of the flagellum (Marshall and Rosenbaum, 2001), the disassembly machinery must be localized to the tip. It is known that the tip contains a morphologically distinct structure known as the "tip structure" (Dentler and Rosenbaum, 1977) but its composition or function are unclear. The microtubule plus-end tracking protein EB1 also localizes to the tip (Pedersen et al., 2003), and this may play a role in regulating turnover, either directly or by recruiting other factors.

C. Phenomenological Studies of Flagellar Length Control

C 1. Measurement of Flagellar Length Distributions

Because flagella are so easy to observe, there is a wealth of quantitative information concerning flagellar length variations under different conditions. These experiments set the boundary conditions that any length control model must satisfy. Flagella are roughly 10-14 microns long, although their average length depends on time of day and cell cycle progression (Tuxhorn et al., 1998). The fact that flagellar length is in a size range that is easy to measure using simple methods of light microscopy is one of the main reasons why this organelle is so useful as a model system to study size control.

The first fact established by observations of flagella is that length appears to be under tight control. Specifically, measurements of the distribution of lengths in a population of *Chlamydomonas* cells appear to indicate that length must be actively adjusted. What, exactly, does this statement mean? Careful measurements on synchronized cells (gametes, for instance) show that flagellar lengths have an approximately Gaussian distribution with an average length around 10 microns and standard deviation in length of approximately 1 micron. Similar distributions of ciliary lengths are seen in other organisms (Wheatley and Bowser, 2000). The low coefficient of variation of these length distributions gives us a visual impression that length control is somehow "tight" in the sense that the variation in lengths is less than what we might expect for a randomly polymerizing structure. Why is this? Let us consider the length distribution that would be expected if there was NO length control. Suppose that flagellar precursor subunits were assembled at random into the flagella. What length distribution would result? Simple calculations show the length distribution for a simple single-stranded linear equilibrium polymer should follow an exponential distribution, with the majority of the polymers having a short length (Nossal & Lecar, 1991). This would obviously not fit the Gaussian distribution seen in actual flagella. On the other hand, it is highly questionable whether a structure as complex as the flagellum should be considered a simple equilibrium polymer at all. Certainly a better approximation might be a multi-stranded dynamic polymer such as a microtubule, especially given experimental data that flagella are dynamic structures undergoing continuous turnover (Stephens, 1999;

Marshall and Rosenbaum, 2001). Multistranded equilibrium polymers still show an exponential length distribution (Howard, 2001), as do dynamic polymers undergoing dynamic instability when confined within a cell, as judged by both experimental measurements and theoretical modeling (Verde et al., 1992; Dogterom and Leibler, 1993). If a dynamic polymer is allowed to grow without bounds, the length distribution can begin to approach a Gaussian (Verde et al., 1992), but theoretical models require that such a distribution must have a constantly increasing average length over time (Verde et al., 1992). The fact that *Chlamydomonas* cells arrested in their growth cycle, for example gametes, can maintain a Gaussian distributed length with a constant average indicates that the length distribution cannot simply be accounted for by the same mechanism that functions in individual microtubules. To summarize this discussion, our naive visual impression that length is somehow restricted in its variation by a specific mechanism, at least in comparison to simple microtubule systems, is likely to be correct.

Two other important results are obtained from simple length measurements. First, while there is a certain degree of variability in lengths among a population of cells, the two flagella within a single cell are always more similar to each other than they are to the population in general. This suggests that there might be an additional mechanism for equalizing lengths within one cell, above and beyond that involved in setting the length in the general population. It also suggests that the dominant source of length variation in a population may be caused by cell to cell variation, as opposed to random

temporal fluctuations within the activity of the length control system itself. Length variation is thus dominated by so-called "extrinsic" noise (Elowitz et al., 2002). Second, flagellar lengths do not noticeably fluctuate in wild-type cells during a normal observation period. Upon extended observation, it can be seen that lengths gradually increase over the course of a day. It would be interesting to know whether this is due to a simple increase in cell mass or biosynthetic capacity as the *Chlamydomonas* cell grows during the light phase, or whether instead this is due to a more direct influence of the cell cycle or circadian clock machinery on the length control system. Careful measurement of variation (i.e. noise) in flagellar lengths in *Chlamydomonas* cells grown under various conditions shows that there is a large reduction in the length variance when gametes are compared to asynchronously growing wild-type cells (our unpublished data). Since gametes are arrested in a G0-like stage of the cell cycle, this difference suggests that variation in progression through the cell cycle is a major contributor to the extrinsic noise in flagellar length. Further evidence that flagellar length is under specific control is obtained from other types of algal cells in which flagellar length varies reproducibly depending on the age of the basal body and cell cycle progression (Beech and Wetherbee, 1990; Lechtreck et al., 1997). Such results indicate that flagellar length must be under active control, and also that the basal body is able to exert an influence *in cis* on its associated flagellum.

C 2. Flagellar Regeneration

Much can be learned about a structure by watching how it is assembled. For most organelles, this is quite challenging because one can't induce the organelle to form in a controlled fashion. Usually, the cell decides when it wants to build an organelle. One major advantage of flagella as a model system for organelle assembly, is that one can, in *Chlamydomonas*, induce flagellar assembly in a highly defined and synchronous manner. This is because *Chlamydomonas* cells are able to sever their own flagella in response to a transient reduction in extracellular pH, a phenomenon known as flagellar autotomy. When cells are exposed to a pH shock, a complex signaling cascade is set in motion which ultimately leads to a katanin-mediated severing of flagellar axonemal microtubules. The flagellum is then shed into the media, and a new flagellum begins to grow. The flagellum generally shows a lag of up to 10 minutes before growth begins, and growth typically reaches full length in less than two hours. An alternative way to induce flagella to grow is to start with cells grown on a plate of agar media. For unknown reasons, *Chlamydomonas* cells grown on plates have flagella that are extremely short or even lacking entirely. Once the cells are washed off into liquid media, they rapidly grow out flagella reaching full length in under half an hour.

The first insight one gains from observing flagellar regeneration is that flagella don't grow at a uniform speed. Plots of growth curves show that flagella grow at their maximum speed when they first start growing, and then continuously slow down, so that they asymptotically approach their final length. Most of the growth is over within the first hour. This type of kinetics has given

rise to several different interpretations. One interpretation is that the slowdown in growth shows that flagella grow under the control of a negative feedback loop such that the growth rate is highest when the length is maximally far from the desired set-point, and then slows down as the set-point is reached. This interpretation seems unlikely to be true for the following reason. If cells are pre-treated with cycloheximide, which blocks new protein synthesis, and then induced to shed their flagella, the new flagella that regenerate only grow to approximately half of the wild-type length. They are thus far from their normal "set-point" when they stop growing. Yet they show the same type of decelerating kinetics as normal flagella, with a rapid growth early on and a gradual approach to the final length over a roughly 1-2 hour period (Rosenbaum et al., 1969). If the growth rate were simply set by a feedback control that measured distance from the set-point, then the slowdown in growth should only be observed when the flagella reach the set-point length, which they never do in the cycloheximide experiment. A second possible explanation for the observed kinetics might be that the induction of flagellar assembly activates a defined intracellular signaling program involving molecular timers, which directly specifies growth rate as a function of elapsed time after initiation. This also seems unlikely based on experiments in which cells with half length flagella, formed by regeneration in cycloheximide, are fused to wild-type cells, such that the wild-type cytoplasm allows the half-length flagella to begin growth to the wild-type length. When the growth kinetics in such experiments are compared to those in wild-type flagellar regeneration, it is seen that the growth rate at any given point in the elongation

process correlates exactly with the length reached at the point, and not with the time elapsed since induction of growth (Marshall et al., 2005). The third interpretation is that growth rate is inherently length-dependent due to a length-dependence of intraflagellar transport. This possibility will be discussed in detail in the section below on models for length control.

Interestingly, when cells first form flagella, they do with a dramatically different type of kinetics. Madey and Melkonian (1990) measured flagellar outgrowth in *Chlamydomonas* cells after mitosis, before hatching from the mother cell wall would normally have occurred. They found that in such cells, flagellar growth was completely linear, occurring at a constant, slow rate of 28 nm/min. This constant linear growth contrasts sharply with the decelerating growth seen during regeneration, and suggests that a different assembly mechanism might be at work. One possibility would be that flagellar assembly at this stage might be strictly rate-limited by a lack of a pre-existing pool of precursor protein. In this case, the assembly rate is never able to become large enough for the length-dependent effects of IFT to become apparent. Consistent with this idea, Madey and Melkonian (1990) found that the post-mitotic flagellar growth phase could be completely arrested by addition of cycloheximide. Thus, there are two types of flagellar assembly kinetics, apparently depending on the degree to which a cell has accumulated a precursor pool. The presence of these same two types of growth kinetics has also been reported in the closely related alga *Volvox carteri* (Coggin and Kochert, 1986) and is therefore probably a general phenomenon. It has recently been shown that flagellar growth in a related green alga,

Spermatozopsis similis, occurs exclusively via an extremely slow linear kinetics (Schoppmeier and Lechtreck, 2003), suggesting that in this organism, unlike *Chlamydomonas*, IFT may either not be involved, or else be under dramatically different regulation. At the very least, the fact that the flagella grow so slowly in *Spermatozopsis* (about 1 micron per hour, compared to *Chlamydomonas* in which a flagellum can grow to 10 microns in 20 minutes) suggests that the growth mechanism in *Spermatozopsis* occurs via a distinct process. While this means that results in this organism cannot be directly used to test the mechanism of length control in *Chlamydomonas* (Beech, 2003), it suggests that a careful analysis of what is actually occurring in *Spermatozopsis*, using genetic and biochemical methods, might eventually provide some extremely useful insights into length control.

The second insight that has resulted from studies of flagellar regeneration is the fact that when flagella elongate, they do so by adding new protein exclusively at their distal ends (Rosenbaum and Child, 1967; Johnson and Rosenbaum, 1992). This conclusion, reached by pulse-labeling cells undergoing elongation, would have been difficult to obtain had it not been so easy to induce flagellar growth at the time of one's choosing. Similarly, studies of mRNA levels as a function of time after flagellar regeneration begins, have revealed that cells execute a complex program of transcriptional activation, with several hundred genes up-regulated (Lefebvre et al., 1980; Stolc et al., 2005) leading to concomitant increases in protein levels of flagellar precursor proteins (Lefebvre et al., 1978). Interestingly, when *Chlamydomonas* flagella are induced to

elongate by addition of the drug Lithium, this elongation also triggers induction of flagellar genes (Pena, 2005). Although the molecular pathway that regulates this gene induction program is unknown, mutants have been identified in which induction no longer occurs (Lefebvre et al., 1988). It will be extremely interesting to learn the precise nature of the pathway that drives flagellar gene expression. Because most current methods used to study gene expression are based on analysis of whole populations of cells, the ability to induce synchronous flagellar regeneration in a whole population of *Chlamydomonas* cells has been invaluable for these studies. The role of this transcriptional program in length control remain unclear, given that cells in which protein synthesis is blocked are still able to reach a defined length, albeit one that is shorter than normal.

C 3. Flagellar Length Equalization

One of the most dramatic phenomena pertaining to flagellar length control is the equalization of flagellar lengths following a transient perturbation. This is observed experimentally by removing one of the two flagella from a cell, and then observing the behavior in real time. Technically, the challenge to this experiment is how to remove just one of the two flagella. In some organisms with very large flagella, this can be done by direct micromanipulation (Tamm, 1967). In *Chlamydomonas*, this has been accomplished by blending a suspension of cells in a Waring blender. If the shear forces are adjusted properly, a significant fraction of the cells will shear off just one flagellum. After shearing, cells are

examined under a microscope, and once a cell is found that has only one flagellum, it can be tracked over time to observe the behavior.

The behavior of cells from which one flagellum has been removed is quite remarkable, and has had a major impact on our conceptual view of flagellar length control as an active process. In such cells, the severed flagellum begins to regenerate, following similar kinetics to those seen in flagellar regeneration as described above. However, while this growth is occurring, the other flagellum begins to shorten! The long flagellum continues to shorten while the regenerating flagellum grows, until they reach the same length. At that point, the two flagella grow out together. If cells are treated with cycloheximide, to poison new protein synthesis, then the two flagella will converge on the same length but will not undergo further growth. In some cases, the long flagellum overshoots the short flagellum transiently, but in such cases it eventually returns to the same length.

This ability of cells to equalize the lengths of their flagella has been taken to indicate that the long flagellum somehow "knows" that it is too long, or that it is "instructed" by the cell to shorten. To some extent, this view was a byproduct of a mistaken idea of flagellar stability. Before studies of flagellar protein turnover were performed (Stephens, 1999; Marshall and Rosenbaum, 2001) it was generally assumed that flagellar microtubules were perfectly stable (Tilney and Gibbins, 1968). This was thought to be the case because flagella do not disassemble when isolated in vitro, nor do they shorten when microtubule depolymerizing drugs are applied. If flagella are in fact stable, then the length

equalization process would necessarily entail an activation of some disassembly machinery. However such a disassembly would not, or so the reasoning went, be active in the regenerating flagellum, or else it would not be able to grow. In order for this machinery to be activated in the long flagellum, but not in the short one, there must be a regulatory pathway that is differentially activated in the long versus the short flagellum. In other words, the long flagellum must know it is too long.

However this argument is based entirely on the mistaken view that flagella are static structures. The fact that flagella are dynamic structures, undergoing continual turnover, provides an alternative explanation for the length equalization. In a cell with two flagella, these two flagella are competing for a common pool of precursor protein. During flagellar regeneration, flagella grow extremely quickly when they are short, and grow with a decelerating kinetics such that their growth rate decreases as length increases. Because turnover continues even after flagella reach full length, the assembly rate never quite becomes zero, but attains some small finite value to balance the ongoing removal during turnover. If one flagellum is suddenly shortened, it will grow with a much faster assembly rate than the full-length flagellum. Since when a flagellum grows, it incorporates precursor protein from the cytoplasmic pool, the rapid growth of the regenerating flagellum will necessarily choke off the supply of precursor from the longer flagellum. In essence, the short flagellum will be able to take more than its fair share of the cytoplasmic protein pool. This will then cause the assembly rate in the long flagellum to decrease to the point that it no longer balances disassembly

during turnover, and as a result the flagellum will begin to shorten. The disparity in assembly rates will hold as long as the two flagella are of unequal length. Numerical simulations have shown that this simple mechanism can account for the length equalization seen when one flagellum is severed and allowed to re-grow (Marshall and Rosenbaum, 2001). Therefore, it can no longer be claimed that flagella know how long they are, in the sense of having regulatory pathways whose activity depends on length, simply on the basis of the flagellar length equalization experiments.

Another example of flagellar length equalization has been reported using mutant cells having recessive mutation that cause their flagella to be longer than wild type. These mutants are discussed in detail in section IV below. When these long flagella cells are fused to wild-type cells, it has been observed that the abnormally long flagella shorten until they reach the same length as the original wild-type flagella from the wild-type cell. Although in this case the length equalization is simply due to the fact that the mutations causing the abnormally long flagellar length are recessive, so that when mixed with wild-type cytoplasm, the recessive mutation is rescued and the length reverts to normal. This experiment, therefore, tells us something about the nature of the mutations, but certainly does not constitute evidence for an active length-change inducing regulatory pathway within flagella. As with the length equalization experiments discussed in the preceding paragraph, the length equalization response in cell fusion experiments with long-flagella mutant cells has also been recapitulated

using numerical simulations that rely only on turnover and do not invoke any specific signaling pathway (Marshall et al., 2001).

To summarize this section, we can say that flagellar length equalization is now understood to reflect the fact that flagella are dynamic structures, undergoing continual turnover, and that their assembly rate depends on length.

D. Genetic Analysis of Flagellar Length Control

Whenever attempting to learn about a new biological system, one way to shine light into the "black box" is genetics. Genetic screens in *Chlamydomonas* have revealed a set of genes affecting flagellar length control.

D 1. Identifying Length Mutants in Chlamydomonas Genetic Screens

Because flagella drive *Chlamydomonas* cell motility, flagellar length defects can be isolated in motility screens. The general procedure is to mutagenize cells, then pick individual colonies into tubes or microwells and then examine cell movements under a dissecting microscope. This method has been used to identify both short flagella mutants (Kuchka and Jarvik, 1987) and long flagella mutants (McVittie, 1972; Jarvik et al., 1976; Jarvik et al., 1980; Asleson and Lefebvre, 1998). Because this screening strategy requires each mutagenized colony to be individually examined by a human observer using a microscope, it is exceedingly tedious and difficult to perform on a large scale. It thus seems likely that the screens conducted to date are far from saturation, and

that many more long and short flagella mutants could be obtained if screening methods with higher throughput could be devised.

The difficulty of identifying long-flagella mutants by visual genetic screens has therefore prompted a search for more efficient strategies. In a very clever approach, Lefebvre's group noticed that many long flagella mutants also show reduced rates of flagellar regeneration after pH-induced flagellar autotomy. Based on this observation, they reasoned that long flagella mutants could be enriched by first screening for mutants defective in flagellar regeneration, followed by a secondary visual screen for length alteration. Using this approach, coupled with a high-throughput screen for flagellar regeneration mutants, they were able to identify long flagella alleles of a new gene, *LF3* (Barsel et al., 1988). We note, however, that not all long flagella mutants show such a delay in flagellar regeneration, indicating that a screen based on this criterion will not be able to identify all potential long flagella mutants, but only those that have this additional phenotype. There is thus still a need for a rapid and scalable screening method based on automated measurement of either flagellar length directly or of motility.

D 2. Phenotypic and Genetic Analysis of Long-Flagella Mutants

It is also important to consider phenotypes other than an overall increase or decrease in length. Indeed, if one considers that length is maintained by a control system, if the system were to be truly broken by a mutation, then one might expect that the predominant phenotype would be a failure to maintain a

unique consistent length. If a mutation causes all cells to shift to a new, longer length, this indicates that the length control system is still functioning, but has simply been reset to a new set-point. Such mutations would therefore reveal genes involved in setting the control point of the system, but not in the functioning of the system itself. Thus, the most interesting mutants would be those which result in a randomization or increased fluctuation in length from cell to cell.

In fact, such mutations have been found, and interestingly, they appear to represent alleles of previously identified length genes. The original *lf2* and *lf3* alleles were all induced by chemical mutagenesis or UV, and may not have resulted in null alleles. It turns out that null mutations in the LF2 and LF3 genes result in a phenotype in which the average flagellar length is not particularly long. Instead, the main defect that is observed is that the flagellar lengths within a given cell are unequal, a phenotype known as "unequal flagellar length" or ULF. This was discovered in insertional mutagenesis screens for mutations that gave the *ulf* phenotype. Two *ulf* mutants identified in this screen, *ulf1* and *ulf3*, were found by genetic analysis to be alleles of LF3 (Tam et al., 2003). These mutant cells mostly lacked flagella, and when flagella were present, they were of unequal lengths and, interesting, shorter than the average wild-type length. It may at first seem puzzling or paradoxical that null alleles of a long-flagella gene have abnormally short flagella, but we must bear in mind that the main phenotype of *lf1*, *lf2*, and *lf3* mutants is the increased variability in length - the average length is actually not that much more than wild-type, and in a population

of *lf* mutant cells, many flagella are quite short while others have flagella that are unusually long. This is true even in many of the original *lf* alleles. These results imply that the LF genes are affecting flagellar dynamics in a subtle way.

D 3. Intraflagellar Transport in Length Mutants

Given the fact that intraflagellar transport is required to maintain flagellar length, it is obvious to ask whether any length mutants affect the process of IFT. Certainly, partial reductions in IFT do in fact result in shorter flagella, for instance *fla2* mutant cells, which have a reduced velocity of IFT particle motion at the permissive temperature (Iomini et al., 2001) have flagella that are significantly shorter than wild type (our unpublished observations). What about long flagella mutants? In this case the evidence is much less clear, but IFT is so obviously a candidate for involvement in length control, that it makes sense to check whether known *lf* mutants might increase the rate of IFT. To some extent, this is like the drunk looking for his keys under the street-lamp for the sole reason that this is where the light is brightest. Since we know more about IFT than we do about most aspects of flagellar assembly, it makes a good starting point for analyzing the effects of *lf* mutations. In any case, detailed information about how distinct alleles of the *lf* genes affect transport and turnover within the flagellum is likely to yield new insights into the length control machinery.

It has been demonstrated that flagella in LF3 null mutants show an increase in the quantity of IFT proteins relative to wild-type (Tam et al., 2003). This result seems at first blush to explain the *lf3* mutant phenotype: *lf3* mutant

flagella have increased IFT, allowing them to grow more rapidly to a longer final length. Unfortunately, this cannot be the whole story since the increased IFT protein levels were measured in an insertional allele of LF3 (*lf3-5*) in which flagella are actually shorter on average than wild-type. If increased IFT protein leads to a longer flagellum, why are the *lf3-5* flagella shorter? In actuality, the apparent increase in IFT proteins in *lf3* mutants is potentially misleading. It has previously been shown, both by immunofluorescence and Western blotting (Marshall et al., 2001; Marshall et al., 2005) that the quantity of IFT protein within the flagellum is independent of length, such that very short flagella contain the same total quantity of IFT protein as very long flagella. Consequently, in cells with short flagella such as those seen in *lf3-5*, the IFT proteins will always represent a disproportionate fraction of the total protein simply because their quantity per flagellum remains constant regardless of length while the total axonemal protein content per flagellum is reduced in shorter flagella, so that if Western blots are run loading the same total protein, as was done by Tam et al (2003), one would expect that any short flagella will show an increase in IFT. Therefore, the increased fraction of total protein represented by IFT proteins in the LF3 null mutant does NOT indicate that the LF3 gene product regulates IFT. Quite to the contrary - this result suggests that IFT levels are normal in the LF3 null mutant. It thus remains unclear how the *lf3* mutation affects length. An interesting clue comes from extensive ultrastructural analysis of *lf3* which revealed linear aggregates of material accumulating at the tips of the short flagella, like a bag full of toothpicks. Although the authors who conducted the

study interpreted this material as IFT protein aggregates, it is equally possible that these linear structures represent defective assembly of axonemal components, suggesting a role for LF3 in regulation of assembly.

D 4. Length Control Proteins - Localization and Function

In addition to serving as tools to probe the behavior of the length control system, length mutants also allow us to identify the protein components of the system itself, once the genes are cloned. A major ongoing effort by the Lefebvre laboratory has resulted in the identification of all four LF genes. Both LF1 and LF3 are apparently novel genes (Tam et al., 2003; Nguyen et al., 2005). However, identification of the genes provides a foot in the door. For instance, epitope tagging has led to new and interesting information about subcellular localization. Both LF1 and LF3 appear to localize in the cell body rather than the flagellum, and both localize in a number of punctate foci. This suggests that LF1 and LF3, and possibly other length control proteins, colocalize together in a cytoplasmic sub-structure which has been dubbed the "lengthosome" (see Figure 1). How the activity of the lengthosome functions to regulate flagellar length remains unknown.

LF4 was found to encode a protein kinase of the MAP kinase family (Berman et al., 2003). LF4p localizes both to the cytoplasm and also within the flagellum and is apparently regulated by a phosphatase located within the flagellum (Wilson and Lefebvre, 2005). The fact that LF4 is a kinase indicates that a signal transduction pathway is involved in length control. It is tempting to

speculate that this might represent a feedback control pathway, in which a length sensor reads flagellar length, modifies the activity LF4 accordingly, and then LF4 signals to a downstream pathway that adjusts length. There is, however, no evidence so far that LF4 actually functions within a feedback loop. It is just as likely, a priori, that LF4 acts in an input pathway to the length control system, by which the cell can specify how long the flagella ought to be. The only evidence in favor of a feedback function, so far, is the presence of LF4 protein within the flagellum. This might seem hard to reconcile with a purely input-pathway function for LF4, unless LF4 has to carry its signal to the flagellar tip, for example, in order to provide its input to the pathway. It is clear that further investigation of LF4 will be of great interest.

To summarize the genetic analyses of flagellar length control, four long-flagella genes have been cloned, LF1 through LF4, of which LF1-LF3 appear to localize together in cytoplasmic "lengthosome" complexes of unknown function, while LF4 is a MAP kinase that can be found within the flagellum. These genes provide a starting point to dissect the molecular pathway of length control. They also provide invaluable tools for testing potential models for the length control mechanism.

III. Models for flagellar length control system

Given the extensive set of genetic and phenomenological data that exist concerning flagellar length control in *Chlamydomonas*, this system represents a best-case situation for developing and testing mechanistic models for length

control. In this section we consider five broad classes of theoretical length-control mechanisms that have been suggested to account for length control in various cellular systems (for review see Marshall, 2004). We will consider which of these may be applicable to the specific problem of flagellar length control in *Chlamydomonas*.

A. Molecular Ruler

One mechanism used in length control is a molecular ruler, in which a protein molecule is produced whose physical length matches the length of the structures whose size is to be controlled. One end of the ruler molecule is anchored at the point where the polymeric structure begins its self-assembly, and then the other end tracks the growing end of the polymeric structure, either promoting assembly directly or acting as a protective cap to block access of the growing end to diffusible growth-inhibiting factors. This type of mechanism is clearly at work in the case of bacteriophage tail fibers (Katsura, 1990) and is also implicated in the control of actin filament length within striated muscles (Fowler et al., 2006). The key prediction of a molecular ruler model is that a protein must be identified whose length matches that of the assembling structure. Such a protein has not yet been identified for the flagellum, although we must admit that failure to discover something hardly constitutes proof of its non-existence. In general, though, molecular rulers tend to be employed for size control in small structures less than a micron long, which makes sense given the fact that the size has to be set by a single protein, and there is a limit as to how long a protein can be.

Again, though, we don't strictly know what this limit is. Moreover, there are ways to get around the need for a single long protein - one can theorize vernier type mechanisms where a pair of proteins of slightly different length assemble alongside one another and only when their two ends line up flush with each other can they recruit a factor to define the assembly termination point. In this case, the length is set by the least common multiple of the lengths of the individual elements. In such a vernier system, it might be very hard to know a priori that a given protein is part of the vernier system, since it would assemble alongside the axoneme and to all intents and purposes be part of it. Since the component proteins of a vernier ruler wouldn't have to be particularly long, there is no obvious feature that would reveal them to us.

Is there any conceivable way to rule out a ruler model then, given that we can't rest on the absence of direct demonstration of the ruler itself? One approach is theoretical - as described by mathematical analyses of the ruler mechanism (Wagenknecht and Bloomfield, 1975) the distribution of lengths produced by a ruler shows a very skewed distribution. Conceptually this can be understood because a protein has a certain degree of flexibility, hence the ruler protein can sometimes flex to a shorter end-to-end length, allowing structures of a reduced length to form with some probability. There is a hard cut-off at longer lengths, however, since there is a limit to how far the ruler can stretch. This leads to a distribution skewed to shorter lengths. Our own measurements (W.M. unpublished data) show that flagellar length distributions in wild-type *Chlamydomonas* cells show a distribution that is essentially Gaussian, based on

statistical calculations of skew and kurtosis. This would seem to rule out ruler models of the simplest type based on a single long flexible ruler protein.

However, for a vernier system that co-assembles alongside the highly rigid axoneme, it is unlikely that shorter structures can be produced. Moreover, if the ruler acts by interacting with a diffusible effector, it might simply set the mean value of a Gaussian distribution of sizes whose variance is determined by the diffusion constant of the diffusing effector. It is thus not possible to completely rule out a ruler model by this type of measurement.

A better argument against rulers is the fact that in a population of cells, flagellar lengths can vary by 1-2 microns. Moreover, even in a single cell, the length varies during the course of the day. Length is also reduced when cells regenerate in the absence of protein synthesis as discussed above. It is quite hard to reconcile these results with a single fixed ruler mechanism. One would have to propose that a ruler or vernier undergoes changes from cell to cell, and throughout the day, and in response to changes in protein levels. While a suitably baroque model could probably be devised to incorporate all of these effects, Occam's razor suggests that our time is better spent evaluating alternative length control methods.

B. Quantal Production

The second type of mechanism we consider is the quantal production of limiting precursor. In this model, there is one (or possibly more) key structural protein constituent of the flagellum whose quantity is limiting. When a cell

initiates formation of a flagellum, a certain quantity of this precursor is synthesized, and then it is incorporated into the growing flagellum. In this model, flagellar growth ceases when the quantity of this limiting precursor is exhausted. Supporting evidence for this type of model comes from experiments in sea urchin cells (Stephens, 1989; Norrander et al., 1995) in which the level of tektin synthesis was found to correlate with the length of cilia in various cells. However, correlation does not prove causality and from this data alone it would be equally plausible that protein production is sensitive to the length or growth of the flagellum.

Direct evidence against the limiting precursor model comes from experiments in *Chlamydomonas* in which cells regenerate flagella in the presence of cycloheximide. In such experiments, flagella do in fact regenerate, albeit to approximately half the normal length. This demonstrates that even after flagellar assembly is completed, the cytoplasm retains a sufficient quantity of all precursor proteins to produce two half-length flagella. Therefore, there cannot be a limiting precursor whose consumption sets the final flagellar length.

Further evidence against the quantal production of limiting precursor model comes from experiments with *Chlamydomonas* mutants having variable numbers of flagella (Kuchka and Jarvik 1982). Such mutants are called *vfl* which stands for "variable flagella". In the Kuchka and Jarvik study, *vfl2* mutant cells having a variable flagellar number between 1 and 4 were examined. If cells produced a fixed limiting quantity of a key precursor that was completely consumed during the process of flagellar growth, then the combined lengths of all flagella in a

single cell must add up to the length of a flagellum that could be constructed from this limiting precursor quantity in a cell with a single flagellum. Hence, cells with two flagella should have flagella half as long as cells with a single flagellum. Flagella would be one third as long in cells with three flagella, and one quarter as long in cells with four flagella. This geometric dependence of length on flagellar number was not, however observed. Instead, the lengths of the flagella decreased only slightly as their copy number increased. More extensive measurements on three different *vfl* mutants (*vfl1*, *vfl2*, and *vfl3*), including measurements under different fixation conditions and in living cells, have confirmed that the dependence of flagellar length on number does not match the geometric dependence predicted by the limiting precursor model (Marshall et al., 2005).

Finally, one can ask whether a limiting precursor model can account for altered lengths in *shf* or *lf* mutants. In the context of this model, an *lf* mutant would increase length by generating increased levels of precursor protein. Such an increase has not been detected by Western blot analysis with known flagellar proteins. It could be argued that one might only see a major increase in protein quantity in those particular cells that make long flagella within a mixed population of *lf* cells showing a high variance in length, some short, some long. Since standard biochemical analyses are population based, they could not detect such a phenomenon at the level of the single cell and might fail to see a significant difference at the population level. We can, however, rule out this possibility by another experiment. If an *lf* mutant makes a drastically larger quantity of a key

precursor protein, then if such cells were fused to wild-type cells, the increased precursor levels in the combined cytoplasm should result in a cell with four longer-than-normal flagella. In fact, when *lf* mutants and wild type are fused, the two long flagella rapidly revert to wild-type length (Barsel et al., 1988). This argues against the idea of a dramatically increased level of a specific precursor protein in such mutants, even if the increase is only seen in a few individual cells. It thus appears that the quantal precursor model is not compatible with the observed genetic and phenomenological data.

C. Cumulated Strain Model

A model has been proposed for bacteriophage tail length control, which theorizes that as additional subunits polymerize onto the growing structure, they undergo an increasingly great conformation alteration, such that the free energy of binding is gradually reduced by a constant increment (Kellenberger, 1972). This model, known as the "cumulated strain model", has been investigated mathematically by Wagenknecht and Bloomfield (1975), who demonstrate that it can lead to an extremely tight distribution around some defined length, using biologically realistic parameters. Their model indicates that for a given precision of length control, the free energy change needed to explain that control becomes less and less as the number of subunits increases. Their model can account for length control in a phage tail with few than 100 subunits without invoking an unreasonable change in binding energy. Therefore, the change in energetics needed to fit length control in flagella, which contain tens or hundreds of

thousands of subunits (depending on whether one considers a subunit a tubulin dimer or a whole 96 nm repeating unit of axonemal structure) will be even less, and therefore certainly within a physically possible realm.

The cumulated strain model is thus capable, in theory, of producing the degree of length regulation (in terms of the standard deviation of the length) observed in real flagella, at least in the sense that the change in free energy of binding that would have to be invoked will be extremely small. So, the model won't violate the laws of physics, which is of course important. But a somewhat more stringent test is to ask whether this model can account for all of the phenomenological and genetic data discussed in sections III and IV. The cumulated strain model predicts that if the ratio between the total quantity of monomer and the number of initiation sites (basal bodies, in our case) is altered, the length should change in defined ways (Wagenknecht and Bloomfield, 1972). Specifically, when the ratio drops, the length should decrease in proportion to the change in the ratio. This predicts that cells with two basal bodies should have flagella twice as long as those with four, a prediction that is not borne out by experiments with *vfl* mutants (Kuchka and Jarvik, 1982; Marshall et al., 2005). Thus, this model fails the same test that excluded the quantal production model.

We can also consider whether the cumulated strain model can account for the known *shf* and *lf* mutants. The only parameters that can really be changed in the model are the free energy change during successive polymerization steps, and the total quantity of monomer present. Therefore if a length mutant is to result in altered length, it must change one or the other of these quantities. It is

not obvious how proteins such as If3, whose products localize to the cell body and are not components of the flagellum itself, could alter the binding energy of flagellar protein subunits. This leaves the alternative, that the If and shf mutants alter the quantity of one or more key flagellar protein subunits. An interesting result of the analysis of the cumulated strain model, as shown by Wagenknecht and Bloomfield, is that while reductions in monomer quantity lead to proportional reductions in length, increases do not. The cumulated strain model is highly resistant to length increases beyond the normal length, such that in order to generate a detectable increase in average length, concentrations of monomer must be increased by several orders of magnitude. Such increases are simply not seen in If mutants for flagellar proteins in general - for instance tubulin does not appear to be made in significantly larger quantities in If mutants. Strictly speaking, however, it is possible that one or more unknown proteins are playing a key role in limiting length, and without a specific antibody to detect them, we might have no way of knowing whether in fact they are suddenly produced in much greater quantities in an If mutant. But as with the quantal precursor model, the fact that If mutant cells with long flagella undergo rapid flagellar shortening to wild type length when fused with wild-type cells, strongly suggests they do not contain elevated precursor levels. Therefore, it seems difficult to make the cumulated strain model work out in the context of long flagella mutants.

Overall, the cumulated strain model is difficult to reconcile with specific experimental details of flagellar length control, at least in its simplest form. Whether a more generalized version of the model, perhaps with a different

dependence of binding energy as a function of polymerization extent, could overcome these problems, remains to be seriously explored.

D. Feedback Model

A fourth type of length control system one could envision is a feedback control system. In this mechanism, a signal transduction pathway somehow senses the length of the flagellum, and then acts to modulate the assembly process in order to attain the correct length. For instance, a length-sensing pathway could inhibit IFT when the flagellum is too long, or up-regulate IFT when the flagellum is too short. In order for such a system to produce a flagellum of a defined length, the feedback would have to be negative feedback. Thus, a length sensing pathway, if it acted upon IFT, would have to inhibit IFT as length increases. Feedback control systems are common in man-made devices, and are known to confer desirable properties of stability and robustness.

Feedback control requires a length sensor to provide the initial input into a signal transduction cascade that ultimately impinges on flagellar assembly machinery. How might length be sensed by a molecular mechanism? One proposal (Rosenbaum, 2003) is that flagella may contain a length-dependent number of calcium channels, so that the total calcium current through the flagellar membrane would be length dependent. How calcium fluxes might lead to changes in flagellar length is unclear but could involve one or more of the known calcium-dependent phosphorylation events that occur within flagella (Bloodgood, 1992). This model is consistent with measurements showing that the number of

calcium channels in the flagellar membrane of *Chlamydomonas* is proportional to flagellar length (Beck and Uhl, 1994). However, as with the studies of tektin levels, correlation does not prove causality, and so it is just as likely that length affects channel number rather than vice versa. An alternative model for measuring length would be to attach a molecular timer, such as a G-protein, onto the IFT complexes, load it with GTP using a GEF at the basal body region, and then check the nucleotide state of the G-protein upon the return of the IFT complex from the flagellum. If the round trip time for a wild-type length flagellum is comparable to the GTPase rate of the G-protein, then deviations in length would result in measurable changes in the GTP/GDP ratio which could in turn modulate the activity of a length-sensitive signal transduction cascade. Many other such models can be easily proposed, but the problem is finding a way to test them.

Ultimately, the only way to determine if a feedback control loop is involved in length control is to identify the potential signaling pathway and then test whether it is activated in a manner consistent with overall negative feedback. The most likely candidate for a length-responsive signaling molecule is the LF4 kinase (Berman et al., 2003). As discussed above, lf4 mutants have abnormally long flagella. The mere fact that a kinase like LF4 results in a length change when mutated does not by any means prove it is part of a feedback loop. For example, one could speculate that the LF4 kinase might instead be present to allow the cell to alter the length of its flagellum in response to various environmental or developmental cues. The feedback control model does,

however, make some simple predictions about LF4 that can be tested. Loss of function mutations in LF4 lead to increased flagellar length, hence the normal function of LF4 must be to oppose net flagellar assembly. Therefore, in order for this molecule to act in a negative feedback loop, its own activity must be an increasing function of flagellar length. In other words, LF4 kinase must be activated when flagella are too long, and inactivated when flagella are too short. It is thus conceptually straightforward to test whether LF4 is part of a length-sensing feedback loop – one has only to measure the activation state of LF4 as a function of flagellar length. However, this measurement has not yet been reported. If the activity of LF4 is not in fact length-dependent, then it cannot be acting in a feedback loop. Other possible signaling molecules involved in length control have been revealed by pharmacological studies (Wilson et al., 2004). However the same caveats apply to these studies as to LF4 – the detection of a signaling molecule does not prove it acts in a feedback pathway. In order to support such a claim, the pharmacological drug targets must be definitively identified (not a simple task in most cases) and then the activation state of these targets measured as a function of flagellar length and compared to the behavior required by the negative feedback constraint. Nevertheless, the identification of signaling molecules that impinge upon length control, primarily due to the groundbreaking work of Wilson and Lefebvre, is a major step forward because it leads to readily testable hypotheses about the molecular mechanism of length control.

E. Balance Point Model

A simple model for length control has been proposed which does not require an explicit length sensor or signaling pathway (as in the feedback model). This model is based on the observation in *Chlamydomonas* showing that axonemal microtubules undergo continuous turnover at their distal tip, and that this turnover is balanced by new assembly, which in turn requires intraflagellar transport (Marshall and Rosenbaum, 2001). The rate of disassembly at the tip appears to be independent of length. Further analysis of IFT particles revealed that the number of IFT particles per flagellum is independent of length (Marshall and Rosenbaum, 2001; Marshall et al, 2005). If a fixed number of transport particles are forced to move over a greater and greater length, the rate at which they can drop off cargo to the tip and return for another load will decrease. Eventually, when the flagellum gets long enough, transport will no longer be efficient enough to balance disassembly, and the flagellum will have to shorten. It has previously been remarked that the deceleratory kinetics of flagellar re-growth in *Chlamydomonas* require that there be a reduction in IFT as elongation progresses (Beech, 2003). In our model, this reduction occurs via simple physics - when there is a fixed number of IFT complexes, traveling at a fixed velocity, then it takes them longer and longer to complete a transport cycle as the flagellum elongates. No special signaling or regulation is required apart from the obvious fact that it takes longer for a moving object to travel a greater distance. The model as formulated is a macroscopic model, phrased in terms of lengths and rates. A more detailed microscopic model that describes the behavior of

individual molecular components, has recently been evaluated and shown capable of producing a stable steady-state length (Bressloff, 2006), confirming that the balance point model is at least theoretically reasonable.

This model predicts that the flagellum will reach a unique length defined by a balance-point between length-independent disassembly and length-dependent assembly. This model can account for many observed aspects of length control, for instance the dependence of flagellar length on number in *vfl* mutants, the growth kinetics upon resumption of growth in half-length flagella, the ability of flagella to equalize their lengths when one flagellum on a biflagellate cell is severed, and the shortening kinetics of long flagella mutant cells when fused to wild-type cells (Marshall et al., 2001; Marshall et al., 2005). For two of these experiments, previous publications had presented data that appeared to be inconsistent with the balance-point model. A previous study (Kuchka and Jarvik, 1982) had reported that flagellar length does not depend on number, however the data reported in that paper actually show just the opposite and confirm the more recent report (Marshall et al., 2005) that cells with more than two flagella have a reduced flagellar length. Kuchka and Jarvik's data suggested that cells with one flagellum and cells with two flagella had equal lengths, but more recent data suggests that this is not generally the case (Marshall et al., 2005). A previous study suggested that when flagella arrested at half-length resume growth by restoration of wild-type gene function to a *shf* mutant, that these flagella initially grow with the same rate as a wild-type flagellum growing starting at zero length (Jarvik et al., 1984). This suggests that growth rate is a function of

time after growth induction, and not a function of length as predicted by the balance-point model. However, re-examination of the published data suggested an erroneous value for wild-type growth rates, and when these experiments were repeated in two different ways, in all cases the results support the model that growth rate depends strictly on length (Marshall et al., 2005). There, we conclude that the balance point model is compatible with all known phenomenological experiments on flagellar length regulation.

The balance point model also accounts for the possibility of shf and lf mutants. In this model, shf mutants can arise in either of two ways: either the rate of turnover is increased, or the rate of transport is decreased. Confirmation of this latter possibility has been obtained by creating a partial reduction in IFT. This partial IFT reduction was achieved by growing temperature-sensitive fla10 mutants cells, carrying a conditional mutation in the fla10 kinesin that drives IFT, at a temperature intermediate between fully permissive and fully nonpermissive. It was confirmed by western blot analysis that such flagella contain a reduced quantity of IFT protein (Marshall et al., 2005). This reduction in IFT was observed to produce a stable, persistent shift in length to a new length roughly half that of wild-type cells (Marshall et al., 2001). This directly demonstrates that the shf phenotype can be obtained by reduction in intraflagellar transport, which is a prediction of the balance point model but NOT of any of the other models. We especially note that feedback control systems, when present, are able to maintain a stable set-point even when the underlying process is perturbed, for example a thermostat can maintain room temperature even if the radiator is

partially blocked by furniture, because it will lead to increase furnace activity to compensate. The fact that reduction in IFT levels leads to a decreased length is thus compatible with the balance point model but not the feedback control model.

The If phenotype can also be explained by the balance point model. Again there are two possibilities: a long flagellum can be generated either by a reduction in the rate of turnover, or an increase in intraflagellar transport. The first possibility is potentially the case for If2 mutants based on the fact that experimental measurements of tubulin dynamics in such mutants have shown them to have a reduced rate of turnover at steady state (Marshall et al., 2001). Similarly, the NIMA kinase Cnk2 exerts an influence on flagellar length apparently, at least in part, by modulating the disassembly rate (Bradley and Quarmby, 2005). In contrast, the long flagella mutant If4 does not appear to alter its rate of turnover compared to wild-type (Song and Dentler, 2001) suggesting that If4 flagella are long for some other reason.

This model therefore seems capable of explaining all known experimental data concerning flagellar length control. However, the model faces one serious problem. The balance point model of length control requires that the number of IFT particles active in the cilium must be held constant. This prediction raises two questions: first, is it actually the case that the number of IFT proteins is constant, and second, by what possible mechanism could this constant quantity be achieved? Direct measurements, including both biochemical analysis of protein levels on Western blots (Marshall et al., 2005), quantitative measurements of immunofluorescence intensity (Marshall et al., 2001), and

counting of IFT particles by immunofluorescence microscopy (Marshall et al., 2005), all show that the quantity of IFT protein complexes within the flagellum is independent of length. Particle counting analysis indicates that the number of particle aggregates is roughly 8 on average, with a range of between 7 and 9 from cell to cell. How can an organelle count the number of particles within it? Recent kymograph data suggests a remarkably simple model for particle counting. Recent kymograph analyses (Dentler, 2005) of IFT particle aggregates moving up and down within the flagellum strongly suggest that individual IFT particle aggregates move up and down within the flagellum without leaving it, as judged by the fact that virtually all of the kymograph traces of a particle moving upwards begin at the end of a trace of a particle moving downwards. Traces indicative of new particles being injected into the flagellum, which would not originate at the end of a downwards trace, were only rarely visible in the published images. These considerations suggest that IFT might resemble a subway, where passengers (cargo) come and go to and from the station (basal body) in order to ride on the trains, but the trains themselves simply go back and forth between stations, never leaving the tracks (flagellar outer doublets). It is also possible that the exit of retrograde IFT particles from the base of the flagellum is tightly coupled with the entry of new IFT particles, such that an uninterrupted kymograph trace results. Distinguishing these two possibilities will require photobleaching analysis of particle turnover in live cells. These kymograph results have many caveats, the most serious being that one cannot tell precisely what a given DIC trace actually represents. We would most

especially like to know what fraction of the total IFT proteins in the flagellum are present in the large visible traces, and what fraction are invisible to the method. Nevertheless, taking this data at face value, it is at least suggestive of a rather tight association of IFT complexes with outer doublet microtubules in vivo.

Electron micrographs of cross sections through *Chlamydomonas* flagella invariably reveal the IFT particle aggregates as long chains of protein tightly apposed to the B tubule of the outer doublet. Given this intimate association of IFT particles with the outer doublets, the new data showing that particles move back and forth without leaving the doublet to which they are attached, and the fact that the number of IFT particle aggregates observed by immunofluorescence is approximately equal the number of outer doublets in the flagellum, we propose a simple mechanism to control particle number.

As illustrated in Figure 2B, we suggest that each outer doublet interacts with a single IFT particle raft. This raft moves back and forth within the flagellar compartment, picking up new cargo at the base and depositing cargo at the tip, without ever leaving the flagellum. The IFT rafts thus behave analogously to elevators moving up and down in an elevator shaft. The entire flagellum thus behaves like an elevator core with nine elevator shafts. In order to keep the number of IFT particle rafts constant at nine per flagellum, it is only necessary for the flagellar pores (Deane et al., 2001) at the base of each doublet to monitor the presence or absence of an IFT particle raft on the doublet. A doublet lacking a raft would signal the pore to inject another IFT particle raft. The main feature of this model is that it solves the problem of how a flagellum can count to nine - it

simply has to count to one, nine times. How does the flagellar pore recognize when it needs to inject an IFT particle? The simplest way would be for retrograde particles to interact with the pore in such a way as to inhibit further introduction of new IFT particles. This would explain why IFT particles accumulate in retrograde IFT mutants - although particles enter the flagellum, because they cannot return to the base, the flagellar pore "thinks" there is no particle raft on its corresponding outer doublet, so it lets in another bolus of IFT protein. This model easily accounts for the fact that retrograde IFT mutants accumulate IFT proteins in their flagella - the lack of returning retrograde particles would be interpreted by the flagellar pore as a lack of active IFT, and in response the pore would inject additional IFT particles. leading to an eventual accumulation.

As mentioned above, it is also possible that IFT particles do enter and exit the flagellum, but that entry and exit are coupled, and in this case the elevator model still works, because if entry of a new particle is coupled to exit of an old particle, the number of particles would never change. This alternate form of the model would, however, have difficulty accounting for the accumulation of IFT particles in a retrograde mutant. This model, which we emphasize is purely speculative at the moment, makes the prediction that length-altering mutations could occur in components of the flagellar pore apparatus.

One conceptual advantage of the balance-point model is that the constant ongoing turnover could potentially allow rapid readjustment of length in response to cellular signaling cues. For instance, cells resorb their flagella prior to division.

Studies in *Chlamydomonas* suggest that this resorption involves intraflagellar transport, either as a trigger for increased disassembly or severing (Parker and Quarmby, 2003) or as part of the disassembly machinery itself (Pan and Snell, 2005). We also note that in the balance-point model, the basal body plays a key role, potentially controlling the entry of both IFT proteins and flagellar precursor proteins into the flagellum. Thus, modifications or regulation of activities localized to the basal body would be expected to result in changes in flagellar length. This could provide a simple explanation for the fact that many cell types can possess flagella of different lengths depending on the maturation age of the corresponding basal bodies (see for example Schoppmeier and Lechtreck, 2003).

IV. Conclusion: What Have We Learned from Flagellar Length Control?

Although flagellar length control in the green alga *Chlamydomonas* is a fascinating biological puzzle, we anticipate that the lessons learned from studying this simple and tractable system will be readily extendible to other contexts.

A. length Control as Pharmacological Target for Ciliary Disease

As noted in the first section of this review, ciliary diseases in humans are often characterized by short cilia, rather than a complete absence of cilia. The degree to which an abnormally short cilium is detrimental may depend on the function of the cilia in a particular tissue. For motile cilia, that need to move fluid via their own motility, reduced length is obviously a severe problem. The same is

true of mechanosensory cilia, such as those of the kidney - a shorter cilium will have different mechanical properties, and is likely to produce less bending at the base in response to a given rate of fluid flow. For chemosensory cilia, short or stumpy cilia may have less surface area into which receptors may be embedded. They may thus lack the sensitivity of a longer cilium. In all cases, shorter cilia are likely to have reduced, but not eliminated function. This partial function may be the reason the disease results in symptoms at all - a disease mutation that results in a complete loss of cilia is most likely to be lethal in early development.

Given that abnormal ciliary length may underlie many human ciliary diseases, what can we do about it? The fact that mutants with abnormally long cilia exist suggests that if pharmacological interventions can be devised that induce an increase in ciliary length, these could be used to treat ciliary diseases with short cilia. For instance, assuming the balance point is correct, a disease caused by a partial reduction in IFT, which would tend to cause a shortening of cilia, could be compensated by a chemical therapy that inhibits turnover. Similarly, the molecular signaling pathways that lead to increased length, such as the LF4 pathway, provide potential targets for drug development - a chemical inhibitor of LF4 ought to lead to an increase in ciliary length.

In order to implement this general scheme for treating ciliary disease, there are two major requirements. First, it is important to determine the extent to which the length control machinery in human cells matches that of *Chlamydomonas*. This is simply a question of repeating, in human cells, the

types of experiments described above in algae. It will be especially interesting to see if reverse genetic knockdown of the human homologs of the LF genes will produce a similar increase in length of primary cilia. Second, efficient and highly parallelizable assays will be needed to allow high throughput screening of compounds for a potential effect on length. By combining GFP constructs specifically targeted to cilia, with automated high throughput imaging devices, it should be possible to rapidly screen through hundreds of thousands of compounds to identify candidates for further study.

B. Flagellar Length Control as Paradigm for General Organelles

A major reason for studying flagellar length control is that the ease of analysis provided by this organelle makes it possible to do large numbers of simple experiments. The hope, however, is that the general models for length control that are derived from experiments in *Chlamydomonas* flagella, will ultimately be applicable to size control of other types of organelles. First, we consider other organelles whose size can be described entirely by length. The most obvious is the microvillus. Microvilli contain parallel bundles of actin filaments. We have previously presented a simple model, analogous to the balance-point model of flagellar length control, to account for length regulation in microvilli (Marshall, 2004). It is known that actin in microvilli undergoes continuous treadmilling, with retrograde movement of the filaments towards the cytoplasm balanced by continuous addition of new actin at the tip. It is also known that actin monomer reaches the tip via diffusion. Solution of the diffusion

equation for a one-dimensional system at steady state with a constant rate of addition at the tip balancing constant treadmilling, results in a system that can achieve a unique, stable steady-state value for its length (Marshall, 2004). This model is, in an abstract sense, very similar to the balance point model for flagellar length control. The only real difference is that the inherent length dependence of assembly derives not from the details of IFT, but rather from the dependence of monomer concentration on length at steady state. So far, this type of model has not yet been tested for microvilli, but there is no reason why it could not be tested. In fact, the very same methods that have been used to test the mechanism of flagellar length control in *Chlamydomonas* (Marshall, 2001; Marshall et al., 2005) can be directly applied to microvilli: specifically one would like to measure the assembly kinetics, resorption kinetics when assembly is blocked, and the dependence of length on number when multiple microvilli are forced to compete for a common pool of precursor. Genetics can also be used to probe the mechanism of length control in microvilli, by identifying partial loss of function alleles in, for instance, the motors that drive treadmilling, and then comparing the observed phenotype with results of simulations.

It remains to be seen how many other linear structures will have their length controlled by similar processes. For instance it now seems likely that the sarcomere size in striated muscle uses a very different mechanism that may be based on a molecular ruler (Fowler et al., 2006). In order to ultimately conduct the same types of length control studies in other cellular systems, a major challenge is the fact that flagella are so much longer than most other linear

structures. Fortunately, several clever new imaging and image processing methods have greatly facilitated precise and accurate length measurement for very small structures (see for example Littlefield and Fowler, 2002), and it seems likely that the development and application of these measuring tools, combined with reverse genetics and mathematical modeling, will soon lead to a clear understanding of length control in general, at which point it will be interesting to see what overall patterns emerge in the types of mechanisms that biology has evolved to control length.

What about organelles that are not simple linear structures? So far, size control in such structures remains very poorly understood. We have previously proposed an abstract version of the balance point model which frees it from a single dimension (Marshall, 2002). To formulate such a model, which is really a schema for generating models rather than a specific model per se, we note that the balance-point model for length control hinges on two features. First, the model requires the structure to be dynamic, such that size control works by setting the assembly and disassembly rates equal at a single value of size. Second, the model requires that assembly is inherently length dependent, due to the properties of IFT. To generalize from this specific model, we say that size control of an organelle can work by a balance-point type of mechanism if two features are present: first, the organelle must be dynamic such that its size (surface area, volume, etc) is constantly changing slightly as the result of ongoing assembly (for example, via fusion of vesicles onto the organelle surface and budding of vesicles off of the surface), and second, that either the assembly

or disassembly rate, or both, is inherently size-dependent. For instance, if a membrane bound organelle is exchanging vesicles with the endoplasmic reticulum (or any other large reservoir of material), then we can assume that the rate of vesicles traveling to the organelle and fusing with its surface will depend only on the rate of vesicle formation at the ER and transit to the organelle, and not on the surface area of the organelle (since we presume the ER has no way of knowing how big the distant organelle actually is). If we further assume that the rate of vesicle budding from the surface is proportional to the surface area, we immediately obtain a simple balance-point model for size control. If we let the rate of vesicle fusion onto the surface be represented by the variable a , and the rate of budding be equal to bS , then the instantaneous rate of change of the surface area S is given by $dS/dt = a - bS$. If we solve for the steady state solution by setting $dS/dt=0$, we find that the system only can maintain a steady state surface area when $S = a/b$. This steady state solution is stable, since if the surface area were to increase, now the budding rate would go up, leading to a reduction in area back down to the steady state solution. Similarly, if the area were to somehow be reduced, now assembly (fusion) would predominate and restore the organelle to its steady state size. This simple generalization of the balance-point model seems reasonable but it has never been tested for any membrane bound organelle so far. Testing the model can proceed using the same methods developed for probing the mechanism of flagellar length control, such as measuring growth kinetics or the dependence of size on the number of organelles present in a given cell.

We conclude that flagellar length control continues to serve as a valuable paradigm for studying the problem of organelle size control in general. The types of length control models that result from the study of flagellar size provide insights into possible models that could regulate size in other systems. The experimental strategies that have been devised to study flagellar length can likewise be used to devise similar approaches for the study of other organelles. More generally, the fact that flagellar length control studies give us easy access to quantitative information which can be used for mathematical modeling, suggests that flagella will be a paradigm not just for size control, but for a more general systems-biology approach to cellular structure.

C. Length Control in Nanotechnology

Current efforts to build more complex and miniaturized machines using the methods of nanotechnology are faced with the same problems that the cell faces in building its sub-structures. How does one specify the size of the structure, or its position, or the number of copies to be made? Much current effort in nanotechnology solves these problems using the type of fabrication processes used in building man-made machines - a blueprint is developed that explicitly encodes all spatial information (size, position, etc) and then this blueprint is used to direct the activity of a fabrication device, such as a lithographic process. Such methods reach a hard limit on size scale, imposed by the physics of the fabrication process. For instance, photolithography is limited in the size of the features it can be produce, by the wavelength of the light used. An alternative

method, that is currently under consideration, is self-organization (Ewaschuk and Turney, 2006). In this paradigm, components of a nano-machine would put themselves together. This type of fabrication gets around the normal physics-imposed constraints, since there is no need to convert a macroscopic blueprint or image into a microscopic structure.

Because self-assembly of the type currently being considered for nanotechnology applications is precisely the fabrication principle used by cells, it makes sense to ask whether the methods employed by cells can be applied to human-designed nano-machines. Controlling the length of polymeric structures is a major issue in nanotechnology (Graveland-Bikker et al., 2006). The same mechanisms employed for length control within cells (molecular rules, cumulative strain, quantal production, feedback, and balance-point regulation) are all potentially applicable to length control in nanotechnology.

Further, the axoneme itself is promising as a potential platform for the fabrication of very small machines. With its precise symmetry, and 96-nm repeating arrangement of dynein arms, it provides a highly structured lattice onto which other small components could be positioned. Pursuit of this specific approach to nano-biotechnology will obviously require a very deep quantitative understanding of how the flagellum is put together. Length control is just one part of this understanding.

Figure 1

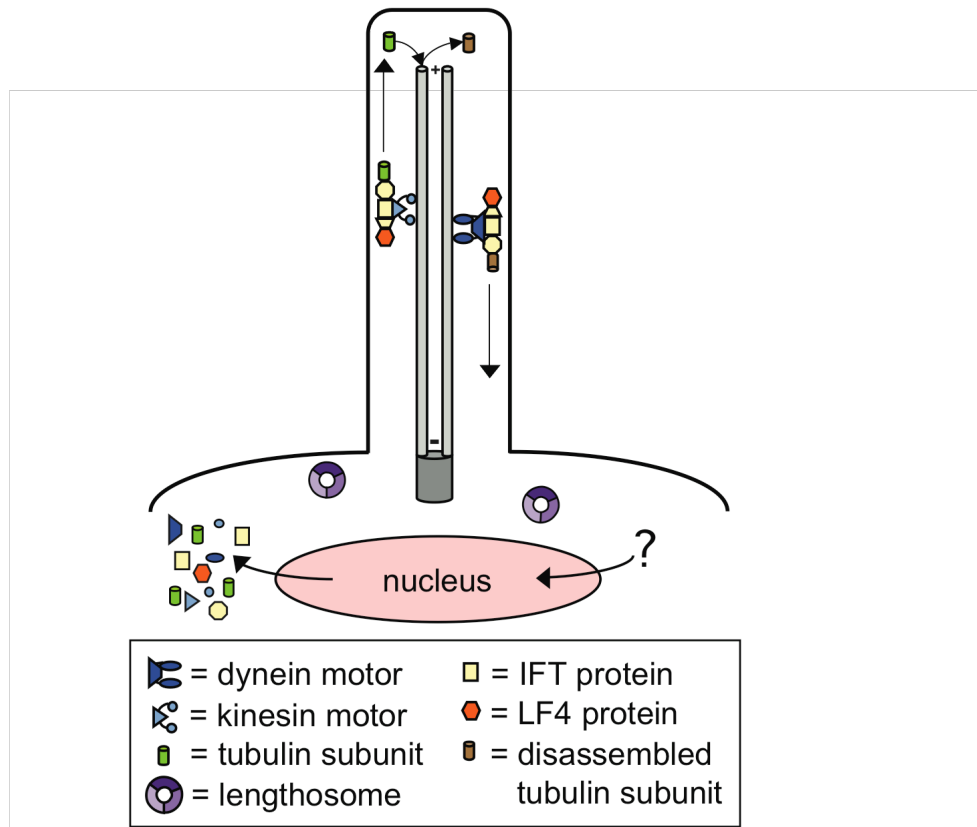


Figure 1. Diagram of flagellum showing components involved in length control.

Intraflagellar transport (IFT) proteins capture flagellar protein precursors from the cytoplasm and transport them to the tip of the flagellum, the site of turnover. This movement is driven by kinesin-II, and the retrograde movement of the IFT complexes back to the cytoplasm is driven by cytoplasmic dynein. IFT also transports the length-regulating kinase LF4, although the function of this protein in the length control system is not yet fully understood. Three other length control proteins, LF1-LF3, localize within the cytoplasm in a structure called the Lengthosome. This complex somehow regulates length, but its mechanism is not known. Genes encoding flagellar proteins are up-regulated when flagellar regeneration is triggered by deflagellation, implying that some sort of signal reaches the nucleus, but the nature of this signal is not known. Thus, while many of the key players are identified, the systems level question of how they act together to produce a well-defined length remains unanswered.

Figure 2

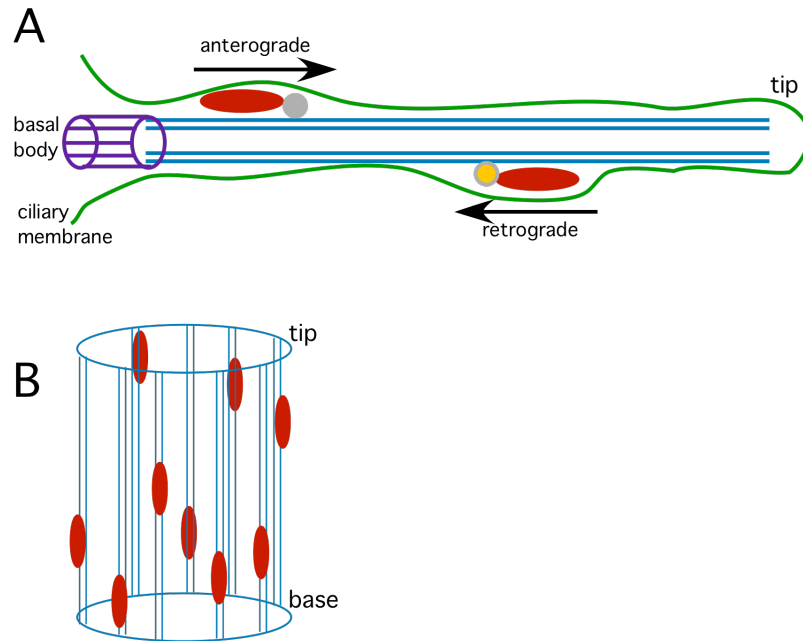


Figure 2. Length-Independent Regulation of Intraflagellar Transport - the Elevator Model.

(A) schematic of cilium, showing basal body embedded in cell cortex (purple) and ciliary membrane (green) which is topologically contiguous with plasma membrane but with a distinct lipid composition. IFT particles (red) are pulled by heterotrimeric kinesin-II (grey) in the anterograde direction, and by cytoplasmic dynein (orange) in the retrograde direction. Cargo proteins such as tubulin are bound by the IFT particles and brought to the tip, where they are assembled onto the growing end of the axoneme. (B) Elevator model. Each outer doublet has a single IFT particle aggregate attached to it, which moves up and down from base to tip and back, like an elevator moving between floors. A defined copy number of nine aggregates per flagellum is thus attained if each doublet recruits exactly one aggregate. This could either be established during initial assembly or maintained by a timer that injects new particles onto unoccupied doublets.

References

- Adams, G.M.W., Huang, B., and Luck, D.J.L. 1982. Temperature-sensitive assembly-defective flagella mutants of *Chlamydomonas reinhardtii*. *Genetics* **100**:579-586.
- Ansley, S.J., Badano, J.L., Blacque, O.E., Hill, J., Hoskins, B.E., Leitch, C.C., Kim, J.C., Ross, A.J., Eichers, E.R., Teslovich, T.M., Mah, A.K., Johnsen, R.C., Cavender, J.C., Lewis, R.A., Leroux, M.R., Beales, P.L., and Katsanis, N. 2003. Basal body dysfunction is a likely cause of pleiotropic Bardet-Biedl syndrome. *Nature* **425**:628-33.
- Asleson, C.M. and Lefebvre, P.A. 1998. Genetic analysis of flagellar length control in *Chlamydomonas reinhardtii*: a new long-flagella locus and extragenic suppressor mutations. *Genetics* **148**:693-702.
- Barsel, S.E., Wexler, D.E., and Lefebvre, P.A. 1988. Genetic analysis of long-flagella mutants of *Chlamydomonas reinhardtii*. *Genetics* **118**:637-48.
- Beck, C. and Uhl, R. 1994. On the localization of voltage-sensitive calcium channels in the flagella of *Chlamydomonas reinhardtii*. *J. Cell Biol.* **125**:1119-1125.
- Beech, P.L. 2003. The long and the short of flagellar length control. *J. Phycol.* **39**:837-839.
- Beech, P.L., and Wetherbee, R. 1990. Direct observations on flagellar transformation in *Mallomonas splendens* (*synurophyceae*). *J. Phycol.* **26**:90-95.
- Berman, S.A., Wilson, N.F., Haas, N.A., and Lefebvre, P.A. 2003. A novel MAP kinase regulates flagellar length in *Chlamydomonas*. *Curr Biol.* **13**:1145-9.
- Bernales, S, Papa, F.R., and Walter, P. 2006. Intracellular signaling by the unfolded protein response. *Ann. Rev. Cell Dev. Biol.* in press.
- Blank, H.M., Totten, J.M., and Polymenis, M. 2006. CDK control of membrane-bound organelle homeostasis. *Cell Cycle* **5**:486-488.
- Bloodgood, R.A. 1992. Calcium-regulated phosphorylation of proteins in the membrane-matrix compartment of the *Chlamydomonas* flagellum. *Exp. Cell Res.* **198**:228-36.
- Bradley, B.A., and Quarmby, L.M. 2005. A NIMA-related kinase, Cnk2p, regulates both flagellar length and cell size in *Chlamydomonas*. *J. Cell Sci.* **118**:3317-26.

- Bressloff, P.C. 2006. Stochastic model of intraflagellar transport. *Phys. Rev. E*. **73**:061916.
- Chemes, H.E., Morero, J.L., and Lavieri, J.C. 1990. Extreme asthenozoospermia and chronic respiratory disease: a new variant of the immotile cilia syndrome. *Int. J. Androl.* **13**:216-22.
- Coggin, S.J., and Kochert, G. 1986. Flagellar development and regeneration in *Volvox carteri* (Chlorophyta). *J. Phycol.* **22**:370-381.
- Cole, D.G. 2003. The intraflagellar transport machinery of *Chlamydomonas reinhardtii*. *Traffic* **4**:435-42.
- Deane, J.A, Cole, D.G., Seeley, E.S., Diener, D.R., and Rosenbaum, J.L. 2001. Localization of intraflagellar transport protein IFT52 identifies basal body transitional fibers as the docking site for IFT particles. *Curr. Biol.* **11**:1586-90.
- Dentler, W. 2005. Intraflagellar transport (IFT) during assembly and disassembly of *Chlamydomonas* flagella. *J. Cell Biol.* **170**:649-59.
- Dentler, W.L. and Rosenbaum, J.L. 1977. Flagellar elongation and shortening in *Chlamydomonas*. III. Structures attached to the tips of flagellar microtubules and their relationship to the directionality of flagellar microtubule assembly. *J. Cell Biol.* **74**:747-59.
- Dogterom, M. and Leibler, S. 1993. Physical aspects of the growth and regulation of microtubule structures. *Phys. Rev. Lett.* **70**:1347-1350.
- Dutcher, S.K. 1995. Flagellar assembly in two hundred and fifty easy-to-follow steps. *Trends Genet.* **11**:398-404.
- Elowitz, M.B., Levine, A.J., Siggia, E.D., and Swain, P.S. 2002. Stochastic gene expression in a single cell. *Science* **297**:1183-6.
- Ewaschuk, R., and Turney, P.D. 2006. Self-replication and self-assembly for manufacturing. *Artif. Life* **12**:411-33.
- Fowler, V.M., McKeown, C.R., and Fischer, R.S. 2006. Nebulin: does it measure up as a ruler? *Curr. Biol.* **16**:R18-20.
- Fung, J.C., Liu, W., de Ruijter, W.J., Chen, H., Abbey, C.K., Sedat, J.W, and Agard, D.A. 1996. Toward fully automated high-resolution electron tomography. *J. Struct. Biol.* **116**:181-9.

- Graveland-Bikker, J.F., Schaap, I.A., Schmidt, C.F., and de Kruif, C.G. 2006. Structural and mechanical study of a self-assembling protein nanotube. *Nano. Lett.* **6**:616-21.
- Grimes, G.W., and Gavin, R.H. 1987. Ciliary protein conservation during development in the ciliated protozoan, *Oxytricha*. *J. Cell Biol.* **105**:2855-9.
- Handel, M., Schulz, S., Stanarius, A, Schreff, M., Erdtmann-Vourliotis, M., Schmidt, H., Wolf, G., and Holtt, V. 1999. Selective targeting of somatostatin receptor 3 to neuronal cilia. *Neuroscience* **89**:909-26.
- Haycraft, C.J., Swoboda, P., Taulman, P.D., Thomas, J.H., and Yoder, B.K. 2001. the *C. elegans* homolog of the murine cystic kidney disease gene Tg737 functions in a ciliogenic pathway and is disrupted in *osm-5* mutant worms. *Development* **128**:1493-505.
- Howard, J. 2001. "Mechanics of Motor Proteins and the Cytoskeleton." Sinauer Associates, Sunderland MA,
- Iomini C., Babaev-Khainov, V., Sassaroli, M., and Piperno, G. 2001. Protein particles in *Chlamydomonas* flagella undergo a transport cycle consisting of four phases. *J. Cell Biol.* **153**:13-24.
- Jarvik, J., Lefebvre, P.A., and Rosenbaum, J.L. 1976. A cold-sensitive mutant of *Chlamydomonas* with aberrant control of flagellar length. *J. Cell Biol.* **70**:149a.
- Jarvik, J., Reinhart, F., and Adler, S. 1980. Length control in the *Chlamydomonas* flagellum. *J. Cell Biol.* **87**:38a.
- Jarvik, J.W., Reinhart, F.D., Kuchka, M.R., and Adler, S.A. 1984. Altered flagellar size-control in *shf-1* short-flagella mutants of *Chlamydomonas reinhardtii*. *J. Protozool.* **31**:199-204.
- Johnson, K.A., and Rosenbaum, J.L. 1992. Polarity of flagellar assembly in *Chlamydomonas*. *J. Cell Biol.* **119**:1605-11.
- Katsura, I. 1990. Mechanism of length determination in bacteriophage lambda tails. *Adv. Biophys.* **26**:1-8.
- Keener, J.P. 2006. How *Salmonella typhimurium* measures the length of flagellar filaments. *Bull. Math. Biol.* **26**:in press.
- Kellenberger, E. 1972. Polymerization in Biological Systems. *Ciba Found. Symp.* **7**:295-299.
- Kuchka, M.R., and Jarvik, J.W. 1982. Analysis of flagellar size control using a

- mutant of *Chlamydomonas reinhardtii* with a variable number of flagella. *J Cell Biol.* **92**:170-5.
- Kuchka, M.R., and Jarvik, J.W. 1987. Short-flagella mutants of *Chlamydomonas*. *Genetics* **115**:685-691.
- Lehtreck, K.F, Reize, I.B., and Melkonian, M. 1997. The cytoskeleton of the naked green flagellate *Spermatozopsis similis* (chlorophyta): flagellar and basal body developmental cycle. *J. Phycol.* **33**:254-265.
- Lefebvre, P.A., Nordstrom, S.A, Moulder, J.E., and Rosenbaum, J.L. (1978). Flagellar elongation and shortening in *Chlamydomonas*. IV. Effects of flagellar detachment, regeneration, and resorption on the induction of flagellar protein synthesis. *J. Cell Biol.* **78**:8-27.
- Lefebvre, P.A., Silflow, C.D., Widen, E.D., and Rosenbaum, J.L. 1980. Increased levels of messenger RNA species for tubulin and other flagellar proteins after amputations or shortening of *Chlamydomonas* flagella. *Cell* **20**:469-578.
- Lefebvre, P.A, Barsel, S.E, and Wexler, D.E. 1988. Isolation and characterization of *Chlamydomonas reinhardtii* mutants with defects in the induction of flagellar protein synthesis after deflagellation. *J. Protozool.* **35**:559-564.
- Littlefield, R., and Fowler, V.M. 2002. Measurement of thin filament lengths by distributed deconvolution analysis of fluorescence images. *Biophys. J.* **82**:2548-64.
- Madey, P., and Melkonian, M. 1990. Flagellar development during the cell cycle in *Chlamydomonas reinhardtii*. *Botanica Acta* **103**:97-102.
- Marshall, W.F., and Rosenbaum, J.L. 2001. Intraflagellar transport balances continuous turnover of outer doublet microtubules: implications for flagellar length control. *J. Cell Biol.* **155**:405-414.
- Marshall, W. 2002. Size control in dynamic organelles. *Trends Cell Biol.* **12**:414-9.
- Marshall, W.F. 2004. Cellular length control systems. *Annu. Rev. Cell Dev. Biol.* **20**:677-93.
- Marshall, W.F. and Nonaka, S. 2006. Cilia: tuning in to the Cell's Antenna. *Curr. Biol.* **16**:R604-14.

- Marshall, W.F., Qin, H., Rodrigo Brenni, M., and Rosenbaum, J.L. 2005. Flagellar length control system: testing a simple model based on intraflagellar transport and turnover. *Mol. Biol. Cell* **16**:270-278.
- Masyuk, T.V., Huang, B.Q., Ward, C.J., Masyuk, A.I., Yuan, D., Splinter, P.L., Punyashthiti, R., Ritman, E.L., Torres, V.E., Harris, P.C., and LaRusso, N.F. (2003). Defects in cholangiocyte fibrocystin expression and ciliary structure in the PCK rat. *Gastroenterology* **125**:1303-10.
- McVittie, A.C. 1972. Flagellum mutants of *Chlamydomonas reinhardtii*. *J. Gen. Microbiol.* **71**:525-540.
- Morris, E.C. 2002. How did cells get their size? *Anat. Rec.* **268**:239-251.
- Norrander, J.M., Linck, R.W., and Stephens, R.E. 1995. Transcriptional control of tektin A mRNA correlates with cilia development and length determination during sea urchin embryogenesis. *Development* **121**:1615-23.
- Nossal, R., and Lecar, H. (1991). "Molecular & Cell Biophysics." Addison-Wesley, Redwood City CA.
- Nguyen, R.L., Tam, L.W., and Lefebvre, P.A. 2005. The LF1 gene of *Chlamydomonas reinhardtii* encodes a novel protein required for flagellar length control. *Genetics* **169**:1415-1424.
- Ortug, C. 2003. Scanning electron microscopic findings in respiratory nasal mucosa following cigarette smoke exposure in rats. *Ann. Anat.* **185**:207-10.
- Otto, E.A., Schermer, B., Obara, T., O'Toole, J.F., Hiller, K.S, Mueller, A.M., Ruf, R.G., Hoefele, J., Beekmann, F., Landau, D., Foreman, J.W., Goodship, J.A., Strachan, T., Kispert, A, Wolf, M.T., Gagnadoux, M.F., Nivet, H., Antignac, C., Walz, G., Drummond, I.A., Benzing, T., and Hildebrandt, F. 2003. Mutations in INVS encoding inversin cause nephronophthisis type 2, linking renal cystic disease to the function of primary cilia and left-right axis determination. *Nat. Genet.* **34**:355-6.
- Pan, J., and Snell, W.J. 2005. *Chlamydomonas* shortens its flagella by activating axonemal disassembly, stimulating IFT particle trafficking, and blocking anterograde cargo loading. *Dev. Cell* **9**:431-8.
- Parker, J.D., and Quarmby, L.M. 2003. *Chlamydomonas* fla mutants reveal a link between deflagellation and intraflagellar transport. *BMC Cell Biol.* **4**:11.
- Pazour, G.J., Dickert, B.L., Vucica, Y., Seeley, E.S., Rosenbaum, J.L., Witman, G.B., and Cole, D.G., 2000. *Chlamydomonas* IFT88 and its mouse homologue,

polycystic kidney disease gene Tg737, are required for assembly of cilia and flagella. *J. Cell Biol.* **151**:709-18.

Pazour, G.J., and Rosenbaum, J.L. 2002. Intraflagellar transport and cilia-dependent diseases. *Trends Cell Biol.* **12**:551-5.

Pedersen, L.B., Geimer, S., Sloboda, R.D., and Rosenbaum, J.L. 2003. The microtubule plus end tracking protein EB1 is localized to the flagellar tip and basal bodies in *Chlamydomonas reinhardtii*. *Curr. Biol.* **13**:1969-74.

Pedersen, L.B., Geimer, S., and Rosenbaum, J.L. 2006. Dissecting the molecular mechanisms of intraflagellar transport in *Chlamydomonas*. *Curr. Biol.* **16**:450-9.

Pena, J. 2005. Correlation of flagellar length and flagellar gene expression in *Chlamydomonas reinhardtii*. (Undergraduate Honors Major Thesis) *Florida State University D-Scholarship Repository Article #95*.

Piperno, G., Mead, K., and Henderson, S. 1996. Inner dynein arms but not outer dynein arms require the activity of kinesin homologue protein KHP1 (FLA10) to reach the distal part of flagella in *Chlamydomonas*. *J. Cell Biol.* **133**:371-9.

Qin, H., Diener, D.R., Geimer, S., Cole, D.G., and Rosenbaum, J.L. 2004. Intraflagellar transport (IFT) cargo: IFT transports flagellar precursors to the tip and turnover products to the cell body. *J. Cell Biol.* **164**:255-66.

Qin, H., Burnette, D.T., Bae, Y.K., Forscher, P., Barr, M.M., and Rosenbaum, J.L. 2005. Intraflagellar transport is required for the vectorial movement of TRPV channels in the ciliary membrane. *Curr. Biol.* **15**:1695-9.

Rosenbaum, J.L., and Child, F.M. 1967. Flagellar regeneration in protozoan flagellates. *J. Cell Biol.* **34**:345-64.

Rosenbaum, J.L., Moulder, J.E., and Ringo, D.L. 1969. Flagellar elongation and shortening in *Chlamydomonas*. The use of cycloheximide and colchicine to study the synthesis and assembly of flagellar proteins. *J. Cell Biol.* **41**:600-19.

Rosenbaum J. 2003. Organelle size regulation: length matters. *Curr Biol.* **13**:R506-7.

Scholey, J.M. 2003. Intraflagellar transport. *Annu. Rev. Cell Dev. Biol.* **19**:423-43.

Schoppmeier, J., and Lehtreck, K.F. 2003. Flagellar regeneration in *Spermatopsis similis* (*Chlorophyta*). *J. Phycol.* **3**:918-922.

- Silflow, C.D., and Lefebvre, P.A. 2001. Assembly and motility of eukaryotic cilia and flagella. Lessons from *Chlamydomonas reinhardtii*. *Plant Physiol.* **127**:1500-7.
- Sloboda, R.D. 2002. A healthy understanding of intraflagellar transport. *Cell Motil. Cytoskel.* **52**:1-8.
- Song, L., and Dentler, W.L. 2001. Flagellar protein dynamics in *Chlamydomonas*. *J. Biol. Chem.* **276**:29754-63.
- Stephens, R.E. 1989. Quantal tektin synthesis and ciliary length in sea-urchin embryos. *J Cell Sci.* **92**:403-13.
- Stephens, R.E. 1999. Turnover of tubulin in ciliary outer doublet microtubules. *Cell Struct. Funct.* **24**:413-8.
- Stephens, R.E. 2000. Preferential incorporation of tubulin into the junctional region of ciliary outer doublet microtubules: a model for treadmilling by lattice dislocation. *Cell Motil. Cytoskel.* **47**:130-40.
- Stolc, V., Samanta, M.P., Tongprasit, W., and Marshall, W.F. 2005. Genome-wide transcriptional analysis of flagellar regeneration in *Chlamydomonas reinhardtii* identifies orthologs of ciliary disease genes. *Proc. Natl. Acad. Sci. U.S.A.* **102**:3703-7.
- Tam, L.W., Dentler, W.L., and Lefebvre, P.A. 2003. Defective flagellar assembly and length regulation in LF3 null mutants in *Chlamydomonas*. *J. Cell Biol.* **163**:597-607.
- Tamm, S.L. 1967. Flagellar development in the protozoan *Paranema trichophorum*. *J. Exp. Zool.* **164**:163-186.
- Tilney, L.G, and Gibbins, J.R. 1968. Differential effects of antimitotic agents on the stability and behavior of cytoplasmic and ciliary microtubules. *Protoplasma* **65**:167-79.
- Toskala, E., Nuutinen, J., and Rautiainen, M. 1995. Scanning electron microscope findings of human respiratory cilia in chronic sinusitis and in recurrent respiratory infections. *J. Laryngol. Otol.* **109**:5090-14.
- Toyama, Y., Sumiya, H., Fuse, H., and Shimazaki, J. 1996. A case of an infertile man with short-tailed spermatozoa. *Andrologia* **28**:81-7.
- Tuxhorn, J., Daise, T., and Dentler, W.L. 1998. Regulation of flagellar length in *Chlamydomonas*. *Cell Motil. Cytoskel.* **40**:133-46.

- Umen, J.G. 2005. The elusive sizer. *Curr. Opin. Cell Biol.* **17**:435-41.
- Verde, F., Dogterom, M, Stelzer, E., Karsenti, E., and Leibler, S. 1992. Control of microtubule dynamics and length by cyclin A- and cyclin B-dependent kinases in *Xenopus* egg extracts. *J. Cell Biol.* **118**:1097-108.
- Wagenknecht, T., and Bloomfield, V.A. 1975. Equilibrium mechanisms of length regulation in linear protein aggregates. *Biopolymers* **14**:2297-2309.
- Wheatley, D.N, and Bowser, S.S. 2000. Length control of primary cilia: analysis of monociliate and multiciliate PtK1 cells. *Biol. Cell* **92**:573-82.
- Wilson, N.F., and Lefebvre, P.A. 2004. Regulation of flagellar assembly by glycogen synthase kinase 3 in *Chlamydomonas reinhardtii*. *Eukaryot Cell.* **3**:1307-19.
- Wilson, N.F, and Lefebvre, P.A. 2005. LF4p, a regulator of flagellar length in *Chlamydomonas*, is a cargo for transport by IFT. *American Society for Cell Biology annual meeting* Abstract #1019.

Chapter 3

Quantitative Analysis of Intraflagellar Transport in *Chlamydomonas* Long-flagella Mutants

Quantitative Analysis of Intraflagellar Transport in *Chlamydomonas* Long-flagella Mutants

Kimberly Wemmer, William Ludington, and Wallace F. Marshall

Department of Biochemistry & Biophysics

University of California San Francisco

San Francisco, CA 94158

email for correspondence: wallace.marshall@ucsf.edu

Introduction

A long-standing but unanswered question in cell biology is: what mechanisms determine the size of organelles? For most organelles, size is inherently difficult to measure because the organelles have complicated three dimensional structures located deep within the cell where imaging can be difficult. Flagella, in contrast, are easy to visualize even when using simple forms of microscopy, and as the only size parameter of a flagellum that can vary is length, the problem of organelle size control is reduced to analyzing a single dimension.

These structures, called both cilia and flagella (two terms I will use interchangeably as they both describe the same structure), are highly conserved from vertebrates to algae and protists. They serve many different functions, from generating fluid flow and propulsion to serving as a antenna for the cell and playing integral roles in signaling pathways.

Flagella are microtubule based structures consisting of nine doublet microtubules that are nucleated by modified centrioles known as basal bodies. The microtubule doublets extend from the cell, and are surrounded by an extension of the plasma membrane. These doublets are all oriented with the microtubule plus-ends located at the distal tip of the flagellum, and the minus-ends located at the basal body located at the cell surface (Figure 1). Consequently, all the turnover within flagella - the addition and removal of subunits making up the flagellar structure - must occur out at the distal tip, and away from the cell body. The maintenance of the flagellar structure depends on

a process called intraflagellar transport, or IFT. IFT is a motile process in which heterotrimeric kinesin-2 moves a complex of proteins known as the IFT particle from the base of the flagellum, where subunits have accumulated at the basal body, out to the distal tip, where a cytoplasmic dynein returns the particles to the cell body (Cole, 2003; Scholey, 2003; Sloboda, 2002). An IFT particle is a complex of at least 16 polypeptides known as IFT proteins (though current research is adding to that number), which are thought to bind cargo, made up of the structural components of flagella, and escort it out to the tip as part of the complex (Qin, 2004; Qin et al., 2005), and cargo is thought to be unable to move into the flagellar compartment without these interactions. IFT particles associate into linear arrays called trains. Due to the constant turnover of subunits that occurs out at the distal tip, IFT is not only required for assembly of flagella, but also their maintenance, such that when IFT is switched off entirely flagella immediately begin to shorten and resorb (Kozminski et al., 1995). When IFT function is down-regulated, rather than terminated, flagella attain intermediate lengths (Marshall and Rosenbaum, 2001). Such results indicate that IFT plays a key role in flagellar length control, and suggest that regulation of IFT may be important for the regulation of length.

Importantly, alterations in length of primary cilia can effect vertebrate development as well as human health and disease, making exploring the mechanisms of ciliary length control a worthwhile project in and of itself. In development, reduction of Notch signaling in the Kupffer's vesicle of zebrafish leads to a decrease in ciliary length, resulting in defects of left-right patterning in

the embryo (Lopes et al., 2010). Intriguingly, this phenotype is rescued by over expression of Foxj1, a transcription factor implicated in regulating many ciliary genes (Thomas et al., 2010), indicating that transcriptional up-regulation of ciliary components may be able to abrogate length defects caused by mutations.

Additionally, there are many examples of ciliary length defects creating pathologies *in vivo*. For example, excessively long cilia in photoreceptors are associated with progressive retinal degeneration in mice (Omori et al., 2010). A rat model of Meckel-Gruber syndrome exhibits tissue-specific length defects; cilia of the kidney collecting ducts are abnormally long, while sperm flagella are excessively short (Tammachote et al., 2009). Animal models for tuberous sclerosis complex (TSC) show increases in ciliary length, which appears to play a role in development of kidney cysts in this disease (DiBella et al., 2009).

Moreover, modulation of length can affect flagellar function, and therefore is likely subject to regulation, giving cells the ability to adjust their cilia to changing conditions. For example, the swimming speed of spermatozoa in a viscous fluid depends linearly on flagellar length (Dresdner and Katz, 1981), and variations in tail length may contribute to sperm selection and rates of fertilization (Holt et al., 2010). This modulation can also have negative consequences, as when the cilia of the respiratory tract are subject to cigarette smoke, causing ciliary shortening and thereby impairing the transport of mucus out of the airway (Leopold et al., 2009; Matsui et al., 1998; Smith et al., 2008).

As indicated above, flagella are highly dynamic organelles, rather than the very stable, static structures that they were once thought to be. In

Chlamydomonas, flagella can be severed easily using a variety of methods, including shocking the cells at low pH or treating them with dibucaine, then re-grown in very high synchrony by returning the culture to neutral pH. This re-growth of flagella induces a large transcriptional increase of flagellar genes to provide the cell sufficient subunits with which to construct the new structures. Additionally, the flagella are resorbed very quickly before cell division, releasing the basal bodies from their location at the cell membrane to allow them to function during cell division. The removal of a single flagellum induces what is termed the 'long-zero' response, a very interesting reaction in which the remaining, or 'long', flagellum resorbs while the severed flagellum, at 'zero' length, re-grows from its original base. The two flagella eventually achieve the same length, then both re-grow together to full length (Rosenbaum et al., 1969). This response demonstrates that there is an intimate connection between the two different flagella on a single cell and that perturbation of a single flagellum affects the entire length regulatory system, indicating that the two different flagella do not exist in isolation from one another. If the two flagella were entirely independent from one another, the prediction is that the remaining flagellum would not change upon removal of the other. Shortening indicates that resources, such as IFT proteins and flagellar components, have been diverted to the other flagellum, and that it has somehow become a better competitor for those resources. Recent evidence (Ludington et al., in preparation) suggests that this competitive advantage is conveyed at the level of recruitment of IFT to individual flagella.

Prior studies thus suggest that regulation of IFT quantity is a key component of the dynamic length control system, but the pathways that regulate IFT are not known. Previous studies (Engel et al., 2009; Marshall et al., 2005) have indicated that the total amount of IFT found within individual wild type flagella is roughly equal, regardless of length. This means that IFT proteins are at much higher concentration within a very short flagellum, as compared to a fully grown one. What mechanism could account for the maintenance of this length-independent content of IFT proteins within each flagellum? If we assume that regulation of IFT is critical for regulation of length, we can then predict that among the set of strains carrying mutations which alter length, some may do so by altering the quantity of IFT within flagella. Currently there are four genes known in *Chlamydomonas* which, when mutated, cause flagella to become abnormally long [*lf1*, *lf2*, *lf3*, *lf4* (Asleson and Lefebvre, 1998; Barsel et al., 1988; McVittie, 1972)] as well as three genes which, when mutated, cause flagella to become abnormally short [*shf1*, *shf2*, *shf3* (Kuchka and Jarvik, 1982; Kuchka and Jarvik, 1987)]. However, in no case is the mechanistic function of these genes understood. LF2 and LF4 encode kinases, but none of their substrates are yet known, nor is it known what upstream regulatory inputs control the activity of these kinases. If it could be shown that one or more of the *lf* genes acted by increasing the content of IFT proteins per flagellum, it would not only confirm the role for IFT in length determination, it would also provide the first mechanistic insight into how the *lf* genes function.

Interestingly, the long flagella or *If* phenotype does not result in uniformly long flagella in all cells in a strain. Instead, a much wider distribution of flagellar lengths is observed, with populations of cells that have flagella longer, shorter, and the same length as wild type cells. The *If* phenotype is frequently coupled with a reduction in coordination of length between the two flagella on a single cell, meaning individual *If* cells are more likely than wild type to have two flagella not of equal length. Additionally, null mutations of *If2* and *If3* result in an unequal length flagella, or *ulf*, phenotype, where all the cells with flagella have very unequal lengths. [*If1*, *If2*, and *If3* strains all carry hypomorphic alleles of these genes, *If4* is a null allele. No null allele of *If1* has yet been identified. (Berman et al., 2003; Nguyen et al., 2005; Tam et al., 2003)]. Double mutants of any combination of *If1*, *If2* and *If3* result in strains with an *ulf* phenotype, meaning very few cells have flagella and those that carry flagella have two of very unequal lengths. This is one line of evidence that suggests that *If1*, *If2* and *If3* act in a complex (Tam et al., 2003) which is thought to function in the cell body of *Chlamydomonas*, rather than the flagella. Co-sedimentation and yeast two hybrid provide further support that *If1*, *If2*, and *If3* act in a complex referred to as either the Lengthosome or Length Regulatory Complex (LRC) (Tam et al., 2007).

Here we quantify IFT in the flagella of *If1*, *If2*, *If3*, and *If4* mutants having long flagella, using live-cell TIRF (total internal reflection fluorescence) microscopy of living cells expressing GFP tagged IFT kinesin KAP subunit (KAP-GFP) (Mueller et al., 2005). We also measure the accumulation of KAP-GFP at the basal body (BB) of these same mutants. Finally, we observe for the first time

the long-zero response of individual *If* cells, allowing us to closely examine the flagellar dynamics in these mutant strains. We find that *If1* and *If4* both have high injection rates at their steady state lengths relative to wild type cells, with an IFT injection profile that resembles that of a wild type cell with short, growing flagella, rather than a cell with fully grown flagella. In *If4* this may be due to an increased level of recruitment of IFT to the basal body at longer flagellar lengths, again relative to wild type. We also find, in agreement with published data, that while they may have similar increased IFT rates, *If1* and *If4* have very different dynamics of flagellar re-growth.

Materials and methods

Strains and culture conditions

Strains used here and their sources are listed in Table 1. All strains were maintained on TAP plates. In this work strains were typically grown in liquid M1 media at 21C in constant light in 18mm culture tubes placed in a roller drum for 1 to 3 days. For the long zero experiments, cultures were grown in 15mL conical tubes in M1 media at room temperature (RT) with agitation under room lights which were switched off at night.

Strain construction

Table 2 contains the strains created during this work. Strains were constructed by crossing parental strains with the desired traits and isolating progeny with the sought genotype using tetrad dissection as described in (Harris, 1989). Strains

were mated in one of two ways. The standard protocol used was used with all strains except crosses involving *If1*, which required a more rigorous protocol.

Standard mating protocol:

A petit pois (or 'small pea', i.e. a large loopful) of cells were taken from TAP plates and added to M-N media in small, 13 mm glass culture tubes with plastic caps. The volume of these cultures is flexible, with a larger volume simply requiring more cells. In this case culture volumes were typically 300 or 600 μL . Cultures were left at room temperature under bench lights with minimal agitation for 4 to 8 hours. Equal volumes of cultures, typically 300 μL , of the two parental strains were taken and well mixed in the 13 mm tubes, then left overnight, again at room temperature under bench lights with minimal agitation. The next morning the formation of a pellicle was assayed visually, though while the presence of a pellicle did indicate a successful mating, lack of a pellicle did not always correlate with a poor mating, and the protocol was continued despite its absence. Cultures were well mixed, then 300 μL of culture per plate were spread onto the center of a 4% agar TAP plate, either using shaking of the plate to spread the culture or the elbow of a glass spreader, leaving the edges of the plate without cells. Plates were put in a clear box right side up, and left under lights at room temperature overnight. In the morning, any plates that were still wet were dried by a flame, then the plates were wrapped in foil and left in a humid box for at least 1 week (strains may remain in this state for weeks, and the protocol continued at a later date). Finally, the plates were unwrapped and zygote isolation and tetrad dissection was performed.

Chemically induced mating protocol:

A petit pois (or 'small pea', i.e. a large loopful) of cells were taken from TAP plates and added to M-N/5 media in small, 13 mm glass culture tubes with plastic caps, mixed, then incubated at room temperature under bench lights without shaking for 3 hours. Dibutyryl cyclic AMP (dbcAMP) and IMBX are added to a final concentration of 300mM and 1mM, respectively. The dbcAMP is freshly prepared in Pipes buffer, pH 7.2, and filter sterilized. Cells are incubated 1 hour further, under the same conditions. The two cultures are then mixed and left again under the same conditions for 1.5 hours. Half of the culture is removed and spread onto the center of a 4% agar TAP plate as described above. The other half is incubated as before overnight, and the formation of a pellicle was assayed visually the next morning. The remaining culture is then plated as before. From this point on, the standard mating protocol was followed.

Verification of strains

Strains were verified by PCR analysis or visual verification of the sought phenotype. Primer used are listed in Table 3. The *fla3^{ts}*, *KAPGFP*, *If2-5*, and *If3-2* alleles were identified using restriction enzyme digest as indicated in Table 3. Strains carrying *If1*, *If2-5*, and *fla10^{ts}* were all assayed for the phenotype visually, then *If1* and *If2-5* were confirmed by sequencing the PCR generated from the primers indicated. For *fla10^{ts}* verification, strains were grown in 5mL liquid culture for 2 days in constant light at 21C in 18mm culture tubes in a roller drum. The cultures were then split, and half was transferred to 34C. The next day, all

cultures were assayed visually. Lines carrying the *fla10^{ts}* allele lacked flagella. Knockout of the *lf4* alleles was tested by PCR, with the absence of the band indicating that the strain lacked this gene. The phenotype was then confirmed visually. PCR to determine mating type was done with the primers indicated in Table 3 as described in (Zamora et al., 2004).

TIRF analysis of IFT

TIRF analysis is described fully in (Ludington et al., in preparation).

Live cell Imaging

Live cell imaging was performed on a Nikon te2000 microscope with a 100x 1.49 NA TIRF oil lens and 491 nm laser illumination through an optical fiber with a near-TIRF illumination field. Emitted light from the sample was reflected to the camera using a 514 nm dichroic mirror and a 525 nm filter. Images were recorded at 29.7 frames per second on a Photometrics QuantEM EMCCD camera with 0.156 microns per pixel. In a set of experiments to control for effects of the illumination field, an identical microscope setup with a Yokogawa C-22 spinning disk was used. A 514nm dichroic mirror was used to separate excitation from emission light. TIRF and spinning disk confocal imaging gave similar trends for injection magnitude versus time preceding and time following an injection, although we did not make a statistical comparison because the two illumination fields produce different injection intensities.

The TIRF field was calibrated for each imaging session by adhering 100nm orange fluorescent beads (Phosphorex Inc) to a coverslip and setting the

TIRF angle to give a mean bead intensity of 75% the maximum fluorescence intensity detected (minimum 45 beads per view frame). To accomplish this, we imaged the beads 3 times over a range of laser angles from below TIR (all light reflected) to above TIR where all of the light is transmitted. The mean bead intensity was calculated at each angle using custom MATLAB software. Then, the mean bead intensity versus laser angle was plotted. The curve shows a characteristic increase up to a maximum and subsequent drop off in intensity as the laser angle increases significantly above TIR. We found empirically that by setting the angle to give a mean bead intensity of 75% the maximum, we could exclude the cell bodies from the illumination field while getting clear illumination of the entire flagellum. This technique of near TIR illumination is described at length in (Tokunaga et al., 2008). This method produces roughly constant flagellar background intensity over a range of flagellar lengths.

Cells were allowed to adhere their flagella to the coverglass and then imaged at 29.7 frames per second.

IFT kymograph analysis

Kymographs were made using hand traces of the flagella in Nikon elements (v3.1) to delineate the initial position of the flagellum. Cell movement was removed using custom MATLAB software based on the algorithm of (Wilson and Theriot, 2006) to automatically determine the region of interest for kymograph generation.

Kymographs were converted to IFT injection time series using custom MATLAB software with the algorithm of (Ludington et al., in preparation). Briefly,

the IFT speed was determined from the dominant trace angle in each kymograph. A median projection across the kymograph at this angle was then rescaled to give a time series of IFT injections into the flagellum with intensity per unit time. Injection intensity was then normalized to the local background. This step detrends the time series and serves as a high pass filter. Local flagellar background is roughly constant over the data set. The time series were then smoothed using 2 iterations of a running median filter with a window width of 3 pixels followed by 1 iteration with a running mean filter of window width 3 pixels. These smoothing steps serve as a low pass filter.

Injection times were determined automatically as the local maxima in the time series. The minimum size injection that we scored was determined by comparing time series maxima to kymograph traces by eye to determine what intensity could reliably be scored as an injection. From this comparison we set the threshold peak intensity at 0.015 relative intensity units. Injection peak sizes were then calculated as the area under the peak above 0.68x maximum peak intensity. Injection sizes were then normalized to the minimum peak size and only injections greater than 10x the minimum injection intensity were counted in the analysis. The parameters used were determined using the ratio of true positives and the ratio of false positives as a function of the signal:noise ratio to optimize results produced from synthetic data. The signal:noise ratio was calculated as the square of the ratio of signal amplitude to noise amplitude. Signal amplitude was calculated as the total signal amplitude from the smoothed

time series, and noise amplitude was calculated as the total amplitude in the time series after subtracting the smoothed signal amplitude.

We generated synthetic kymograph data sets using a model convolution approach (Gardner et al., 2010) by re-sampling the injection series from the real data, convolving the synthetic series by the point-spread function of the microscope, and then adding background and noise to the level measured in the background of real flagella. We then built synthetic data sets over a range of signal:noise values representative of the real dataset. Over the range of measured signal:noise, the highest false positive rate was 6% and the lowest true positive rate was 98%, with a maximum total error of 8%. At the mean signal:noise of the data set, the true positive rate was 100% with 6% false positives. The algorithm tends to have a very high true positive hit rate due to the median projection across the kymographs.

Taking the median projection greatly reduces the rate at which noise obscures the true signal. Though this method is simple and robust, it does limit the type of kymographs that can be input: there must be a consistent IFT velocity for all particles over the entire flagellum for the entire course of the time series. Therefore, we manually selected time series where the IFT velocity was consistent over the entire kymograph.

In terms of total injected material detected, the algorithm detects 98.4% of the actual input from synthetic data when realistic noise is overlaid on the synthetic kymographs. However, on an injection-by-injection basis, the accuracy is lower, and this inaccuracy increases for larger magnitude injections. Therefore,

when doing analysis of injection magnitude versus times preceding or following an injection, we implemented an additional filtering algorithm to eliminate kymographs that did not have sufficient quality data to determine whether or not a trend exists. We did this by first calculating the 95% confidence interval around the Pearson correlation coefficient between injection magnitude and time preceding [or following] an injection event for each kymograph. We then eliminated kymographs where the width of the 95% confidence interval was above a set threshold value. We tested the filtering algorithm on both the injection magnitude versus time interval preceding an injection event and on the magnitude versus time interval following an injection event, and we varied the threshold value from 0.5 to 2.0, where 2.0 = no filtering.

Statistics

All statistical tests were performed in MATLAB using the Statistical Analysis Toolbox. Akaike information criterion tests were performed using custom MATLAB software to test whether one line or two lines give a better fit to magnitude versus time interval point scatters. All correlation values given are the standard Pearson product-moment correlation coefficient (r). P-values for correlation are for the test of whether the correlation is non-zero, where $P=1$ gives 100% certainty of a zero correlation.

Analysis of KAPGFP at basal bodies

Fixation of cells

Methanol fixation was modified from (Feldman and Marshall, 2009). Briefly, coverslips were coated in poly-L-lysine. Cells were adhered for 2 minutes, then incubated in 2 times in 100% methanol at -20C for 5 minutes per wash. Subsequent washes for 5 minutes in: 2:1 methanol:1x PBS, 1:2 methanol:1x PBS, and 1x PBS were performed to gradually remove the methanol. A follow up 10 minute wash in 1x PBS was followed by two 30 minute blocking steps, first with cold water fish gelatin-BSA and then with cold water fish gelatin-BSA supplemented with goat serum.

The coverslips were then inverted over a solution of 5% block diluted in 1x PBS overnight in a humid chamber. The next day they were washed six times for 5 minutes in 1x PBS, then fixed to a glass slides with VECTSHIELD mounting media (Vector Labs, H-1000).

Fixed cell imaging

Fixed samples were imaged on a Deltavision microscope with an 100X oil immersion lens (NA 1.40 PlanApo) for a 0.4 second exposure time with a FITC filter. Z-stacks were acquired with a 0.2 micron z-step. Deconvolution was performed using Deltavision software.

KAPGFP intensity quantification

Custom software was written in MATLAB. Manual segmentation was used to identify cells and basal body regions. For each cell, background was subtracted from the z-stack as the mean intensity of the pixels in the 3D bounding box perimeter, and then pixels with intensity greater than one-third the maximum intensity were summed to give injector intensity. The one-third cutoff

was chosen because it consistently produced a good visual overlap with the injector region. Intensity ratios of the two individual flagella on a single cell were compared by one-way ANOVA, then multiple pairwise comparisons were made using Bonferroni's correction for alpha.

Long-zero experiments

These experiments were done in collaboration with the Berns Lab at the University of California, San Diego, using their Robolase IV system, similar to the system described in (Botvinick and Berns, 2005). A femtosecond laser set at a power of 121mW was used to strike individual flagella, inducing flagellar excision of one of the two flagella on a cell, resulting in a cell with one long flagellum while completely lacking any of the second, struck flagellum. The Robolase system is built on a Zeiss Axiovert 200M, with a 40X oil 1.3NA Phase III objective lens we used to visualize the cells. We imaged cells held in place in a microfluidic *Chlamydomonas* trap plate from CellAsic (C04A), which has chambers that catch the cells in pockets and hold them in place, allowing the same cell to be followed over time. Cells were imaged initially to allow determination of their pre-cut flagellar lengths, then one flagellum on a number of cells were sequentially struck with the laser at recorded times. The cells were then imaged over time, allowing us to observe the length changes that occurred after flagellar excision. Lengths were measured by manually tracing the flagella using ImageJ software.

Results

Increased IFT content in the flagella of some If mutants

As discussed above, one might predict that the long-flagella phenotype could arise from an increase in the quantity of IFT particles within the flagellum. To test whether any of the existing *Chlamydomonas* If mutants in fact have increased IFT within their flagella, we constructed strains expressing GFP-tagged KAP (fla3) in each of the four *If* mutant backgrounds, and confirmed that the long flagella phenotype seen in parental strains was still present in the GFP-KAP expressing derivatives (Supplementary Figure 1). We then imaged IFT using TIRF microscopy as previously described (Engel et al., 2009) and generated kymographs for each cell by stacking up images of flagella as a function of time (Figure 1). Within such a kymograph, the processive motion of an IFT train is revealed as a diagonal streak or trace running from the base to the tip of the flagellum.

Intraflagellar transport within a kymograph can be described by three parameters: speed, which is the average rate at which an IFT train moves out to the tip and is calculated by the slope of the traces in the kymographs; frequency, which is the number of times a new IFT train is released from the base of the flagellum; and magnitude, which is the intensity of GFP fluorescence in a trace. We extracted these three quantitative parameters from each kymograph using an automated algorithm previously reported (Ludington et al., in preparation). In this work, the frequency and magnitude parameters combined give the overall rate of IFT injection into the flagellum. These parameters also allow the calculation of

the total amount of IFT within the flagella of a strain, and measurement of the length of the kymograph allows us to correlate the data generated to the length of individual flagella. We would like to note that we feel the speed of IFT trains is unlikely to be a relevant parameter in our studies of flagellar length control. This is because the rate of arrival of IFT trains at the distal tip actually depends on their injection rate into the flagella, and not on the speed of the trains themselves. The IFT trains in flagella are like eggs on a conveyor belt, being transported to their egg crates. If the eggs are placed on the belt at a rate of 1 every 10 seconds, then they will arrive at the boxes at that same rate, 1 egg every 10 seconds. Changing the speed of the conveyor belt will change the spacing of the eggs on the belt, but will not change the rate at which they arrive at their destination.

From these automated measurements of KAP-GFP kymographs, we calculated IFT quantity in each flagellum (see Materials and Methods), and plotted this value for wild type and the four *If* mutants in Figure 3. The results show that *If1*, *If2-1*, and *If4-V13* all showed a significant increase in the quantity of IFT particles as judged by KAP-GFP traces observed in IFT kymographs, though the statistical significance of the increase in *If2-1* is low (Figure 3). There are, however, strong increases in the IFT content in both *If1* and *If4*, providing the first insight into how *If* flagella achieve their increased length.

Injection rate is increased in some If mutants

The fact that *If1*, likely *If2-1*, and *If4-V13* have increased IFT content per flagellum suggests that these genes may encode part of the machinery responsible for regulating IFT injection as a function of length. We note that the quantity of IFT protein in the flagellum at steady state is the product of the rate of IFT protein injection into the flagellum and the time spent by each IFT train in the flagellum. Since the residence time of a train (i.e. the total time a train spends within the flagellum) is proportional to the length of the flagellum, the possibility is raised that perhaps the increase in IFT content is a trivial consequence of the increased length in *If* mutants. This seems unlikely *a priori* as, in wild-type cells, the total IFT content is constant and independent of length.

However to address this question more directly, we calculated the injection rate on a cell by cell basis from the kymographs. The injection rate is plotted versus length for wild type and *If* mutants in Figure 4D. For each strain, we calculate the best fit trend-line, then measured the deviation in these trend lines to the trend line seen in wild-type cells. These deviations from the WT trend line are plotted in Figure 5. These results show that all four *If* mutants show an alteration in the dependence of injection rate on length, though again only *If1* and *If4* have statistically significant increases. This indicates that the rate at which IFT trains are injected into the flagella of *If1* and *If4* cells is higher than would be expected for a wild-type cell if it had flagella at that length, based on the wild-type trend line. Stated another way, *If1* and *If4* cells with flagella at wild type lengths, say 10 μm , have higher injection rates than wild type cells with flagella at the same length. However, it is important to note that the injection rate still varies

with flagellar length in these *lf* mutants; that is, shorter flagella still have higher injection rates than longer flagella, even though the levels of injection are altered relative to wild type.

We therefore conclude that the increase in IFT content in *lf1* and *lf4* is largely due to an increase in injection rate, and that these strains appear to alter the dependence of injection rate on flagellar length, without altering the fact that injection rate still does change with length; therefore, in no case does injection rate become length independent.

Measurement of IFT system parameters in lf mutants

The rate of injection, in turn, is the product of the frequency with which an IFT train enters the flagellum and the quantity of protein in the individual trains being inserted into the flagellum. It is known that IFT trains consist of a linear array of IFT particles, and that the quantity of IFT proteins in a train can vary (Engel et al., 2009), resulting in small or large trains. We note that previous work has shown that IFT train size decreases as a function of flagellar length (Engel et al., 2009). Therefore, for any given injection frequency, injection of larger trains would mean a higher total rate of entry of IFT proteins into the flagellum. Consequently, if a mutation causes either an increase in the injection frequency or an increase in the protein content of the injected trains, it would lead to an increase in IFT quantity, all else being equal, which, as discussed above, could cause extension of flagellar length. Alternatively, an increase in the speed of IFT would lead to a higher rate of delivery out to the distal tip of the flagella, also

resulting in an extension of flagellar length. We therefore measured the speed, injection frequency, and injection magnitude of IFT traces from kymographs for each of the *If* mutants analyzed above, in order to ask which of these parameters may have changed in order to shift the steady state quantity of IFT per flagellum.

In order to interpret these results, we must emphasize the fact that the inherent length dependencies of these parameters must be taken into account. In wild-type cells, IFT protein content is independent of length as judged by both biochemical means (Marshall et al., 2005) and TIRF analysis (Engel et al., 2009). As discussed above, longer flagella should tend to have higher quantities of IFT protein due to the increased residence time of each particle within the flagellum, however this is not the case. This apparent anomaly is resolved by the observation that the magnitude of the injections, that is, the quantity of IFT proteins per train, decreases in long flagella (Engel et al., 2009). This decrease in magnitude is coupled with a small increase frequency, a phenomena discussed later. Conversely, short flagella that are growing out to steady state length have an IFT pattern of lower frequency, higher magnitude IFT trains. This inverse relationship between train size and flagellar length is thus the basis for the maintenance of a constant, length-independent quantity of IFT protein per flagellum. Since *If* mutants have longer flagella, if all parameters followed the same trend as wild-type it would be possible for the injection frequency to decrease on average simply as a byproduct of having extremely long flagella. For this reason, we do not simply compare the average values of the three key parameters (speed, frequency, magnitude), rather, we measure each parameter

as a function of length and ask whether the dependence of each parameter on length has shifted in any of the mutants.

The dependence of frequency and magnitude of IFT trains on flagellar length are plotted in Figures 4A and 4C, respectively. Speed varies only weakly with length in wild-type and the same is true in the mutants (data not shown). In wild-type cells, it was formerly thought that frequency of IFT injection was length-independent (Dentler, 2005; Engel et al., 2009), although more recent studies have found there is a weak, but highly significant, dependence of frequency on length (Ludington et al., in preparation).

When we measured these parameters in *lf* mutant strains, we observed a very interesting result. The pattern of IFT in the two *lf* strains with significantly increased amounts of IFT per flagellum and rates of IFT injection, *lf1* and *lf4*, more closely resembled that of short, growing wild-type flagella rather than the pattern typically found in steady state, fully grown flagella. In other words, the IFT of *lf1* and *lf4* cells is skewed toward higher magnitude, lower frequency IFT injections than would be found in wild-type flagella of equal length. The flagella of these two strains do not appear to adhere to the switch in IFT profile that is typical of wild-type flagella, in which the pattern of lower frequency, higher magnitude IFT trains in short flagella changes to higher frequency, lower magnitude pattern as the flagella approach steady state.

We note, however, that in all *lf* mutants the magnitude and frequency are still length dependent, so these mutations have not eliminated the length response. It may seem surprising that each of these mutations affects two

apparently separate parameters, magnitude and frequency. However, we have recently obtained evidence that there is an intrinsic scaling relation between these two parameters, probably reflecting the physical mechanism of IFT injection (Ludington et al., in preparation). As plotted in Figure 4, the scaling relation between injection and magnitude is not altered in any of the *If* mutants.

Quantification of basal body recruitment of IFT proteins

A pool of IFT proteins are known to be docked at the basal bodies (Deane et al., 2001), and in recent work we have observed a length dependent accumulation of IFT material at the basal body, with short, rapidly growing flagella accumulating more fluorescent KAP-GFP at their basal bodies than do steady state, fully grown flagella (Ludington et al., in preparation). Additionally, within a single cell that is exhibiting a long-zero response, the shorter flagellum has greater accumulation of material at its base than the long, resorbing flagellum. We have proposed that the profile of IFT injection, and the coupling of injection magnitude and frequency, is due to the physical constraints put on the injection system by this accumulation of material at the basal body. Because the *If* mutants appear to increase the overall rate of IFT while maintaining the relationship between the injection frequency and magnitude, we next asked whether the *If* mutations might increase IFT recruitment to the basal bodies.

Such an effect would help explain another question that has long existed in the field: although the LF4 protein is located in both flagella and cytoplasm, it has been found to be in its active form in the cytoplasm, and the remaining LF

proteins are found exclusively in the cytoplasm in complexes called Lengthosomes. How might these cytoplasmic proteins affect IFT dynamics within the flagellum? One possibility is that perhaps these proteins modulate IFT docking to the basal bodies, thereby indirectly affecting the rate of IFT injection into flagella.

To answer this question we again turn to the *lf*: KAP-GFP strains we generated. We performed quantitative fluorescence analysis to measure the quantity of KAP-GFP accumulated at the basal body of cells, and measured the length of the flagella on these cells using DIC microscopy (see Figure 6 for representative examples from each strain). As shown in Figure 7, the intensity of staining at the basal body relative to length is significantly elevated in two *lf* strains, *lf2-1* and *lf4-V13*. This data indicates that these two strains fail to properly down-regulate the recruitment of material to basal bodies as their flagella elongate to their steady state lengths, in contrast to wild type cells.

This information provides further detail into the mechanism behind the long flagella of *lf4* strains. We propose that the elongation of *lf4* flagella is caused by the up-regulation of flagellar IFT content, which, in turn, is due to an increase in the rate of injection of IFT proteins and their cargos. This increase in rate is owing to a lack of down-regulation of recruitment of flagellar materials to the basal body, which is typically seen with long, steady-state flagella, resulting in a pattern of IFT injection that more closely resembles that of short, growing flagella, even when the flagella of *lf4* are at their full length. This chain of consequences leads from increased materials at the basal bodies of *lf4* flagella,

relative to wild-type cells with flagella at the same length, to longer flagella on *If4* cells.

Long-zero response in LF mutants

As described above, when a single flagellum is detached from a *Chlamydomonas* cell it quickly re-grows in less than 1 hour, and while it is re-growing the other flagellum rapidly shortens until the two flagella attain equal length, at which point both flagella grow out together. This long zero response is a hallmark feature of the flagellar length control system and suggests an intimate coordination between the two flagella of a single *Chlamydomonas* cell.

Previous studies have examined the long-zero response in *If1*, *If2*, and *If3* (Barsel et al., 1988), however, this work was, of necessity, performed following the responses of a large population of cells. Because there is extensive diversity of re-growth of flagella from individual *If* cells in some strains, notably in *If1* and *If2-1*, we wanted to know if this diversity was also apparent in long-zero response of these strains (see the Discussion section for a summary of previously generated work). Therefore, we used a laser scalpel to ablate single flagella on cells held in a microfluidic chamber, which allowed us to observe the behaviors of single cells over time.

Interestingly, we recorded different responses from different strains, in contrast to what was previously seen in the population based studies. While we observed reactions typical of wild type in strains *If3-2* and *If4-V13*, we saw very altered behaviors in *If1* and *If2-1* (Figures 8 and 9). *If1* cells did exhibit a

response to the removal of a single flagellum, and resorbed their long flagellum. However, re-growth from the zero length flagella was extremely delayed and appeared highly variable, with very few cells exhibiting any re-growth during our time courses.

In contrast to these behaviors, the limited number of *If2-1* cells we were able to observe appeared to exhibit no response to the removal of a single flagellum at all. The remaining flagellum did not shorten, and some even lengthened over time. This variability in re-growth in response to long-zero perturbations reflects the variability of regeneration of both flagella seen after pH shock in these strains (see Table 4), though it is in stark contrast to previously performed population studies, indicating that further research is needed before we will be able to draw definitive conclusions from these experiments.

Conclusions

These experiments add greatly to our knowledge of the mechanisms behind the lengthening of *If* mutant flagella. This information, combined with the wealth of data that has been generated by others in the field (see Table 4), allows us to expand upon ideas that have been proposed previously.

Existing models for the role of IFT in flagellar length control do predict that mutations increasing IFT would result in a long flagella phenotype. One such model, called the "balance point model", was based on experimental observations that the microtubules of the axoneme undergo continuous turnover even after the full length of the flagellum has been attained, due to the basal rate

of disassembly at the distal tip. This disassembly is balanced by constant assembly, which is fed by the delivery of material to the tip by IFT (Marshall and Rosenbaum, 2001; Song and Dentler, 2001; Stephens, 1999). The steady state length of the flagella must therefore be set by the length at which the rate of assembly and disassembly at the distal end are equal. Because IFT is required for assembly at the tip, it was hypothesized that variation of IFT efficiency as a function of length, such that IFT was more efficient in short flagella and less efficient in long flagella, could account for the flagellar length regulation (Marshall and Rosenbaum, 2001). This model was supported by the fact that microtubule turnover at the tip occurs at a length-independent rate (Marshall and Rosenbaum 2001), and that the quantity of IFT proteins per flagellum is length-independent (Marshall et al., 2005; Engel et al., 2009).

The balance-point model has been able to successfully predict many aspects of flagellar length control - for example, the ability of a cell to equalize the length of its flagella after one is severed, the dependence of flagellar growth rate on length, and the dependence of steady state flagellar length on the number of flagella per cell (Marshall et al., 2005). However, the model depends critically on the ability of the cell to maintain a constant quantity of IFT particles per flagellum, independent of flagellar length. Because the residence time of an IFT particle within the flagellum is proportional to the length of the flagellum, the only way to maintain a length-independent, steady state quantity of IFT particles inside the flagellum is to have injection of the particles be regulated as a function of length. If the injection rate is inversely proportional to the length, then the total

quantity at steady state, which is the product of the residence time and the injection rate, would become constant. Ludington et al. (in preparation) have recently demonstrated that this is in fact the case, observing that injection rate is inversely proportional to flagellar length. But what mechanism could regulate IFT injection as a function of length? This is currently unknown, but clearly it would seem to require some sort of length sensor that can measure flagellar length and adjust IFT injection accordingly.

We note that our data on *lf4* fits nicely with the balance-point model. We propose that the molecular action of the LF4 protein is to inhibit the accumulation of IFT proteins and flagellar components at the basal body, and that it is activated once a certain length is attained to cause a down-regulation of this material at the base of the flagella.

We have observed that when LF4 is absent, there is an excessive accumulation of material at the basal bodies, relative to the length of its flagella. We propose that this over abundance of material results in an increased rate of IFT injection into the cell, as predicted by the avalanche model proposed in Ludington et al. (in preparation). The elevated injection rate then results in long flagella, in accordance with the balance-point model. This is the first model suggesting the molecular mechanism of flagellar lengthening in an *lf* strain.

It has recently been reported that the aurora like kinase CALK shows length-dependent phosphorylation, further supporting the idea that a length sensor might exist in the flagellum (Luo et al., 2011). We note that the existing evidence does not show that CALK is part of the length sensor or feedback

system (CALK RNAi strains do not have altered length) however, its phosphorylation state is altered in response to such a system. Obviously, further studies of CALK function in length control will be extremely interesting.

This information allows us to speculate further on the role of LF4 in regulating IFT injection into the flagellar compartment. We assume there is a basal level of IFT proteins and flagellar materials transported to the centrioles at the base of flagella. We propose that perhaps CALK is able to increase the rate of recruitment of materials to the basal body, while LF4 inhibits it. The level of recruitment of material to the basal bodies impacts the rate of IFT injection into the flagella, which in turn can effect flagellar length, resulting in a length state that is responsive to input from both CALK and LF4 signaling pathways. This model implies that the length of flagella is the result of finely balanced and nuanced signaling from the cell body.

A possible model for the activity of the lengthosome complex has been proposed by Tam et al. (2007; 2003), who suggest that *If1*, *If2*, and *If3* play a role in IFT particle remodeling. We find that there is significant evidence to support this model (see Table 4). Several mutant alleles of these genes, particularly *If1* and *If2-1*, cause slow, asynchronous regeneration of flagella after pH shock, and these same alleles have difficulty re-growing flagella in a long-zero setting. Additionally, while *If1*, *If2*, and *If3* mutant strains are able to genetically complement each other in stable diploids, they cannot complement in quadriflagellated cells, implying that when the wild-type proteins are introduced into a mutant background, they need a significant period of time before they can

correct molecular error that has occurred in the mutant strain. Furthermore, the null alleles of these same genes results in an unequal length of flagella, or *ulf*, phenotype, indicating that entirely removing the function of these proteins results in an even more severe defect in properly loading IFT into flagella. All of these strains, *lf1*, *lf2*, *lf3*, and the *ulfs*, frequently exhibit swelling at the distal tips of their flagella (Tam et al. 2003, Figure 6), implying that material is accumulating there because of insufficient transport to return it back to the cell body. Finally, we have observed a disparity in basal body accumulation and IFT injection in these cells, possibly suggesting that the accumulation of material at the base of flagella and rate of injection into flagella has been de-coupled in these strains. How these strains still maintain their length dependence on rate of injection is unknown.

It must be acknowledged that we do not observe any changes in the parameters of IFT injection into flagella in the *lf3-2* strain. We see at least two possible reasons for this. First, it is formally possible that *lf3-2* mutants increase the size of their flagella using an entirely different mechanism than the other strains, which in no way impacts the IFT content of its flagella. We feel that this is unlikely, given LF3 is thought to act in a complex with LF1 and LF2 proteins, and it is difficult to image a way in LF3 alone could cause such a disparate affect. Alternatively, perhaps the changes to IFT occur only in cells with flagella of significantly increased length, and we did not observe a high enough number of those to effect the statistics of the parameters we observe.

Finally, we were hoping that this study would address the question of length control using an unbiased approach, with the idea that a mutation that eliminated the length sensor, or the feedback pathway that responds to the sensor, would result in cells that are no longer able to maintain constant IFT per flagellum. We imagine that this would, in turn, cause highly variable flagellar lengths. Since high variability in flagellar length is a hallmark of most *lf* mutants, we expected that *lf* mutants might remove the length-dependence of IFT injection. A somewhat surprising result was that of the *lf* strains we examined, all appear to alter, but do not abrogate, the feedback system controlling IFT quantity, meaning that all *lf* mutants analyzed still showed length-dependent injection rates. This was a disappointing result because we had hoped that analysis of *lf* mutants might reveal essential components of the length sensor that presumably regulates IFT quantity.

The failure to observe a loss of length-dependent injection among the *lf* mutants might simply indicate that current screens are not saturating, and if additional *lf* or variable length mutants could be identified, we may find some that lose length dependence of IFT injection. Alternatively, we might be mistaken in our prediction of the phenotype of a feedback-loss mutant. Perhaps without length-dependent feedback control of IFT injection, flagella would be short rather than abnormally long, or such mutants might not assemble flagella at all. In the latter case, the components of the sensor and feedback system are to be sought among the large number of flagella-less "bald" mutants. However, it is not

obvious how to discriminate among the set of flagella-less mutants which specific ones lack flagella because a defect in feedback control of IFT.

Clearly further research is required to understand more about the complicated system responsible for flagellar length regulation.

Figure 1

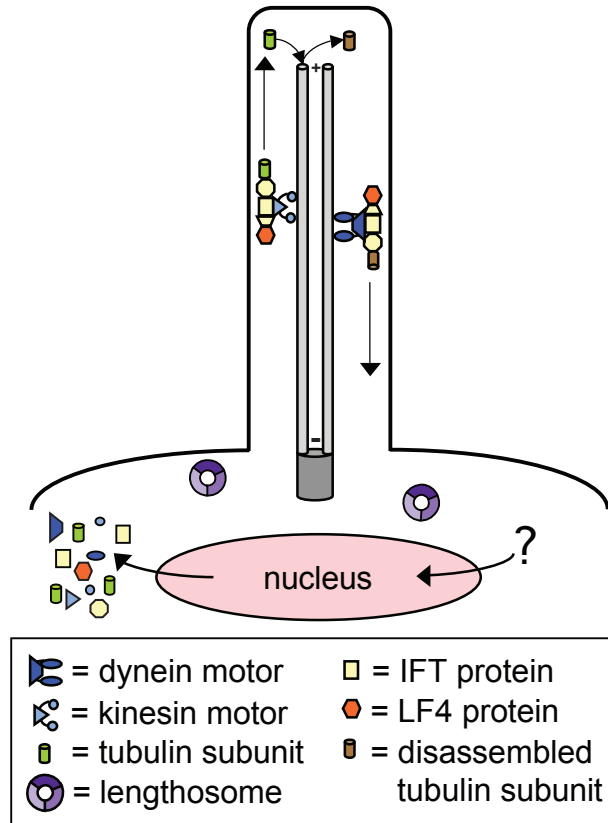


Figure 1. Diagram of flagellum showing components involved in length control.

Intraflagellar transport (IFT) proteins capture flagellar protein precursors from the cytoplasm and transport them to the tip of the flagellum, the site of turnover. This movement is driven by kinesin-II, and the retrograde movement of the IFT complexes back to the cytoplasm is driven by cytoplasmic dynein. IFT also transports the length-regulating kinase LF4, although the function of this protein in the length control system is not yet fully understood. Three other length control proteins, LF1-LF3, localize within the cytoplasm in a structure called the Lengthosome. This complex somehow regulates length, but its mechanism is not known. Genes encoding flagellar proteins are up-regulated when flagellar regeneration is triggered by deflagellation, implying that some sort of signal reaches the nucleus, but the nature of this signal is not known. Thus, while many of the key players are identified, the systems level question of how they act together to produce a well-defined length remains unanswered.

Figure 2

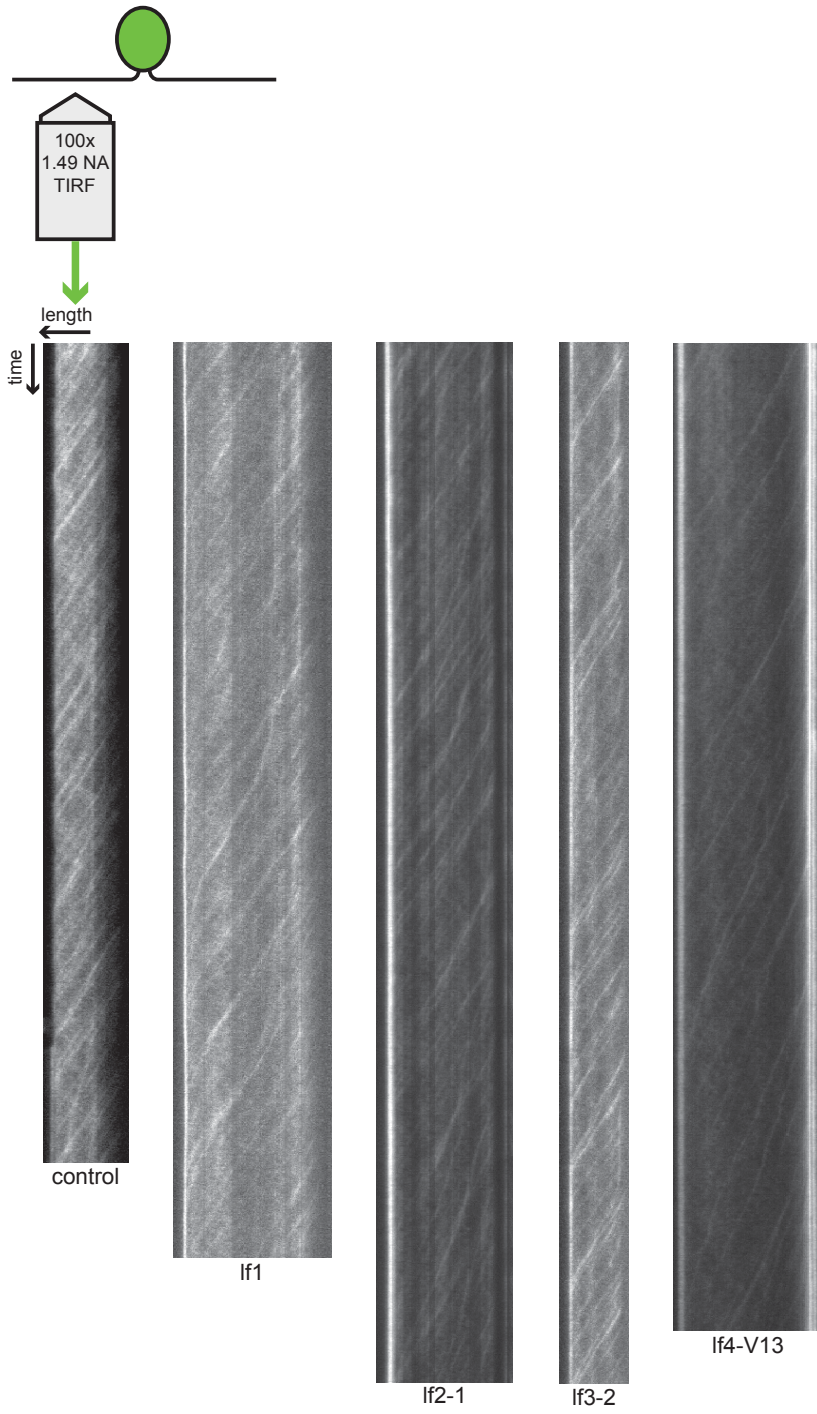


Figure 2. Example kymographs from control and *lf* cells.

These images depict one kymograph representative of each strain. These have been altered to allow visualization of the traces, therefore the intensity of the image does not necessarily reflect that actual measured data. The width of the kymograph is indicative of the length of the flagellum, and the length of the kymographs represents the length of the movie taken.

Figure 3

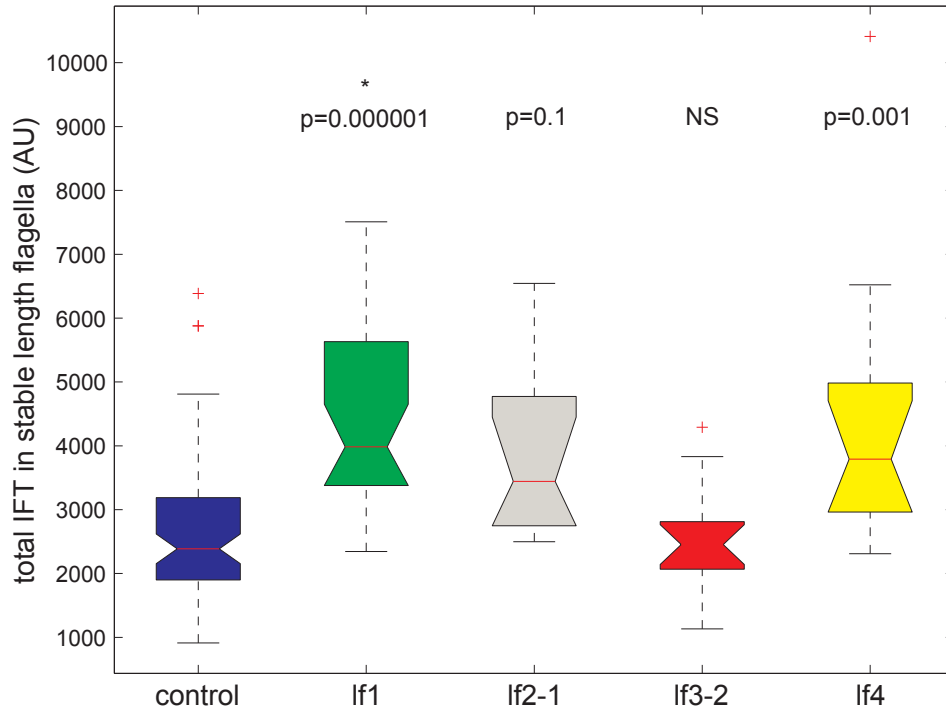


Figure 3. IFT content in flagella is increased in some *If* mutants.

Box and whisker plot of the total IFT content in fully grown flagella shows increases in *If1*, *If2-1*, and *If4*. AU, arbitrary units. Box and whicker plots: top and bottom of each colored box represent the 25th and 75th percentile respectively. The horizontal line within the box is the median. Whiskers extend to the last data point within 1.5 times the interquartile range. Red crosses represent outlier values.

Figure 4

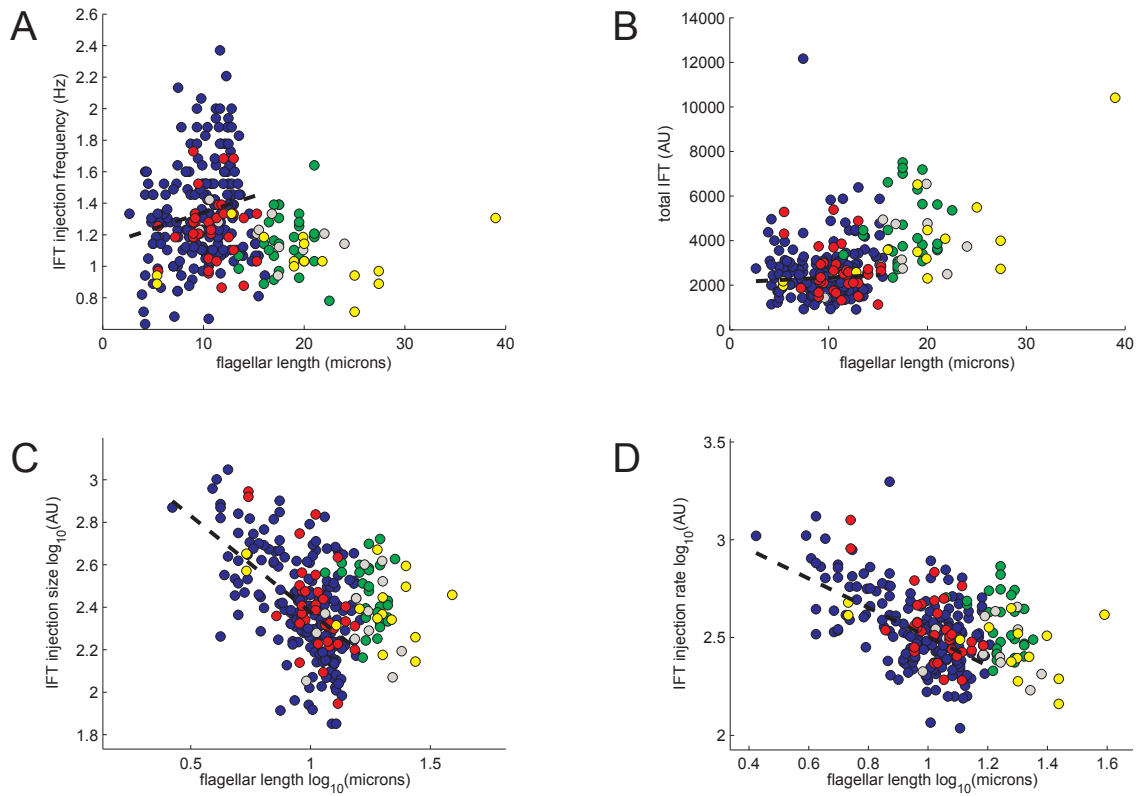


Figure 4. Analysis of IFT Parameters in *If* mutants.

These graphs plot data from control (blue), *If1* (green), *If2-1* (grey), *If3* (red), and *If4* (yellow) cells. The trend line for the control is represented as a black dashed line (trend line for the other strains were omitted for clarity). Hz, hertz. AU, arbitrary units.

Figure 5

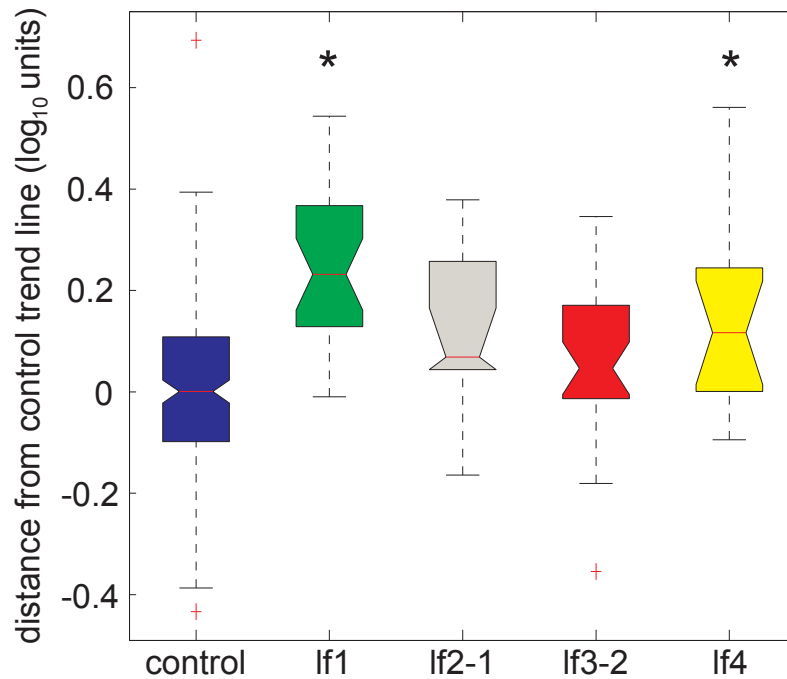


Figure 5. Altered dependence of IFT injection rate on length.

Box and whisker plot showing the distance from the control trend line of IFT injection rates for *lf1*, *lf2-1*, *lf3-2*, and *lf4* cells. *lf1* and *lf4* cells both show significant deviation from the control strain. The Y-axis is in arbitrary units.

Box and whicker plots: top and bottom of each colored box represent the 25th and 75th percentile respectively. The horizontal line within the box is the median.

Whiskers extend to the last data point within 1.5 times the interquartile range.

Red crosses represent outlier values.

Figure 6

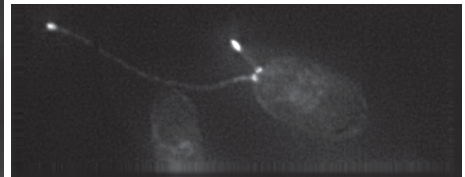
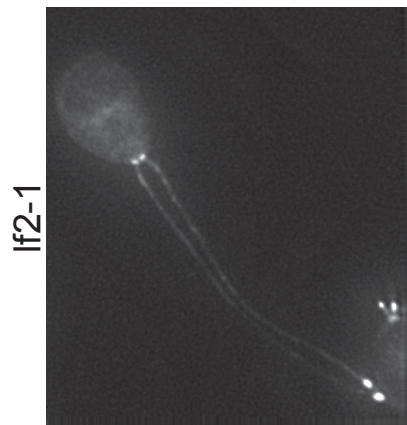
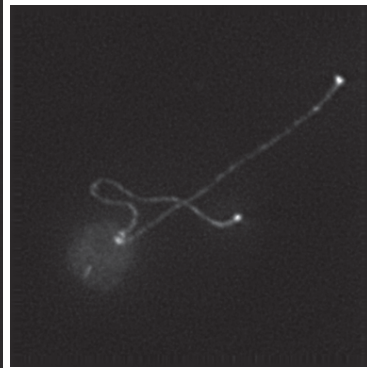
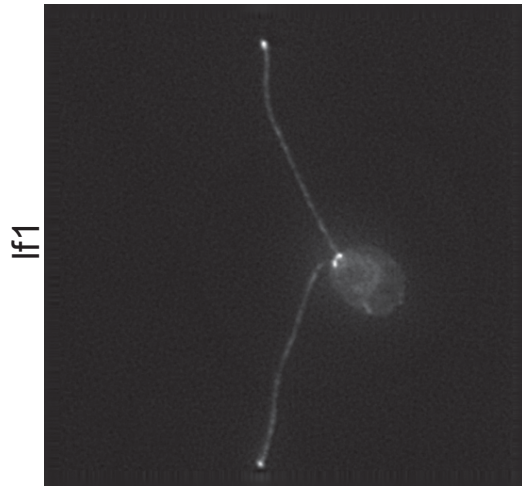
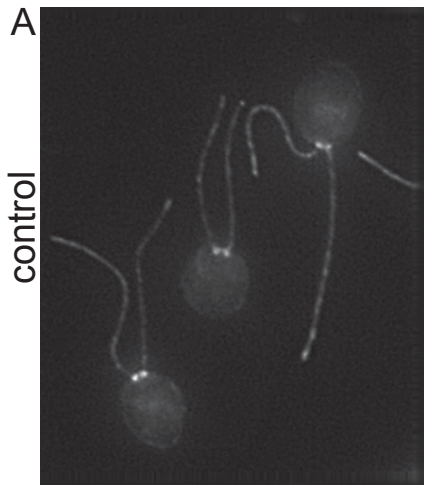


Figure 6 continued

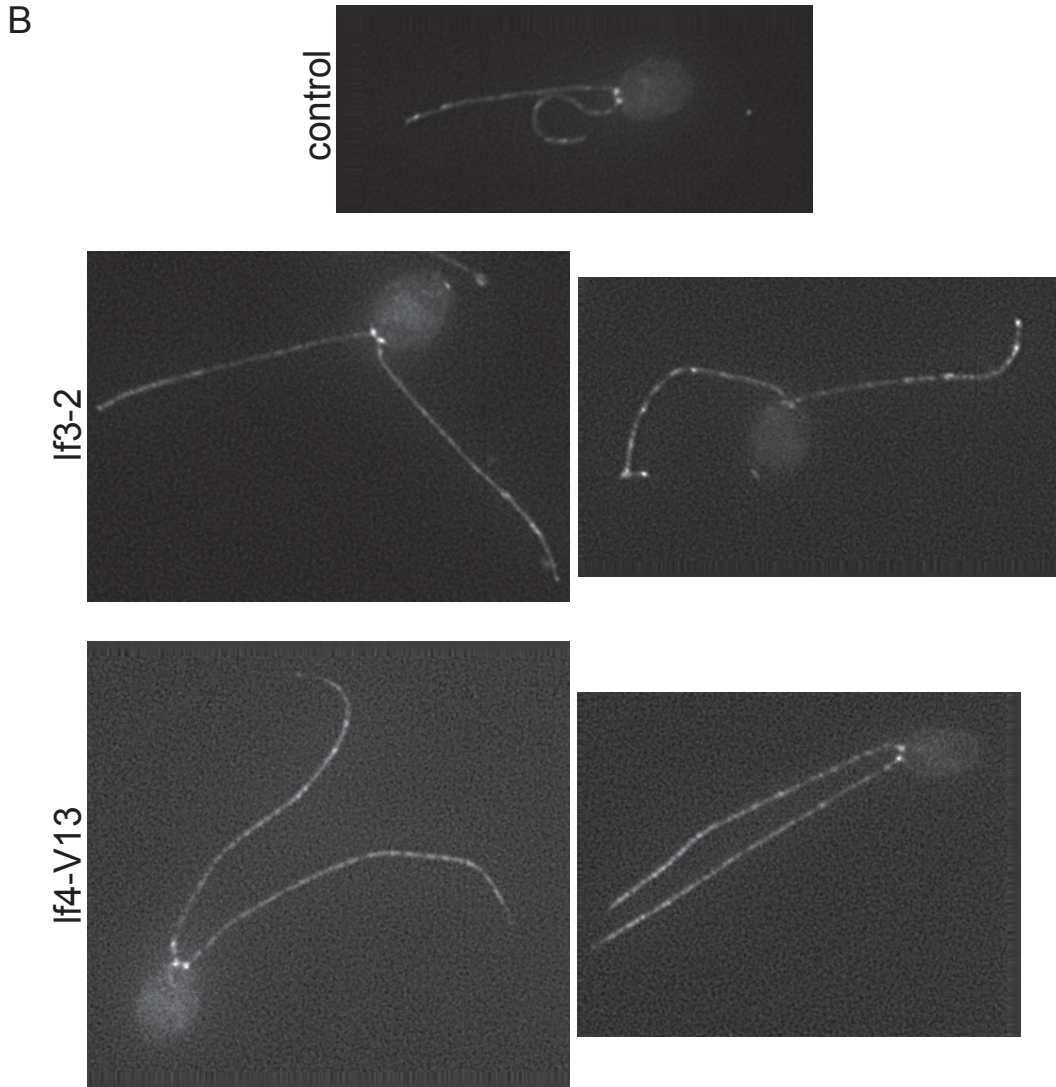


Figure 6. Examples of KAP-GFP fluorescence in *If* strains.

Microscopic images showing the fluorescence of the heterotrimeric kinesin-2 KAP subunit tagged with GFP (KAP-GFP). A significant amount of KAP-GFP localizes to the basal body, and is also found in puncta along the length of the flagella. We often observe an accumulation of this protein at the what appear to be the swollen tips of flagella in *If1* and *If2-1* cells, and occasionally in *If3-2* as well. We almost never see this behavior in control or *If4-V13* flagella. (A) One image from control strain KAP-GFP, two images each from *If1* and *If2-1*. (B) One image from control strain KAP-GFP, two images each from *If3-2* and *If4-13*.

Figure 7

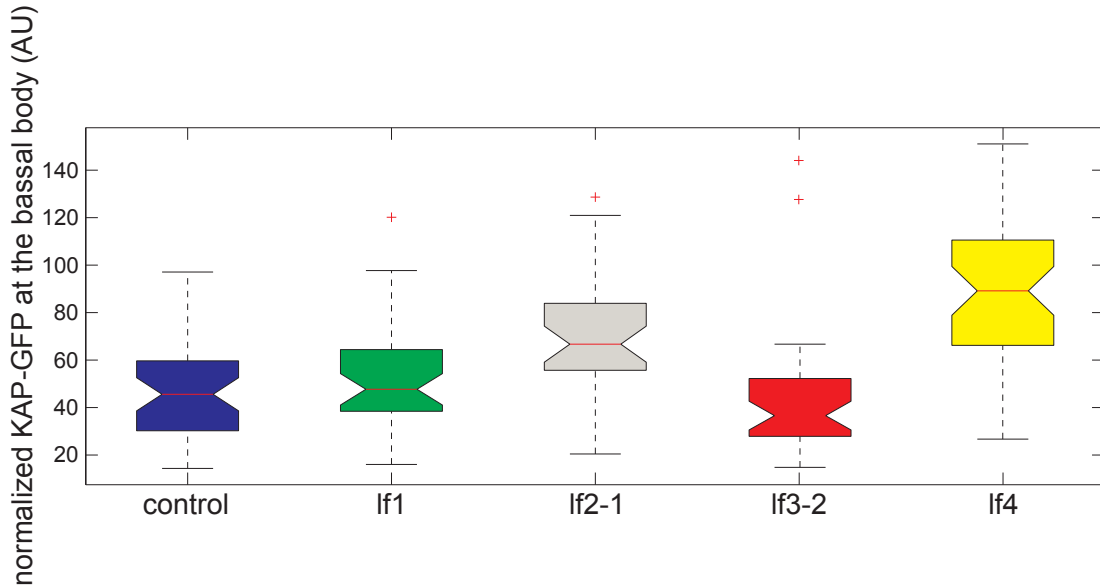


Figure 7. Accumulation of KAP-GFP at the basal bodies of *lf* strains.

This box and whisker plots demonstrates the increased recruitment of KAP-GFP to *lf2-1* and *lf4* basal bodies, relative to the control strain. The levels of *lf2-1* and *lf4* are significantly elevated, $p < 0.001$. AU, arbitrary units. Box and whicker plots: top and bottom of each colored box represent the 25th and 75th percentile respectively. The horizontal line within the box is the median. Whiskers extend to the last data point within 1.5 times the interquartile range. Red crosses represent outlier values.

Figure 8

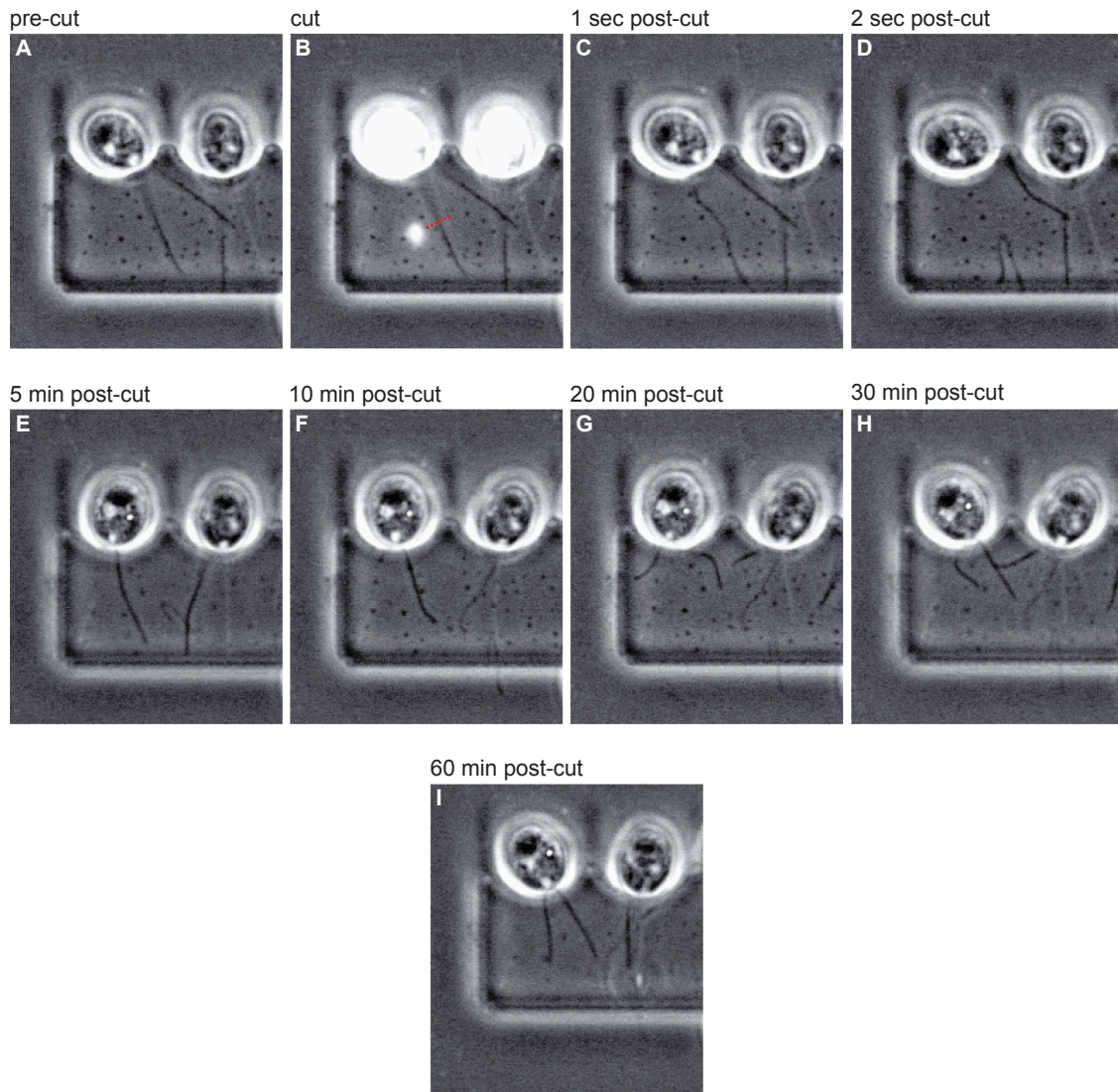


Figure 8. A wild type cell undergoes the long-zero response.

WT cells held in two pockets of a *Chlamydomonas* trap plate from CellAsic. Initially (A), the cell has two full length flagella. In B, the laser is visible, with the dashed red line indicating the path it will follow. C and D show the severed flagellum moving away from the cell body. E through I show the cell at subsequent time points, re-growing its short flagellum, while the long retracts and then re-grows (sec are seconds, min are minutes).

Figure 9

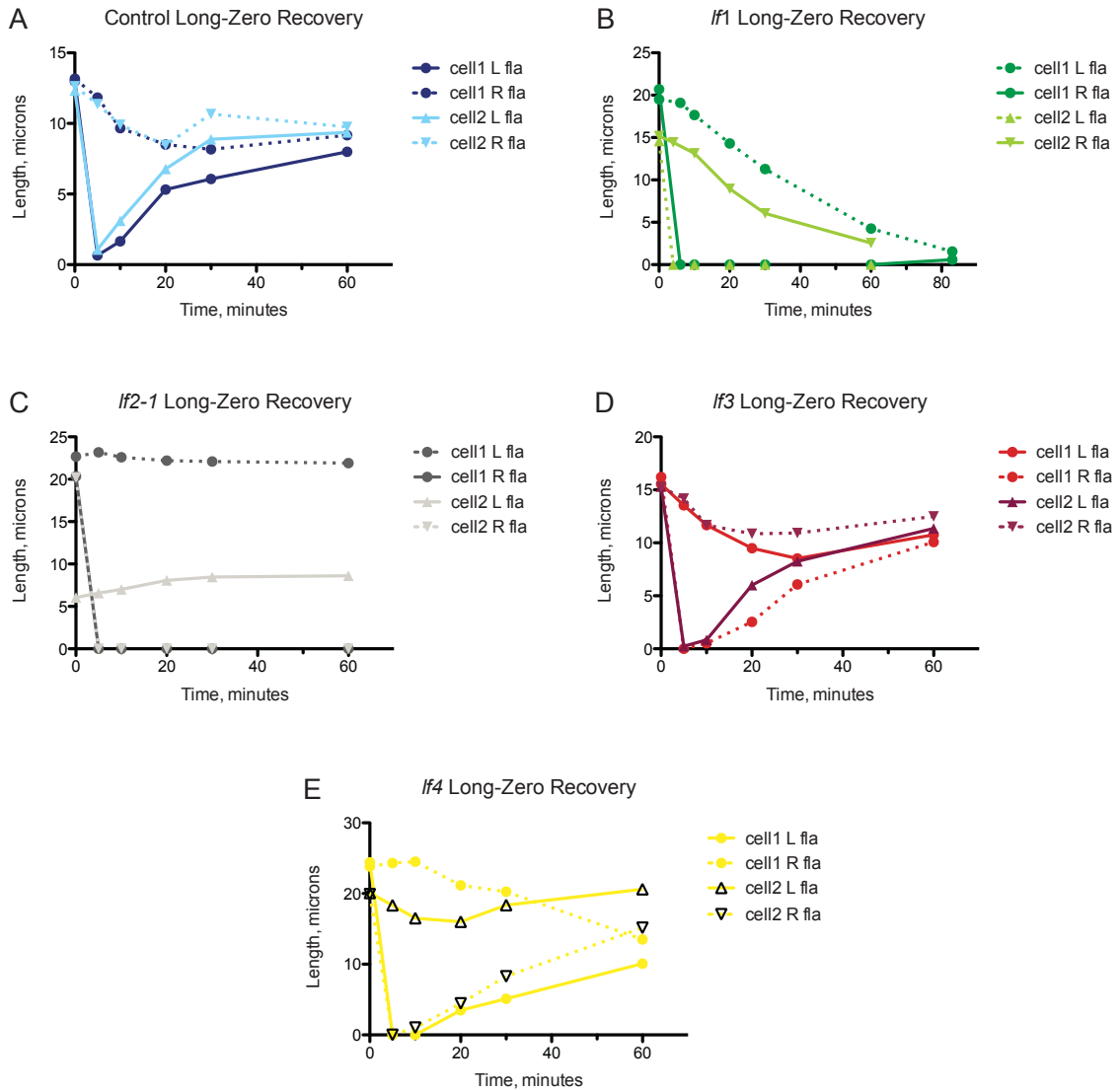


Figure 9. Some *If* strains have altered long-zero responses.

Graphs showing the flagellar dynamics of cells exhibiting the long-zero response. (A) Control cells demonstrate typical responses, with variability seen between individual cells. (D) *If3* and (E) *If4* cells have similar responses to control cells, with fast growth from the zero-length flagellum and retraction, then re-growth, of long flagellum. (B) *If1* cells have extremely delayed and highly variable re-growth of the short flagellum, with the long continuously retracting. (C) *If2-1* cells fail to exhibit a response; there is no growth from the short flagellum or retraction of the long; the long flagellum may even lengthen slightly rather than resorb.

Table 1. *Chlamydomonas* strains used in this work.

strain name	genotype	source	key references
cc125	WT	CC	see www.chlamy.org
cc1678	lf1	CC	McVittie, 1972; Barsel et al, 1988; Asleson & Lefebvre 1998; Nguyen et al, 2005
cc803	lf2-1	CC	McVittie, 1972; Barsel et al, 1988; Asleson & Lefebvre 1998; Tam et al, 2007
cc2287	lf2-5	CC	McVittie, 1972; Barsel et al 1988; Asleson & Lefebvre 1998; Tam et al, 2007
cc3662	lf3-2	CC	Barsel et al 1988; Asleson & Lefebvre 1998; Tam et al, 2003
lf4-V13	lf4-V13	Dr Gregory Pazour	Asleson & Lefebvre 1998; Berman et al, 2003
lf4-V86	lf4-V86	Dr Gregory Pazour	Asleson & Lefebvre 1998; Berman et al, 2003
cc1919	fla10 ^{ts}	CC	Adams et al, 1982; Walther et al, 1994; Kozminski et al, 1995; Vashishtha at al, 1996
fla10 ^{ts} mt+	fla10 ^{ts}	Dr Lynn Quarmby	Adams et al, 1982; Walther et al, 1994; Kozminski et al, 1995; Vashishtha at al, 1996
KAPGFP	fla3 ^{ts} ::KAP-GFP	Dr Mary Porter	Mueller at al, 2005

Table 2. *Chlamydomonas* strains created for this work.

strain created	line used here	parental strain mating type -	parental strain mating type +
KAPGFP Bx1 mt-	6B	KAPGFP	cc125
If1; fla3 ^{ts} ; KAPGFP	If1-2A	cc1678	KAPGFP Bx1
If2-1; fla3 ^{ts} ; KAPGFP	If2-1-1A	KAPGFP	cc803
If2-5; fla3 ^{ts} ; KAPGFP	If2-5-3B	cc2287	KAPGFP Bx1
If3-2; fla3 ^{ts} ; KAPGFP	If3-2-3B	KAPGFP	cc3662
If4-V13; fla3 ^{ts} ; KAPGFP	If4-V13-6A	KAPGFP	If4-V13
If4-V86; fla3 ^{ts} ; KAPGFP	If4-V86-18B	KAPGFP	If4-V86
If1; fla10 ^{ts}		cc1678	fla10 ^{ts} mt+
If2-1; fla10 ^{ts}		cc1919	cc803
If2-5; fla10 ^{ts}		cc2287	fla10 ^{ts} mt+
If3-2; fla10 ^{ts}		cc1919	cc3662
If4-V13; fla10 ^{ts}		cc1919	If4-V13
If4-V86; fla10 ^{ts}		cc1919	If4-V86

Table 3. Primers used in strain verification.

allele	primers	band size (bp)	method of ID	digest results
fla3 ^{ts}	fla3-1 CAPS-F2 CTGCTGCAGGACAAGAACAA	520	XhoI	WT: 520 fla3-1: 268+252
	fla3-1 CAPS-R2 TAGTCCACCTCCGTCTCGTC			
lf1	LF1-F1 TCTGCATCGTGCAGTAAGCACT	321	sequence PCR product	NA
	LF1-R1 TATGTCAATACGGAGCGTGGCCT			
lf2-1	LF2-1-F1 GGCGCAAATACTTGTGAGAGCACA	536	sequence PCR product	NA
	LF2-1-R1 TATCGGCACACCTAACTCCGTCA			
lf2-5	LF2-5-F1 TGCAGGCAAGGACTATTGTTGCAC	463	Ddel	WT: 357+106 lf2-5: 260+106+97
	LF2-5-R1 ATGAACCCTACGGCCATTCCCAAT			
lf3-2	LF3-F1 CCCATTGAGACCTGTCAACC	414	HinfI	WT: 223+147+44 lf3-2: 267+147
	LF3-F1 GCAACAAAGCCCAAATCTGT			
lf4 both V13+V86	LF4-F5 CTGCTGCTGTCATGTCGTTT	161	presence or absence of the band	NA
	LF4-F5 ATCTTACTCGGCCAGCTCAA			
MT plus	MT P2 forward GCTGGCATTCTGTATCCTTGACGC	423	presence or absence of the band	NA
	MT P2 reverse GCGGCGTAACATAAAGGAGGGTCCG			
MT minus	MT M3 forward CGACGACTTGGCATCGACAGGTGG	689	presence or absence of the band	NA
	MT M3 reverse CTCGGCCAGAACCTTTCATAGGGTGG			

NA indicates 'not applicable'.

Table 4. Summary of flagellar phenotypes of *If Chlamydomonas* strains.

strain	length phenotype of strains here	parameters from kymograph	KAP-GFP at the BB	regeneration	long-zero response	double mutant with <i>If1/If2/If3</i>	double mutant with <i>If4</i>
KAP-GFP	WT	WT	WT	WT quick regeneration	WT long retracts short re-grows	WT	WT
<i>If1</i>	mix of long and short, a few very long	high injection rate relative to control	no difference from WT	asynchronous with very slow growth	long retracts, short has extremely slow re-growth	<i>uIf/aIf</i> lagellate	<i>If</i> , regenerates ~WT
<i>If2-1</i>	a few very long, some WT, some <i>uIf</i>	elevated injection rate, with low significance	high	extremely poor growth with a very long lag	no retraction or re-growth	<i>uIf/aIf</i> lagellate	<i>If</i> , poor regeneration
<i>If3-2</i>	many ~WT, a few very long	no difference from WT	no difference from WT	~WT	~WT	<i>uIf/aIf</i> lagellate	<i>If</i> , (regeneration unknown)
<i>If4-V13</i>	often ~20 μ m, a few short or WT length	high injection rate relative to control	high	~WT	~WT	<i>If</i>	NA

References

- Asleson, C.M., and P.A. Lefebvre. 1998. Genetic analysis of flagellar length control in *Chlamydomonas reinhardtii*: a new long-flagella locus and extragenic suppressor mutations. *Genetics*. **148**:693-702.
- Barsel, S.E., D.E. Wexler, and P.A. Lefebvre. 1988. Genetic analysis of long-flagella mutants of *Chlamydomonas reinhardtii*. *Genetics*. **118**:637-648.
- Berman, S.A., N.F. Wilson, N.A. Haas, and P.A. Lefebvre. 2003. A novel MAP kinase regulates flagellar length in *Chlamydomonas*. *Curr Biol*. **13**:1145-1149.
- Botvinick, E.L., and M.W. Berns. 2005. Internet-based robotic laser scissors and tweezers microscopy. *Microscopy research and technique*. **68**:65-74.
- Cole, D.G. 2003. The intraflagellar transport machinery of *Chlamydomonas reinhardtii*. *Traffic*. **4**:435-442.
- Deane, J.A., D.G. Cole, E.S. Seeley, D.R. Diener, and J.L. Rosenbaum. 2001. Localization of intraflagellar transport protein IFT52 identifies basal body transitional fibers as the docking site for IFT particles. *Curr Biol*. **11**:1586-1590.
- Dentler, W. 2005. Intraflagellar transport (IFT) during assembly and disassembly of *Chlamydomonas* flagella. *The Journal of cell biology*. **170**:649-659.
- DiBella, L.M., A. Park, and Z. Sun. 2009. Zebrafish Tsc1 reveals functional interactions between the cilium and the TOR pathway. *Human molecular genetics*. **18**:595-606.
- Dresdner, R.D., and D.F. Katz. 1981. Relationships of mammalian sperm motility and morphology to hydrodynamic aspects of cell function. *Biology of Reproduction*. **25**:920-930.
- Engel, B.D., W.B. Ludington, and W.F. Marshall. 2009. Intraflagellar transport particle size scales inversely with flagellar length: revisiting the balance-point length control model. *J Cell Biol*. **187**:81-89.
- Feldman, J.L., and W.F. Marshall. 2009. ASQ2 Encodes a TBCC-like Protein Required for Mother-Daughter Centriole Linkage and Mitotic Spindle Orientation. *Current Biology*. **19**:1238-1243.
- Gardner, M.K., B.L. Sprague, C.G. Pearson, B.D. Cosgrove, A.D. Bicek, K. Bloom, E.D. Salmon, and D.J. Odde. 2010. Model Convolution: A Computational Approach to Digital Image Interpretation. *Cell Mol Bioeng*. **3**:163-170.

- Harris, E.H. The *Chlamydomonas* sourcebook. 1989. Academic Press, San Diego, CA.
- Holt, W.V., M. Hernandez, L. Warrell, and N. Satake. 2010. The long and the short of sperm selection in vitro and in vivo: swim-up techniques select for the longer and faster swimming mammalian sperm. *J Evol Biol.* **23**:598-608.
- Kozminski, K.G., P.L. Beech, and J.L. Rosenbaum. 1995. The *Chlamydomonas* kinesin-like protein FLA10 is involved in motility associated with the flagellar membrane. *J Cell Biol.* **131**:1517-1527.
- Kuchka, M.R., and J.W. Jarvik. 1982. Analysis of flagellar size control using a mutant of *Chlamydomonas reinhardtii* with a variable number of flagella. *J Cell Biol.* **92**:170-175.
- Kuchka, M.R., and J.W. Jarvik. 1987. Short-Flagella Mutants of *Chlamydomonas reinhardtii*. *Genetics.* **115**:685-691.
- Leopold, P.L., M.J. O'Mahony, X.J. Lian, A.E. Tilley, B.G. Harvey, and R.G. Crystal. 2009. Smoking is associated with shortened airway cilia. *PLoS ONE.* **4**:e8157.
- Lopes, S.S., R. Lourenço, L. Pacheco, N. Moreno, J. Kreiling, and L. Saúde. 2010. Notch signalling regulates left-right asymmetry through ciliary length control. *Development.*
- Ludington, W.B., K.A. Wemmer, K.F. Lechtreck, G.B. Witman, and W.F. Marshall. Manuscript in preparation. Avalanche-like behavior generates periodicity in eukaryotic intraflagellar transport.
- Luo, M., M. Cao, Y. Kan, G. Li, W. Snell, and J. Pan. 2011. The Phosphorylation State of an Aurora-Like Kinase Marks the Length of Growing Flagella in *Chlamydomonas*. *Curr Biol.*
- Marshall, W.F., H. Qin, M. Rodrigo Brenni, and J.L. Rosenbaum. 2005. Flagellar length control system: testing a simple model based on intraflagellar transport and turnover. *Mol Biol Cell.* **16**:270-278.
- Marshall, W.F., and J.L. Rosenbaum. 2001. Intraflagellar transport balances continuous turnover of outer doublet microtubules: implications for flagellar length control. *J Cell Biol.* **155**:405-414.
- Matsui, H., S.H. Randell, S.W. Peretti, C.W. Davis, and R.C. Boucher. 1998. Coordinated clearance of periciliary liquid and mucus from airway surfaces. *J Clin Invest.* **102**:1125-1131.

- McVittie, A. 1972. Flagellum mutants of *Chlamydomonas reinhardtii*. *J Gen Microbiol.* **71**:525-540.
- Mueller, J., C.A. Perrone, R. Bower, D.G. Cole, and M.E. Porter. 2005. The FLA3 KAP subunit is required for localization of kinesin-2 to the site of flagellar assembly and processive anterograde intraflagellar transport. *Mol Biol Cell.* **16**:1341-1354.
- Nguyen, R.L., L.W. Tam, and P.A. Lefebvre. 2005. The LF1 gene of *Chlamydomonas reinhardtii* encodes a novel protein required for flagellar length control. *Genetics.* **169**:1415-1424.
- Omori, Y., T. Chaya, K. Katoh, N. Kajimura, S. Sato, K. Muraoka, S. Ueno, T. Koyasu, M. Kondo, and T. Furukawa. 2010. Negative regulation of ciliary length by ciliary male germ cell-associated kinase (Mak) is required for retinal photoreceptor survival. *Proc Natl Acad Sci USA.*
- Qin, H. 2004. Intraflagellar transport (IFT) cargo: IFT transports flagellar precursors to the tip and turnover products to the cell body. *J Cell Biol.* **164**:255-266.
- Qin, H., D.T. Burnette, Y.K. Bae, P. Forscher, M.M. Barr, and J.L. Rosenbaum. 2005. Intraflagellar transport is required for the vectorial movement of TRPV channels in the ciliary membrane. *Curr Biol.* **15**:1695-1699.
- Rosenbaum, J.L., J.E. Moulder, and D.L. Ringo. 1969. Flagellar elongation and shortening in *Chlamydomonas*. The use of cycloheximide and colchicine to study the synthesis and assembly of flagellar proteins. *J Cell Biol.* **41**:600-619.
- Scholey, J.M. 2003. Intraflagellar transport. *Annual review of cell and developmental biology.* **19**:423-443.
- Sloboda, R.D. 2002. A healthy understanding of intraflagellar transport. *Cell motility and the cytoskeleton.* **52**:1-8.
- Smith, D.J., E.A. Gaffney, and J.R. Blake. 2008. Modelling mucociliary clearance. *Respir Physiol Neurobiol.* **163**:178-188.
- Song, L., and W.L. Dentler. 2001. Flagellar protein dynamics in *Chlamydomonas*. *The Journal of biological chemistry.* **276**:29754-29763.
- Stephens, R.E. 1999. Turnover of tubulin in ciliary outer doublet microtubules. *Cell structure and function.* **24**:413-418.

- Tam, L.W., W.L. Dentler, and P.A. Lefebvre. 2003. Defective flagellar assembly and length regulation in LF3 null mutants in *Chlamydomonas*. *J Cell Biol.* **163**:597-607.
- Tam, L.W., N.F. Wilson, and P.A. Lefebvre. 2007. A CDK-related kinase regulates the length and assembly of flagella in *Chlamydomonas*. *J Cell Biol.* **176**:819-829.
- Tammachote, R., C.J. Hommerding, R.M. Sinderson, C.A. Miller, P.G. Czarnecki, A.C. Leightner, J.L. Salisbury, C.J. Ward, V.E. Torres, V.H. Gattone, 2nd, and P.C. Harris. 2009. Ciliary and centrosomal defects associated with mutation and depletion of the Meckel syndrome genes MKS1 and MKS3. *Human molecular genetics.* **18**:3311-3323.
- Thomas, J., L. Morlé, F. Soulavie, A. Laurençon, S. Sagnol, and B. Durand. 2010. Transcriptional control of genes involved in ciliogenesis: a first step in making cilia. *Biol Cell.* **102**:499-513.
- Tokunaga, M., N. Imamoto, and K. Sakata-Sogawa. 2008. Highly inclined thin illumination enables clear single-molecule imaging in cells. *Nat Methods.* **5**:159-161.
- Wilson, C.A., and J.A. Theriot. 2006. A correlation-based approach to calculate rotation and translation of moving cells. *IEEE Trans Image Process.* **15**:1939-1951.
- Zamora, I., J.L. Feldman, and W.F. Marshall. 2004. PCR-based assay for mating type and diploidy in *Chlamydomonas*. *BioTechniques.* **37**:534-536.

Chapter 4

Biological Noise in an Organelle Size Control System

Biological Noise in an Organelle Size Control System

Kimberly A. Wemmer and Wallace F. Marshall

Dept. of Biochemistry & Biophysics
University of California, San Francisco

Abstract

Stochastic variations (noise) in gene expression have been extensively characterized, but the ramifications of this variation for cellular structure and function remain unclear. To what extent are cellular structures subject to noise? In this report we answer this question using the length control system of the eukaryotic flagellum as a model system. We show that flagellar length undergoes significant fluctuations that can be decomposed into intrinsic and extrinsic noise components. This length variation is functionally relevant, based on the fact that cells with the highest deviation from their length set-point show impaired swimming. To investigate the molecular basis of biological noise in flagella we identify genes that increase noise. These two genes, *If1* and *If4*, which both increase the average flagellar length, have dramatically different effects on intrinsic versus extrinsic noise, suggesting they operate in different length-regulating pathways, with *LF1* making a larger contribution to the suppression of intrinsic noise. Using a theoretical model for flagellar length control based on the balance between IFT-mediated assembly and length-independent disassembly, a linear noise analysis predicts that parameter changes that lead to increased length should increase noise, as we have observed, and also that such parameter changes should increase low-frequency fluctuations. We confirmed this prediction by analyzing the power spectrum of length fluctuations in *If1* mutants. Taken together our results show that biological noise can clearly affect the size control of cellular structures, with a corresponding effect on cell function.

Introduction

Stochastic variation (noise) is well documented in gene expression (Elowitz et al, 2002; Raser et al, 2004; Kaern et al., 2005), but the biological effect of this variation remains to be determined. At the level of the whole cell, structure and function arise from the joint action of dozens or hundreds of individual genes. It is not clear whether the independent fluctuations in the genes contributing to a given biological process would not simply average out. We therefore quantified the level of noise in biological structure at the cellular level, by examining stochastic variations in the length of the eukaryotic flagellum, an organelle chosen for these studies because of its simple geometry. Cilia and flagella are interchangeable terms for the microtubule-based organelles that project from the surface of most eukaryotic cells (Pazour and Rosenbaum, 2002). Cilia perform important motile and sensory functions. Because these organelles are simple linear structures, it is easier to analyze the length regulation of cilia and flagella than it is to analyze size control in more complicated organelles. The flagellum is thus an excellent test-bed for exploring the systems biology of cellular structure (Randall, 1969; Wemmer and Marshall, 2007). The lengths of cilia and flagella are known to vary from cell to cell in a variety of organisms (Randall, 1969; Wheatly and Bowser, 2000; Adams et al., 1985) suggesting these organelles can be used to analyze biological noise in cellular structure.

Materials and Methods

Strains, media, and imaging

All strains were obtained from the *Chlamydomonas* Genetics Center, Duke University, with the exception of If4 mutant strain V13 which was a gift of Greg Pazour, UMASS Medical Center. The If4 mutation was confirmed in this strain by PCR (data not shown). For asynchronous culture, cells were grown in 2ml cultures in TAP media (Harris, 1989) under continuous illumination. Cultures arrested in G1 were obtained by growing cells in M1 media for 2 days in continuous illumination and then switching them to continuous darkness for 24 hours. Gametes were grown overnight in M-N media.

For measurement of length in fixed cells, cells were fixed in 1% glutaraldehyde, and imaged using DIC optics with an Olympus 60x air lens and an air condenser on a DeltaVision 3D microscopy system. Three dimensional data collection was performed using a 0.2 mm step in the Z-axis. Lengths were then measured by tracing the flagella in three dimensions using the DeltaVision distance measuring function using the multi-segment length calculation method.

For measurements of length fluctuations in live cells, cultures were grown in TAP media at 21C in constant light on a roller drum. For embedding live cells, 1% w/v agarose was melted in TAP media, then cooled to 41C. A square of vaseline was made on a glass slide, then 5uL of culture was mixed with 20uL agarose in TAP within the square. The slide was then inverted over a coverslip, compressing the agarose in TAP into a flat, square pad. The cells were allowed to recover at room temperature in light for 2 hours to overnight, then imaged. The

slide was imaged using DIC microscopy on a Deltavision microscopy system, at room temperature in ambient light. Embedded cells were imaged using a 100x oil immersion lens (NA 1.40 PlanApo) with a z step size of 0.2 microns. One z stack was taken through the entire cell every 10 minutes for 2 hours. The length of the flagella was measured using Deltavision software.

Computing intrinsic and extrinsic noise

We define intrinsic and extrinsic noise in a purely operational sense by treating the two flagellar length measurements from each cell as though they were two fluorescence intensity measurements in a dual-reporter gene expression noise protocol, and computing intrinsic and extrinsic noise using the relations previously described for gene noise (Elowitz et al., 2002), as follows:

$$h_{int}^2 = \langle (L_1 - L_2)^2 \rangle / 2\langle L_1 \rangle \langle L_2 \rangle$$

$$h_{ext}^2 = \{ \langle L_1 L_2 \rangle - \langle L_1 \rangle \langle L_2 \rangle \} / \langle L_1 \rangle \langle L_2 \rangle$$

For each given cell measurement, we arbitrarily defined L1 as referring to the length of the flagellum whose base was closest to the left edge of the CCD camera field of view.

Estimation of measurement noise

We used time-lapse imaging to obtain two separate estimates for measurement error. First, as plotted in Figure 1B, we imaged cells fixed in glutaraldehyde at multiple sequential time points and then calculated the mean squared change in length. As expected for measurement errors which are uncorrelated with each other, the slope of the best fit line to this data was less than 5×10^{-5} , showing the difference in measured length was independent of time lag. The average value of the mean squared difference in length was 0.0438 square microns, corresponding to an average measurement error of 0.2 microns.

As an alternative measure, we analyzed the fluctuations in live cells and calculated the mean squared change in difference between L1 and L2, and plotted this versus time. This plot gave a roughly linear behavior for the first several time points. We then fit a straight line to the first ten time points and obtained a Y intercept of 0.597. For a one-dimensional random walk such as that executed by the difference in length between the two flagella, the Y intercept of this plot should correspond to 4 times the mean squared measurement error in each measurement. We therefore obtain an estimated measurement error of 0.39 microns. We thus obtain two independent estimates of measurement error, both of which are on the same order of magnitude as the XYZ voxel size.

Measurement of swimming speed versus flagellar length by high speed video

To obtain simultaneous measurements of swimming speed and flagellar lengths we mounted cells between a slide and coverslip supported by a 1 mm Vaseline

ring, and imaged the cells on a Zeiss Axiovert 200M microscope with a 40X air objective lens using DIC optics and an infrared-blocking filter, collecting data with a Phantom MiroEx4-1024MM video camera at a frame rate of 1000 fps, exposure time 998 mSec. Cells were imaged at a dilution that ensured at most one or two cells per field of view. Following collection of each dataset, individual cells were manually tracked for 10 cycles of flagellar beating, marking the position of the cell at the beginning and end of this period. The difference in position divided by the elapsed time was taken as the average swimming speed. Since our data collection was only two-dimensional, many cells swam out of focus during the imaging and those images were discarded. Only cells where the flagella remained in focus through the entire 10 beat cycles were used for distance measurements. Distance measurements of swimming and length measurement of flagella were performed using the Phantom Miro software.

Small signal linear noise analysis of balance-point length control model

We have previously described a simple model for length control of cilia and flagella that has been termed the balance-point model to distinguish it from more elaborate models based on active length sensors (none of which have yet been discovered). The balance point model is based on observations that the axonemal microtubules undergo continuous turnover at their plus-ends, with assembly taking place at a constant rate regardless of length, and assembly taking place at a rate limited by intraflagellar transport (Marshall and Rosenbaum, 2001). A key component of the model is the hypothesis that

intraflagellar transport is inherently length-dependent. This dependency arises because the quantity of IFT proteins in the flagellum is independent of length (Marshall and Rosenbaum, 2001; Marshall et al., 2005). For each IFT particle, moving at a constant velocity, the round-trip transit time is obviously proportional to length, hence the frequency with which a particle can deliver protein cargo to the tip is proportional to $1/L$. Because the total number of IFT proteins moving in the flagellum is length-independent, the overall efficiency by which the IFT system taken as a whole can move protein out to the tip for assembly is therefore proportional to $1/L$. The constant of proportionality depends on the number of IFT proteins in the flagellum, their velocity, etc. Because assembly is rate-limited by transport, it follows that the assembly rate is proportional to $1/L$ while the disassembly rate is independent of length. Therefore, the assembly rate versus length curve will intersect the disassembly versus length curve at a unique value of the length, which reflects the steady state length of the flagella.

Following our previous formulation of the balance-point length control model, we define three parameters, A, P, and D. Parameter A describes the efficacy of intraflagellar transport and encapsulates the speed of the IFT particles, the number of IFT particles in a flagellum (a quantity known to be independent of length), and the cargo carrying-capacity of the particles. The parameter P describes the total pool of flagellar protein in a cell, including protein incorporated into the two flagella as well as unincorporated precursor stored in the cytoplasm (Rosenbaum et al., 1969). Parameter D describes the rate of flagellar disassembly. We have previously estimated values for these parameters in wild-

type cells as follows: $D=0.22$ mm/min (measured from the rate of shortening in fla10 mutant cells), $P=40$ mm (measured from the ratio of flagellar lengths before and after regeneration in the presence of cycloheximide (Marshall and Rosenbaum, 2001)). Note that the pool size is expressed in units of length, the conversion factor being the quantity of protein required to assemble a 1 mm segment of the axoneme. We previously estimated parameter $A \sim 0.11$ (this is a unit-less quantity).

The balance-point model for length control can then be encapsulated by a pair of nonlinear differential equations, one for each of the two flagellar lengths L_1 and L_2 :

$$\dot{L}_1 = f(L_1, L_2) = A \frac{(P - L_1 - L_2)}{L_1} - D$$

$$\dot{L}_2 = g(L_1, L_2) = A \frac{(P - L_1 - L_2)}{L_2} - D$$

The steady state solution is:

$$L_1 = L_2 = L_{ss} = \frac{P}{2 + \frac{D}{A}}$$

With the parameter values given above this predicts a steady state length of 10 mm. With this model we would like to predict how changes in the parameters would affect noise rejection by the system, in order to ask whether parameter changes that increase the steady-state length would be predicted to increase

noise. To do this, we employ a linear noise analysis by modeling the response to small perturbations in length. Increased sensitivity to small perturbations would tend to result in a noisier system.

We begin our noise analysis by introducing a change in variables:

$$x = L_1 - L_2 \qquad y = L_1 + L_2 - 2L_{ss}$$

The new variables x and y relate to the intrinsic and extrinsic noise, respectively, that will be produced by a fluctuation applied to one of the flagella. We next consider the effect of applying a small perturbation to L_1 at time $t=0$. Initially this perturbation would increase both x and y , but then over time the system will restore itself to the steady state lengths. We ask how fast this restoration will occur. To do so, we linearize the problem as follows. First we note that x and y can be expressed in terms of the deviations from the steady state in L_1 and L_2 as follows:

$$u = L_1 - L_{ss}$$

$$v = L_2 - L_{ss}$$

$$x = u - v$$

$$y = u + v$$

Assuming the perturbations are small, u and v will be close to zero. The rate of change of the deviations u and v is approximated by the Jacobian:

$$\begin{pmatrix} \dot{u} \\ \dot{v} \end{pmatrix} = \begin{pmatrix} \left. \frac{\partial f}{\partial L_1} \right|_{L_1=L_2=L_{ss}} & \left. \frac{\partial f}{\partial L_2} \right|_{L_1=L_2=L_{ss}} \\ \left. \frac{\partial g}{\partial L_1} \right|_{L_1=L_2=L_{ss}} & \left. \frac{\partial g}{\partial L_2} \right|_{L_1=L_2=L_{ss}} \end{pmatrix} \begin{pmatrix} u \\ v \end{pmatrix}$$

Evaluating the elements around the steady-state value $L_1=L_2=L_{ss}$ we obtain the linearized system:

$$\begin{pmatrix} \dot{u} \\ \dot{v} \end{pmatrix} = A \begin{pmatrix} \frac{(L_{ss} - P)}{L_{ss}^2} & -\frac{1}{L_{ss}} \\ -\frac{1}{L_{ss}} & \frac{(L_{ss} - P)}{L_{ss}^2} \end{pmatrix} \begin{pmatrix} u \\ v \end{pmatrix}$$

we then express the behavior of x and y in the linear approximation according to

$$\dot{x} = \dot{u} - \dot{v}$$

$$\dot{y} = \dot{u} + \dot{v}$$

this yields, finally, a pair of uncoupled differential equations for x and y :

$$\begin{aligned} \dot{x} &= u \left(\left. \frac{\partial f}{\partial L_1} \right|_{L_1=L_2=L_{ss}} - \left. \frac{\partial g}{\partial L_1} \right|_{L_1=L_2=L_{ss}} \right) + v \left(\left. \frac{\partial f}{\partial L_2} \right|_{L_1=L_2=L_{ss}} - \left. \frac{\partial g}{\partial L_2} \right|_{L_1=L_2=L_{ss}} \right) \\ &= (u - v) \left\{ A \frac{(L_{ss} - P)}{L_{ss}^2} + \frac{A}{L_{ss}} \right\} \\ &= \left\{ A \frac{(L_{ss} - P)}{L_{ss}^2} + \frac{A}{L_{ss}} \right\} x \end{aligned}$$

$$\dot{y} = u \left(\frac{\partial f}{\partial L_1} \Big|_{L_1=L_2=L_{ss}} + \frac{\partial g}{\partial L_1} \Big|_{L_1=L_2=L_{ss}} \right) + v \left(\frac{\partial f}{\partial L_2} \Big|_{L_1=L_2=L_{ss}} + \frac{\partial g}{\partial L_2} \Big|_{L_1=L_2=L_{ss}} \right)$$

$$= \left\{ A \frac{(L_{ss} - P)}{L_{ss}^2} - \frac{A}{L_{ss}} \right\} y$$

we define constants:

$$\alpha = A \frac{(L_{ss} - P)}{L_{ss}^2} + \frac{A}{L_{ss}}$$

$$\beta = A \frac{(L_{ss} - P)}{L_{ss}^2} - \frac{A}{L_{ss}}$$

hence:

$$\dot{x} = \alpha x$$

$$\dot{y} = \beta y$$

with solutions

$$x(t) = x(0)e^{\alpha t}$$

$$y(t) = y(0)e^{\beta t}$$

We now consider what happens if we add random fluctuations to the system governing flagellar length. We model intrinsic fluctuations by adding a noise term to the equation governing x , thus:

$$\dot{x} = \alpha x + \sigma \eta$$

Where s denotes the magnitude of the fluctuations and η denotes gaussian white noise with zero mean and variance 1. This is the stochastic differential equation that describes an Ornstein-Uhlenbeck process, and it is a standard result (Honerkamp, 1994; Van Kampen, 1992) that the stationary solution to this equation has a mean of 0 and a mean squared value of:

$$\langle x^2 \rangle = \frac{\sigma^2}{2\alpha}$$

Since we do not know the microscopic molecular source of the fluctuations, we do not know the value of s , however we assume it is the same for wild type and mutant cells. Hence the mean squared difference in length between the two flagella should be proportional to $1/a$. Substituting the value of a derived above and then using the value of L_{ss} in terms of the three parameters A , D , and P , we obtain

$$\langle (L_1 - L_2)^2 \rangle \sim \frac{1}{\left\{ A \frac{L_{ss} - P}{L_{ss}^2} + \frac{A}{L_{ss}} \right\}} = \frac{P}{D(2 + D/A)}$$

Which is given as equation (2) in the Results section.

Results

Flagellar length control system exhibits both extrinsic and intrinsic noise

In order to analyze noise in flagellar length, we measure lengths in the unicellular green alga *Chlamydomonas* (Merchant et al., 2007). These cells have two flagella per cell, each of which is approximately 10 μm in length on average (Figure 1A inset). This organism has long been used in studies of flagellar length control because its flagella are easy to measure and because mutants exist in which flagellar length is altered (Wemmer and Marshall, 2007).

Our quantitative analysis of noise in a population of fixed cells is based on approaches previously developed for gene expression analysis. Two distinct types of noise have been previously described for studies of gene expression: - extrinsic noise, which describes the variation in overall expression levels from cell to cell, and intrinsic noise which describes variations in transcription rates at an individual promoter (Elowitz et al, 2002; Raser et al., 2004). The distinction between the two types of noise is measured in gene expression studies using a dual-reporter method (Elowitz et al., 2002), in which two different fluorescent protein reporter constructs are driven by identical promoters, so that variation in expression of both constructs can be measured on a cell-by-cell basis. To make a similar distinction in the case of flagellar length, we take advantage of the fact that *Chlamydomonas* cells naturally have two identical flagella. We therefore measure the lengths of these two flagella in a population of cells (see Figure 1A) and from these measurements we can compute the intrinsic and extrinsic noise

using the same mathematical definitions used for gene expression studies (See Materials and Methods).

As shown in Figure 1A, and summarized in Table S1, we find that flagellar lengths in wild-type cells demonstrate measurable levels of both intrinsic and extrinsic noise. Intrinsic noise describes the variations in length between the two flagella within one cell and may represent fluctuations within the length-control machinery intrinsic to each flagellum, while extrinsic noise describes the cell to cell variation in length and may represent fluctuations in cell-wide features relating to size control, for instance cell size (see below). We found that the extrinsic noise is greater in magnitude than the intrinsic noise. The intrinsic noise is, however, significantly greater than the estimated measurement error, thus we can conclude that flagella are subject to biological noise.

The data of Figure 1A show that flagellar length varies across a population of cells, leading us to ask whether the variation reflects fixed variation in different cells or random fluctuations over time within each cell. To do so, we embedded cells in agarose and acquired time-lapse 3D movies using DIC microscopy. We then measured the lengths of the flagella and plotted the mean-squared change in length as a function of time-interval (Figure 1B). This plot shows that flagellar lengths undergo diffusive dynamics at short time scales, because the mean squared length difference is linearly proportional to the time interval. At longer time-scales, the mean squared length difference reaches a plateau suggesting that the magnitude of the length variation is constrained. This constraint is a

manifestation of the flagellar length control system, whose molecular basis remains largely unknown (Wemmer and Marshall, 2007).

We next investigated the source of extrinsic noise. A dominant contribution to extrinsic noise in gene expression is variation in cell size (Raser et al., 04), presumably because larger cells have more ribosomes thus making more protein per mRNA molecule. Flagellar length can be affected by changing levels of flagellar precursor proteins (Rosenbaum et al., 1969), predicting that larger cells might have longer flagella due to increased numbers of ribosomes. Indeed it has been noted that larger cells sometimes have longer flagella in various mutants (Adams et al., 1985). We asked whether cell size correlated with extrinsic variations in flagellar length by comparing flagellar lengths to cell diameters on a cell by cell basis (Figure 1C). For wild-type cells, we obtained a correlation coefficient of 0.61. However with the restricted range of cell sizes in normal wild-type populations, the scatter of lengths made it hard to observe a convincing trend. Therefore we extended the range of cell sizes by also examining *mat3* mutant cells which have smaller cell size due to alteration of the cell size control machinery (Umen and Goodenough, 2001). These measurements are also plotted in Figure 1C. When we take the combined wild-type and *mat3* data, we obtain a correlation coefficient between length and diameter of 0.71, suggesting that cell size makes a major contribution in determining flagellar length, although as in other studies cell size is apparently not the only determinant of extrinsic noise (see for example Taniguchi et al., 2010).

Extrinsic noise can also result from variations in cell cycle state. We compared noise in asynchronous cultures (which were used to derive the data discussed above) to noise in cells arrested in G1 by growth in the dark in minimal media, and to gamete cultures which are arrested in a G0-like state in preparation for mating. Extrinsic noise was significantly reduced in both cases (Table S1), suggesting that cell-to-cell variations in cell cycle state contributed to increased extrinsic noise in the asynchronous cultures. As shown in Table S1, for G1 arrested wild-type cells, the correlation between cell size and flagellar length is even stronger than in asynchronous cultures of wild-type cells (correlation coefficient 0.75) suggesting that when variation due to cell cycle progression is eliminated, the remaining extrinsic noise is increasingly dominated by cell size variation. Our results indicate that variation in cell size makes a significant contribution to extrinsic noise, as has been reported in prior studies of noise in protein production (Raser et al., 2004). We hypothesize that much of this extrinsic noise may be due to variation in synthesis of flagellar precursor proteins from cell to cell, consistent with prior demonstrations that flagellar growth is limited by availability of precursor protein in the cytoplasm (Rosenbaum et al., 1969; Coyne and Rosenbaum, 1970), such that larger cells, which have more ribosomes, produce more flagellar precursor and thus grow longer flagella. We also note that it has been shown that the clean decomposition of total noise into intrinsic and extrinsic components requires that the extrinsic component must vary on a time scale that is long compared to the intrinsic fluctuation time scale (Hilfinger and Paulsson, 2011). Both cell size changes and cell cycle

progression in *Chlamydomonas* take place on a time scale of many hours, while flagellar length changes typically take place on a time scale of tens of minutes, hence the delineation of intrinsic and extrinsic noise seems justified in this system.

Biological noise in flagellar length affects cell function

The fact that genes exist whose action reduces noise in flagellar length raises the possibility that noise is under selective pressure due to effects on cellular fitness. We therefore asked whether noise affects flagellar motility. *Chlamydomonas* cells bend their two flagella in opposite directions in order to swim forward in a breast-stroke like motion. Inequality in lengths due to intrinsic noise might thus be expected to prevent a cell from swimming forward effectively in a straight line. To test this prediction, we observed *Chlamydomonas* cells swimming using a high speed camera. For each cell, we measured the lengths of its two flagella while it was swimming, allowing us to determine the length inequality as measured by the absolute difference in lengths and at the same time measure the swimming speed. As shown in Figure 2, we found that optimal swimming occurred when both flagella were of approximately equal length and when their lengths were in the range 8-12 microns. Outside of this range, swimming speed fell off dramatically. The defects in swimming were different depending on the type of length variation. When both flagella were too long, the extra length of flagellum appeared to flail ineffectively through the media, presumably impeding forward progress. On the other hand, if both flagella were

too short, the flagella were unable to generate an asymmetrical bending motion, and so the flagella just move back and forth but cannot generate overall forward motion because symmetrical swimming movements do not produce motion at low Reynolds number. If the two flagella were of unequal length, the cells were seen to move in circles, not unexpected if the two flagella are generating different forces.

These results indicate that to the extent that a length control system may have evolved to ensure effective swimming, it must satisfy two goals: ensure equality of flagellar length, and ensure that the two flagella are in roughly the right average length range. With this evolutionary consideration in mind, we can propose a fitness-based test for the existence of a length control system: if flagellar lengths are regulated, we would expect them to be distributed in a manner that mirrors the length ranges giving optimal swimming. In fact, this is precisely what we observe. As indicated by the dots in Figure 2, wild-type gametes have a joint distribution of lengths for their two flagella that exactly match the optimal range of flagellar lengths for fast swimming. We conclude that a flagellar length control system is likely to exist. Also, noting that inequality of flagellar lengths was generally more deleterious for swimming, it appears that flagellar length represents a situation in which suppression of intrinsic biological noise is functionally important for fitness in the organism.

Noise analysis of balance-point model for flagellar length control

The noise measurements reported here provide a new way to test hypothetical flagellar length control system models, since any model for such a system must be able to account for not only the average steady-state behavior of the system, but also the fluctuations that occur within the system. We have previously described a model, outlined in Figure 3A and B, for flagellar length control based on the intrinsic length-dependence of intraflagellar transport (Marshall and Rosenbaum, 2001; Marshall et al., 2005). This model contains three parameters, A, D, and P, which reflect the efficiency of IFT, the rate of disassembly at the tip, and the level of flagellar structural protein synthesized by the cell. As previously derived (Marshall and Rosenbaum, 2001), the steady-state average flagellar length for this model is:

$$\langle L \rangle = \frac{P}{2 + \frac{D}{A}} \quad (1)$$

Clearly, average length can be increased either by increasing A, increasing P, or decreasing D. How would length-increasing parameter changes affect noise? To answer this question we have performed a small-signal linear noise analysis as derived in Materials and Methods. We do not know the ultimate source of intrinsic noise in this system, but we postulate that it may result from random fluctuations in the growth rate at the tip, so that the length executes a one-dimensional random walk, with the length-dependent growth or shrinkage rate created by the balance point model providing a restoring force to return the

length back to its set point after any fluctuation. The system is thus analogous to the classical problem of Brownian motion of a particle attached to a spring, where in our case the noise source is due to random variation in assembly rates at the tip rather than thermal collisions, and the fact that we use a linearized model provides a Hookian restoring force term. Under this assumption, as derived in Materials and Methods, length noise is predicted to depend on model parameters as follows:

$$\langle (L_1 - L_2)^2 \rangle \sim \frac{P}{D \left[2 + \frac{D}{A} \right]} \quad (2)$$

Predicted results from this equation are plotted in Figure 3C. Note that any parameter change that increases length is predicted by equation 2 to result in increased intrinsic noise, but changes in different parameters can have different relative effects on intrinsic noise. Changing either the pool size or the IFT efficacy have almost identical effects on noise, and in both cases the increase in the mean squared difference in the length of the two flagella (intrinsic noise) is linearly proportional to the increase in length, so a mutation that causes a doubling of average length should cause approximately a doubling of mean squared length differences. In contrast, changes to the disassembly rate D have a much larger, non-linear effect. It may thus be possible to predict which parameters of the model are affected by distinct mutations, by determining how

much each mutation increases noise relative to average length. In any case a strong prediction of this model is that any parameter change that leads to an increase in length should also increase intrinsic noise in the balance-point length control system.

A second prediction of this model, derived in Materials and Methods, is that the effect of fluctuations will be less quickly damped out in mutants with long flagella. Indeed, the reason that the variance in length is predicted to increase in this model is that the effect of individual fluctuations should damp out more slowly in long-flagella mutants, allowing multiple fluctuations to add up to produce larger deviations from the average solution. The reason this occurs in long-flagella mutants relates to the shape of the assembly versus length curve in the balance-point model (Figure 3B). Considering only small fluctuations, the rate at which any given fluctuation is corrected is roughly the product of the magnitude of the fluctuation times the slope of the assembly versus length curve in the region of the steady-state solution, since the disassembly curve is a horizontal line. Since the assembly versus length curve is an hyperbola, its slope is a continuously decreasing function of length. For long flagella obtained via a decrease in disassembly rate, it is self evident that longer flagellar mutants will have a decreased slope of their assembly curve at the steady state solution, thus fluctuations will persist for longer than wild-type. For long flagella obtained via an increase in either the precursor pool size or the efficacy of IFT, both types of parameter changes have the effect of rescaling the length dependence of the

assembly curve to produce a lower slope at every value of length, again leading to slower damping of fluctuations.

Identifying genes that regulate noise in flagellar length control system

The model derived above predicts that mutants with long flagella should have increased noise and slower fluctuation correlation times. To test these predictions, we measured intrinsic and extrinsic noise in two mutants, *lf1* (McVittie, 1972; Nguyen et al., 2005) and *lf4* (Berman et al., 2003), which cause cells to have abnormally long flagella. It was previously reported that the *lf1* mutation leads to increased variance in length (McVittie, 1972). As indicated in Figure 4A, we find that both mutations lead to increased noise, but in different ways: *lf1* mainly increases intrinsic noise while *lf4* increases both types of noise (Table 1). This suggests the two genes act in fundamentally different ways within the length control system, with the LF4 gene product acting to cell-to-cell variation in length and the LF1 gene product acting to promote equality in length of the two flagella within a cell regardless of their average length. For both mutants, the quantitative effect of the *lf* mutations on noise is much greater than their effect on average length (Table 1), suggesting that the LF genes may have evolved primarily as a means to control length variation, as opposed to setting any particular average length.

In order to determine if the increased intrinsic noise in *lf1* mutants was due to larger dynamic fluctuations, we analyzed fluctuations in individual *lf1* mutant cells using time-lapse microscopy. As shown in Figure 4B, we found that the

fluctuation magnitude of individual flagella was approximately double in lf1 compared to wild type (as judged by the autocovariance value for zero lag). This is the same order of magnitude increase as predicted by the theoretical noise model for mutations affecting either IFT or pool size, but would not be consistent with an alteration in disassembly rate. Moreover, the fluctuations damped out much more slowly in lf1 compared to wild-type as judged by the decay of the autocovariance function. A best fit exponential to the data of Figure 4B indicated a decay time constant of 101 min for wild-type and 183 min for lf1. The linear noise model presented above suggested that lf mutants should have larger variance in length due to slower damping of fluctuations as measured by a slower predicted decay of the autocorrelation function, precisely as we observed for lf1.

The increase in extrinsic noise (cell to cell variation) in the lf4 mutant raises two alternative possibilities about the function of the LF4 gene. One possibility is that LF4 is involved in constraining cell size, such that the lf4 mutant would have a wider variation in size thus leading to a larger level of extrinsic noise. It is indeed the case that the standard deviation in cell diameter increases slightly in lf4 compared to wild type, by a ratio of 1.3, however this is far less than the increase in standard deviation in lengths, so increased cell size variability is unlikely to be the sole explanation for the increased extrinsic noise in lf4. The other possibility is that the lf4 mutation may cause length to depend more strongly on cell size than in wild type. This possibility is supported by the fact that the slope of the best-fit line relating flagellar length to cell diameter increases

from 0.96 in wild type to 1.74 in lf4 cells. This steeper dependence of length on cell diameter could be accounted for by several distinct mechanisms, for example if lf4 mutants had increased IFT in their flagella so that flagellar growth could be sustained at a lower level of precursor protein, or if lf4 mutants had elevated transcription of flagellar precursor protein encoding genes. The present data cannot distinguish these possibilities.

These experimental results reveal that LF1 and LF4 genes act to reduce biological noise in flagellar length. In fact, both genes seem to have a larger effect on noise than they do on the average length, suggesting that noise suppression may be their primary evolutionary purpose.

Discussion

The results presented here show that the flagellar length system exhibits both intrinsic and extrinsic noise. The overall effect of these noise sources is that in a wild-type cell, the coefficient of variation (standard deviation divided by length) is in the range 10-20%, which is comparable to the measured variability in length of vertebrate cilia (Wheatley and Bowser, 2002) and in the length of bacterial flagellar hooks (Koroyasu et al., 1998). While it is commonplace to compare cells and cellular structures with man-made machines, such a high level of size variability would not be tolerable in most man-made machines. It is therefore interesting to consider whether the level of variability and noise that is observed indicates that cells cannot do any better, or alternatively that they do not need to do any better. The close matching between the distribution of flagellar lengths in wild-type cells and the length range for optimal swimming speed (Figure 2) strongly suggests that the latter explanation is correct - there is no evolutionary pressure to reduce variability in size to a level below the minimum tolerable for effective swimming.

Our results show that the dependence of noise on length can in principle be explained by a dependence of the noise damping rate on parameters of the flagellar maintenance system that regulate length. Attempts to use noise measurements to define parameters precisely is currently hampered by the fact that we do not know the ultimate source of the noise. One possibility is that intraflagellar transport may show fluctuations in its rate over time, thus producing

random variations in the growth rate at the tip. Other sources of variation could include stochastic fluctuations in cargo loading or transport through the flagellar pore. Future studies using quantitative imaging methods will be necessary to determine which microscopic features of the system correlate with macroscopic fluctuations in length.

Finally we consider how best to exploit this analysis for understanding the function of new length-control mutants. The ability to discriminate the effects of mutations on different parameters based on different effects on noise is potentially quite powerful. However, while we currently have at least a first order approximate model to describe the effect of length-altering parameter changes on intrinsic noise, we lack a similar formalism for interpreting differences in extrinsic noise. One clear question that remains to be answered in this regard is the mechanistic basis for the linear correlation between cell diameter and flagellar length. The simplest possibility is that larger cells have more ribosomes and therefore make more precursor protein to support longer flagella, however in such a case we might have naively expected flagellar length to scale with cell volume rather than diameter. The mechanisms that ensure proper scaling of organelle size with cell size are largely unknown (Chan and Marshall, 2010), and we suggest that flagella may be an excellent model system in which to investigate the origin of such scaling relations

Conclusions and prospects for future studies

Our results show that concepts of intrinsic and extrinsic noise are not merely of theoretical interest in high-precision gene expression studies, but rather are directly applicable to biologically relevant structure and function at the level of cells and organelles.

Figure 1

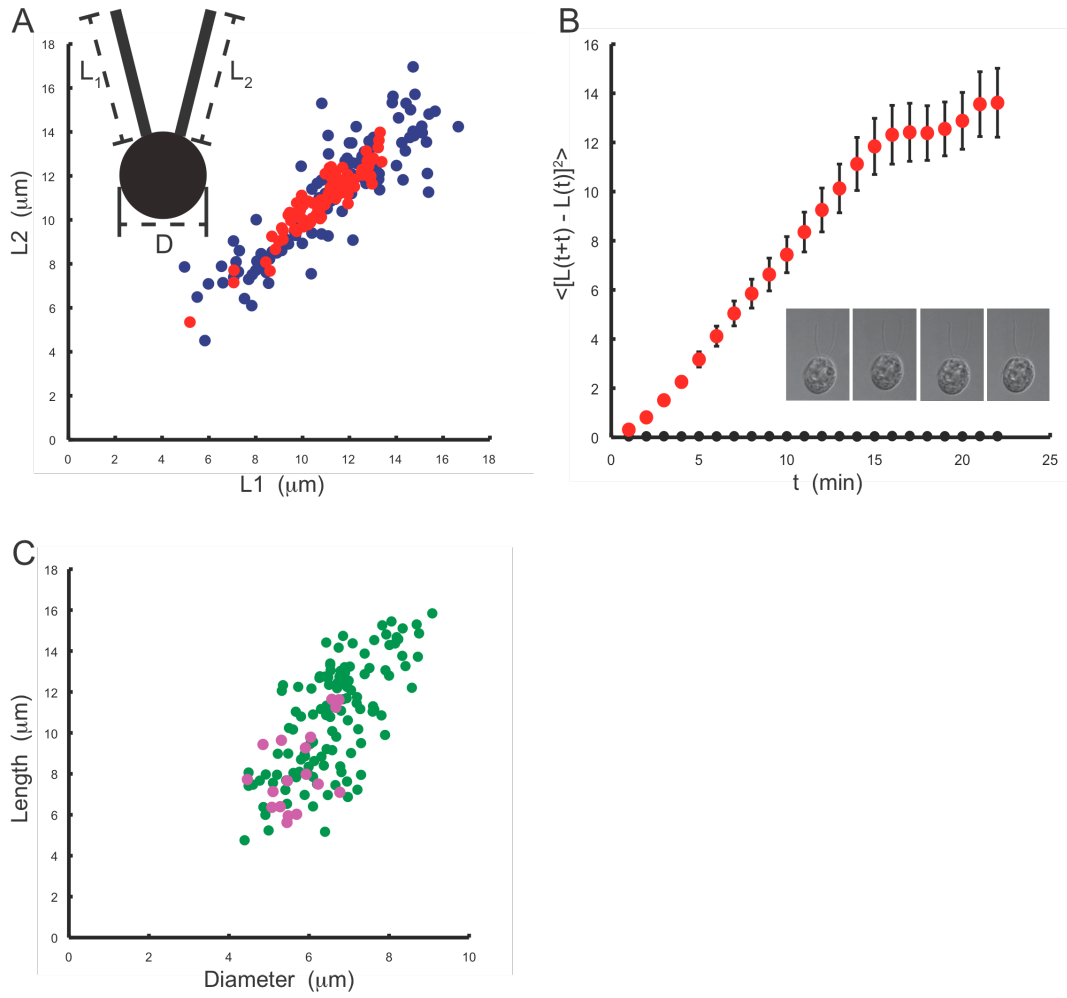


Figure 1. Measuring intrinsic and extrinsic noise in flagellar length control system.

(A) Intrinsic and extrinsic noise can be visualized in measurements of flagellar length in cells with two equivalent flagella. Graph plots length of one flagellum versus length of the other flagellum. Extrinsic noise is reflected by scatter along the diagonal $L_1=L_2$. Intrinsic noise is reflected by scatter perpendicular to this axis. (Blue) wild-type asynchronous culture, (Red) wild-type gametes. (Inset) Cartoon of a *Chlamydomonas* cell showing the three measurements used in this paper. (B) Fluctuations in length observed in living cells. (Red) Mean squared change in length plotted versus time, showing constrained diffusion-like behavior. Error bars signify standard error of the mean. (Black) Mean squared change in length in glutaraldehyde-fixed cells as an indicator of measurement error. (Inset) Four successive time points of a 3D time series of a single living cell embedded in agarose and imaged with DIC microscopy, as used to generate the data in this plot. (C) Contribution to extrinsic noise from cell size variation measured by correlation between length with cell diameter in asynchronous cultures. (Green) Wild-type cells. (Pink) *mat3* mutant cells that have smaller average size than wild-type.

Figure 2

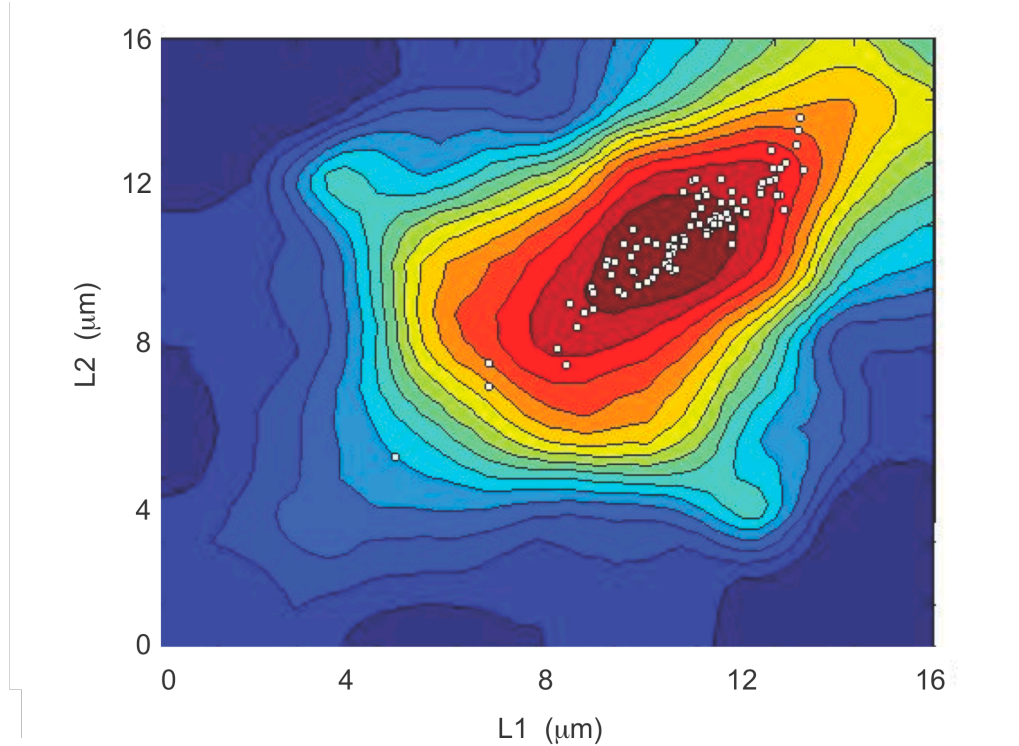


Figure 2. Noise affects fitness.

Contour plot of swimming speed (red fastest, blue slowest) versus the lengths of the two flagella. White dots signify lengths of wild-type gametes superimposed on swimming speed distribution, showing that wild-type cells have flagellar lengths optimally tuned to the ideal range for maximal swimming speed.

Figure 3

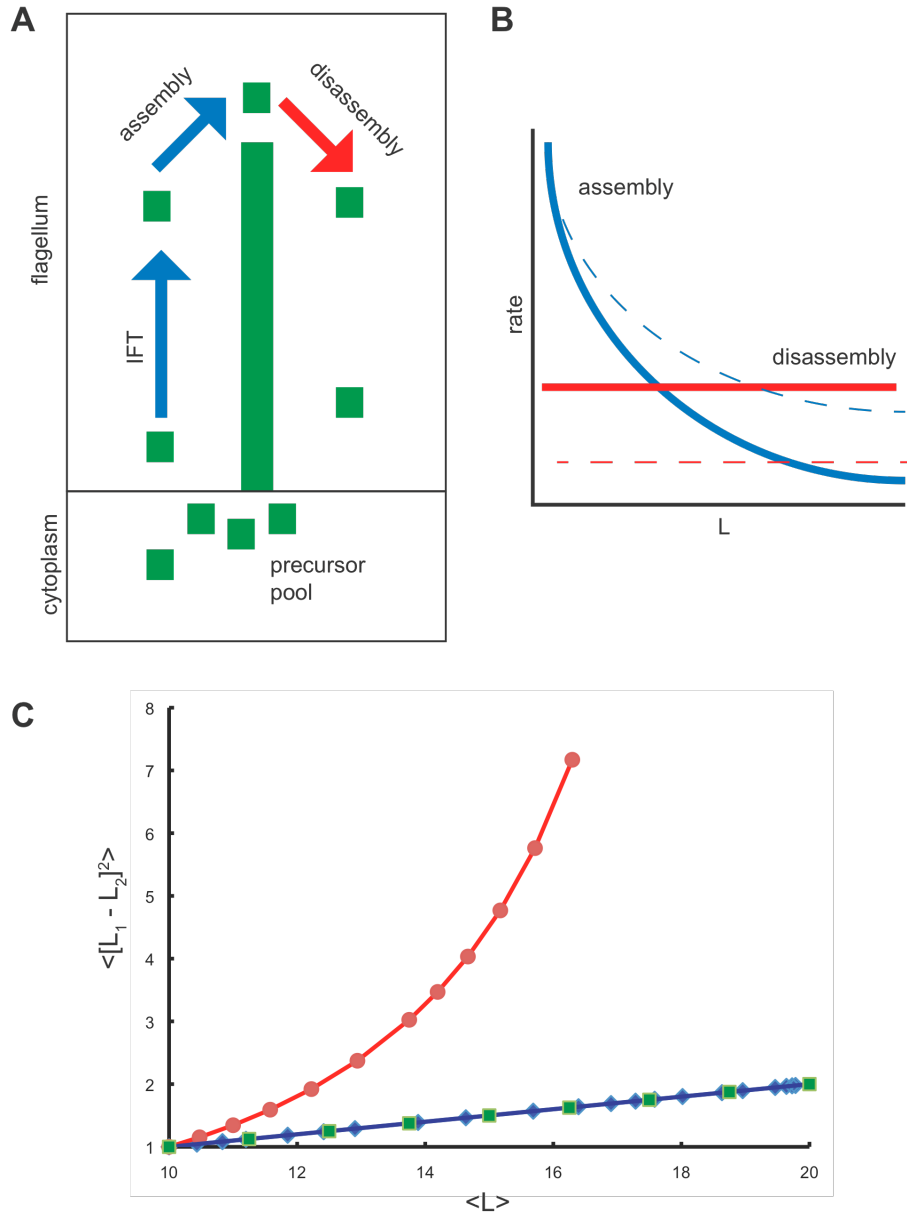


Figure 3. Noise analysis of a length control system model.

(A) Schematic of balance-point mode for flagellar length control. Flagellar microtubules undergo constant disassembly (red arrow) at a length-independent rate D . This disassembly is balanced by assembly, which occurs at a rate limited by the rate of intraflagellar transport (blue arrow). Assuming the number of IFT particles is length-independent, the frequency of cargo delivery at the tip is proportional to $1/L$. Precursor protein from the cytoplasm binds with first order binding. The available free precursor pool is the total pool P minus the quantity of precursor already incorporated into the two flagella. Hence the net assembly rate is given by $A(P-2L)/L$. (B) Steady-state length is determined by the balance point between length-independent disassembly (Red line) and length-dependent assembly (blue line). Mutations can increase flagellar length either by increasing assembly (blue dotted line) or decreasing disassembly (red dotted line). (C) Results of small signal noise analysis. Plot shows the mean squared difference in the length of the two flagella plotted versus length as parameters A (describing the efficacy of IFT), D (describing the rate of steady state axoneme disassembly), or P (describing the total pool of flagellar precursor protein) are changed so as to increase length from 10 to 12 microns. (red circles) results of decreasing D , (blue diamonds) results of increasing A , (green squares) results of increasing P . Since the strength of the noise source is not known, all results are normalized to a value of 1 at the wild-type length of 10 microns. Parameter values for the wild-type case are those previously derived from experimental measurements (Marshall and Rosenbaum, 2001).

Figure 4

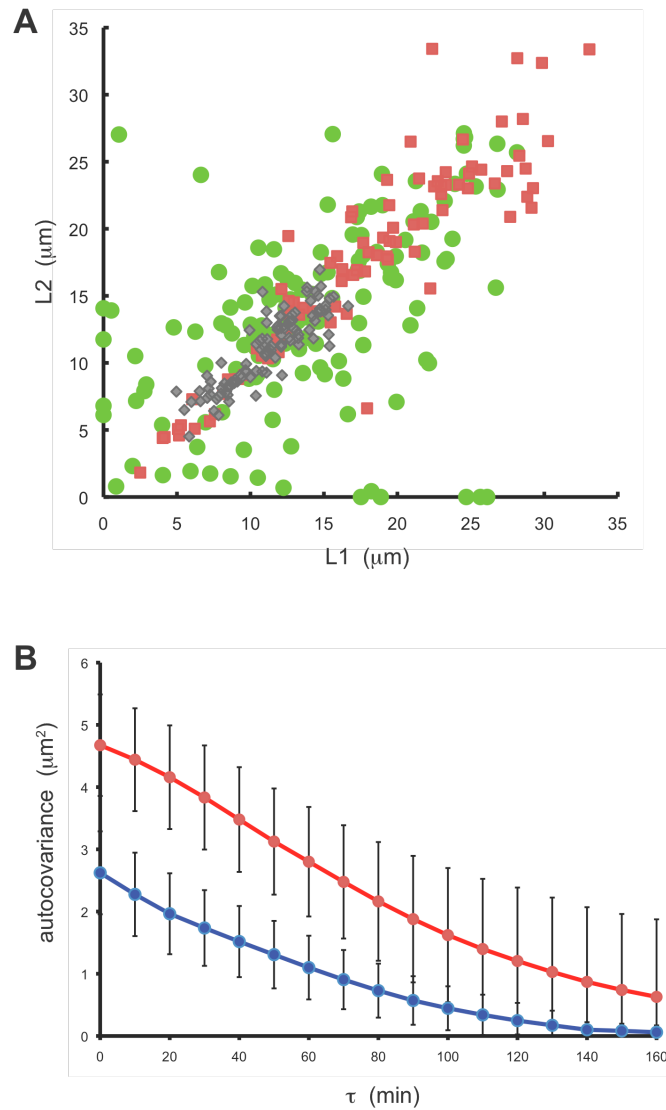


Figure 4. Identification of genes that participate in flagellar length noise suppression.

(A) increased intrinsic and extrinsic noise in long flagella mutants. (green circles) *If1*, (red squares) *If4*, (gray diamonds) wt. All data shown is from asynchronous cultures. (B) Autocovariance of *If1* (red) versus wild-type (blue) based on measurements of length fluctuations in living cells, showing higher mean squared fluctuations (based on covariance at zero lag) and slower decay as predicted for *If* mutants by linear noise model.

Table 1. Results of noise calculations. <L> denotes average flagellar length, with standard deviation listed. <D> is the average cell diameter. r is the correlation coefficient between flagellar length and cell diameter. Noise measures h^2 listed are the actual measurements multiplied by 100. n is the number of cells measured. 95% confidence intervals for noise measures are given in parentheses.

Strain	<L>	<D>	r	$h^2_{int} (x10^{-2})$	$h^2_{ext} (x10^{-2})$	n
<u>Asynchronous cultures</u>						
wt	11.1±2.7	6.8±0.9	0.61	0.73 (0.54-0.95)	5.0 (4.0-6.1)	105
If1	13.8±6.9	6.1±1.2	0.27	13.5 (9.1-18.7)	10.8 (6.9-15.0)	141
If4	17.8±7.4	6.2±1.2	0.22	1.5 (0.92-2.08)	15.6 (11.4-20.0)	88
<u>Cell-cycle arrested</u>						
wt (dark)	9.9±0.9	6.2±1.0	0.75	0.32 (0.25-0.41)	0.57 (0.38-0.78)	70
wt (gamete)	10.9±1.4	5.2±0.7	0.07	0.12 (0.09-0.15)	1.6 (1.0-2.3)	92
If1 (gamete)	13.9±5.7	4.5±0.9	0.36	2.2 (1.1-4.2)	12.2 (5.8-18.3)	18
If4 (gamete)	23.5±8.4	5.2±0.7	0.06	1.8 (0.57-3.7)	10.8 (3.6-20.9)	22
<u>Functional selection</u>						
fast divers	11.1±1.2	6.1±1.0	0.51	0.42 (0.25-0.64)	0.73 (0.51-0.94)	106
slow divers	9.4±2.4	6.0±1.0	0.39	2.9 (1.7-4.4)	3.6 (1.8-5.7)	108

References

- Adams, G.M., R.L. Wright, and J.W. Jarvik. 1985. Defective temporal and spatial control of flagellar assembly in a mutant of *Chlamydomonas reinhardtii* with variable flagellar number. *J. Cell Biol.* **100**:955-64.
- Berman, S.A., N.F. Wilson, N.A. Haas, and P.A. Lefebvre. 2003. A novel MAP kinase regulates flagellar length in *Chlamydomonas*. *Curr. Biol.* **13**:1145-9.
- Chan, Y.H. and Marshall W.F. 2010. Scaling properties of cell and organelle size. *Organogenesis* **6**:88-96.
- Coyne, B., and Rosenbaum, J.L. 1970. Flagellar elongation and shortening in *Chlamydomonas*. II. Re-utilization of flagellar proteins. *J. Cell Biol.* **47**:777-81.
- M.B. Elowitz, A.J. Levine, E.D., Siggia, and P.S. Swain. 2002. Stochastic gene expression in a single cell. *Science* **297**:1183-6.
- E.H. Harris. The *Chlamydomonas* sourcebook. Academic Press, San Diego, CA 780 pp. (1989)
- Hilfinger, A, and Paulsson, J. 2011. Separating intrinsic from extrinsic fluctuations in dynamic biological systems. *Proc. Natl. Acad. Sci. U.S.A.* **108**:12167-72.
- J. Honerkamp. Stochastic dynamical systems. Wiley-VCH, New York, NY. 535.(1994).
- Kaern M, Elston TC, Blake WJ, Collins JJ. 2005. Stochasticity in gene expression: from theories to phenotypes. *Nat. Rev. Genet.* **6**:451-64.
- Koroyasu S, Yamazato M, Hirano T, Aizawa S. 1998. Kinetic analysis of the growth rate of the flagellar hook in *Salmonella typhimurium* by the population balance method. *Biophys. J.* **74**:436-443.
- W.F. Marshall and J.L. Rosenbaum. 2001. Intraflagellar transport balances continuous turnover of outer doublet microtubules: implications for flagellar length control. *J. Cell Biol.* **155**:405-14.
- W.F. Marshall, H. Qin, M. Rodrigo Brenni, and J.L. Rosenbaum. 2005. Flagellar length control system: testing a simple model based on intraflagellar transport and turnover. *Mol. Biol. Cell* **16**:270-8.

- S.S. Merchant, et al. 2007. The *Chlamydomonas* genome reveals the evolution of key animal and plant functions. *Science* **318**:245-50.
- R.L. Nguyen, L.W. Tam, and P.A. Lefebvre. 2005. The LF1 gene of *Chlamydomonas reinhardtii* encodes a novel protein required for flagellar length control. *Genetics* **169**:1415-24.
- Randall J. 1969. The flagellar apparatus as a model organelle for the study of growth and morphopoiesis. *Proc. Roy. Soc. B.* **173**:31-62.
- Raser, J.M. and O'Shea, E.K. 2004. Control of stochasticity in eukaryotic gene expression. *Science* **304**:1811-14.
- J.L. Rosenbaum, J.E. Moulder, D.L. Ringo. 1969. Flagellar elongation and shortening in *Chlamydomonas*. The use of cycloheximide and colchicine to study the synthesis and assembly of flagellar proteins. *J. Cell Biol.* **41**:600-19.
- J.L. Rosenbaum and G.B. Witman. Intraflagellar transport. 2002. *Nat. Rev. Mol. Cell Biol.* **3**:813-25.
- G.J. Pazour and J.L. Rosenbaum. 2002. Intraflagellar transport and cilia-dependent diseases. *Trends Cell Biol.* **12**:551-5.
- C.D. Silflow and P.A. Lefebvre. 2001. Assembly and motility of eukaryotic cilia and flagella. Lessons from *Chlamydomonas reinhardtii*. *Plant Physiol.* **127**:1500-7.
- Taniguchi, Y., Choi, P.J., L, G.W., Chen, H., Babu, M., Hearn, J., Emili, A., and Xie, X.S. 2010. Quantifying E. coli proteome and transcriptome with single-molecule sensitivity in single cells. *Science* **329**:533-8.
- Umen, J.G., and Goodenough, U.W. 2001. Control of cell division by a retinoblastoma protein homolog in *Chlamydomonas*. *Genes Dev.* **15**:1652-61.
- Van Kampen, N.G. 1992. Stochastic processes in physics and chemistry. North Holland Press, Amsterdam.
- K.A. Wemmer and W.F. Marshall. 2007. Flagellar length control in *Chlamydomonas* - a paradigm for organelle size regulation. *Int. Rev. Cytol.* **260**:175-212.
- D.N. Wheatley and S.S. Bowser. 2000. Length control of primary cilia: analysis of monociliate and multiciliate PtK1 cells. *Biol. Cell* **92**:573-82.

Chapter 5

Identification of New Protein Components of the *Chlamydomonas* Central Pair

Identification of New Protein Components of the
***Chlamydomonas* Central Pair**

Kimberly A. Wemmer, Juliette Azimzadeh, and Wallace F. Marshall

Dept. of Biochemistry & Biophysics
University of California, San Francisco

Introduction

Flagella are microtubule-based structures that propel cells through the surrounding fluid. The internal structure of most motile cilia and flagella consists of nine parallel doublet microtubules arranged around a central pair of singlet microtubules (Figure 1). Force for propulsion is provided by thousands of dynein motors, anchored in two rows along one side of each doublet and organized into multi-headed complexes called the inner and outer dynein arms, that can walk along the microtubule of the adjacent doublet. In order to produce coordinated bending of the flagellum, these dynein motors must produce their power strokes in synchrony, like the oarsmen on an ancient Mediterranean war-galley. But while the oar-strokes were coordinated by a continuous drum-beat, flagellar dynein motors are synchronized in a much more complicated manner. In *Chlamydomonas* flagella, there is significant evidence that the coordination of dyneins occurs through the influence of the central pair microtubules via other axonemal structures.

While flagella may beat without the presence of a central pair - for example, cilia in the mouse node and paralyzed *Chlamydomonas* flagella that carry suppressing mutations (Porter et al., 1992) - when the central pair is present and active it imposes a higher-order regulation on the movement of the axoneme and enables the formation of a more complex three-dimensional waveform (Omoto et al., 1999). While we focus on this very common type of ciliary movement here, a type found, for example, in the human airway and very well studied in *Chlamydomonas* flagella, it is worth noting that types of ciliary waveform are

potentially as diverse as the organisms that perform them. Trypanosomes, for instance, have a very unusual type of flagellar motility and exhibit a central pair with a fixed orientation (Branche et al., 2006), in stark contrast to the more commonly found waveform described below.

As discussed in Chapter 1, the central pair is a complex sub-structure within the flagellum, which contains not only a pair of microtubules, C1 and C2, but also an elaborate set of projections (Figure 1). Various projections from the central pair are responsible for different behaviors, for example, studies in sea urchin sperm and *Chlamydomonas* show that only those dynein arms located near one side of the central pair C1 microtubule are active, while the rest are inactive (Nakano et al., 2003; Wargo and Smith, 2003). By demonstrating that this region of the central pair stimulates dynein activity, these studies and others have identified an important functional role for the asymmetry seen in central pair projections.

The regulation of the axonemal dyneins to produce a highly effective flagellar waveform is a fascinating area of study. The dynein arms, located all around the circumference and down the length of flagella, must be differentially regulated; if all the motors were active simultaneously no effective beating, and therefore no net propulsion, could be produced.

The central pair regulation of the dynein arms is a complicated signaling pathway that runs through many of the structures found in the flagellar axoneme. The projections on the central pair interact with the radial spoke head (Kohno et al., 2011), inducing a change in state on the radial spoke. The resulting signaling

cascade is not well understood, but likely involves use of secondary messengers, especially calcium, signaling to the dynein regulatory complex located on the A tubule of the outer doublets (this complex is also known as the nexin link, Heuser et al., 2009). The involvement of calcium in this signaling pathway is suggested by the abundance of calcium binding proteins found in these structures, and well as studies that have found that changes in the concentration of calcium can alter the behaviors of isolated axonemes *in vitro* as well as swimming patterns *in vivo* (Kawai et al., 2009; Omoto and Brokaw, 1985; Smith, 2002). Additionally, pH and cAMP signaling have been implicated in effecting flagellar beating (Rubin and Filner, 1973).

The central pair itself must be a dynamic structure in order to cycle through the various stages of a single beat of a flagellum, and then reset for the next stroke. Isolated central pairs have an inherent twist, with the C1 tubule found along the outer edge of curves in the microtubules. This same orientation of the C1 and C2 tubules are found *in vivo* in bends in the *Chlamydomonas* flagellum (Mitchell and Nakatsugawa, 2004). As the central pair apparatus rotates within a flagellum, the C1 microtubule contacts specific subset of radial spokes, which in turn relay a regulatory signal to the dynein arms on a particular region of certain doublet microtubules, activating only those motors and generating a sliding force between designated outer doublet microtubules. As the microtubules of the axoneme are anchored at their base in a cell, this force generates a bend in the flagellum.

Intriguingly, the propagation of this bend itself drives the rotation of the

central pair within the flagellum, thereby causing the activation of a new set of dyneins and generating force between a different set of out doublets, changing the shape of the stroke being executed as the stroke is happening (Mitchell and Nakatsugawa, 2004). The fact that upon the completion of a stroke the flagellum is able to begin another indicates, therefore, that the inherent geometry of the axoneme itself helps to drive the mechanical changes that must occur to make a flagellum beat.

In order for all these interactions to occur in their prescribed manner, cells must properly assemble the axoneme. This apparently complicated task becomes simplified when the modular structure of the flagellum is taken into account. Each outer doublet consists of a 96nm repeat structure, which contains a fixed set of dynein arms and radial spokes (Mastronarde et al., 1992). Because this basic structure is repeated through the length of the structure, the cell is able to focus on assembling many copies of one small structure over and over rather than a single, large, complicated one. The 96nm repeat functional module can be further broken down into smaller pieces, such as the radial spoke and the dynein arms, which self-assemble within the cytoplasm, either entirely or in smaller sub-assemblies. They are then added onto the growing structure, rather than building each protein subunit onto the microtubules themselves (Fowkes and Mitchell, 1998; Qin et al., 2004; Yang et al., 2001). This kind of organization and building plan would allow the cell to build an intricate structure very simply, by assembling a few pieces that fit well together, rather than trying to place each protein into a specific position along the entire length of the flagellum.

However, when structural abnormalities in the axoneme do occur, they can cause paralysis of the cilia, leading to disease. Motile cilia are important to the functioning of several different tissues in animals; this type of cilia is found on respiratory epithelia, ependymal cells on the ventricular surface of the brain, on the middle ear epithelia, on the fallopian tube epithelia, and makes up the tail of sperm cells. Moreover, motile cilia are crucial to establishing the left-right axis in vertebrates, as they function to create fluid flow in organs analogous to the mouse node, and this flow directs the first left-right asymmetric signaling in the embryo. When motility of cilia is impaired in humans, it can cause diseases such as primary ciliary dyskinesia (PCD) and Kartagener's syndrome, with patients commonly exhibiting chronic sinusitis, bronchiectasis, neonatal respiratory distress, male infertility, and situs inversus. These patients occasionally also have hydrocephalus, female infertility, otitis media, or retinitis pigmentosa (Lee, 2011). Nearly all of the pathologies affecting people with ciliary motility disorders can be traced to a defect in moving fluid through the tissues in which these cilia are found, causing increased rates of infection and inflammation. The severity of the disease is likely directly proportional to the severity of the mutation, and therefore the degree of ciliary impairment. Given the diverse number of ways ciliary motility may be eroded, it is to be expected that a wide spectrum of phenotypes may be seen in patients with different genetic lesions.

Additionally, signaling pathways may be involved in regulation of the central pair structure. Fused, a component of the Hedgehog signaling pathway, has recently been shown to be essential for construction of the central pair in mouse,

leading of course to defects in ciliary beating and the resulting developmental defects (Wilson et al., 2009).

In *Chlamydomonas*, there are several different types of mutants that cause paralysis of flagella, effecting all the various components of the axoneme important to generating ciliary beating: the dynein arms, the radial spokes, and the central pair (examples include: *pf24* and *pf15*; Yang et al., 2004; Dymek et al., 2004). Here, we utilize two *Chlamydomonas* mutants, *pf15* and *pf18* (Dymek et al., 2004; Warr et al., 1966), which completely lack the central pair of their flagella, to identify new components of the central pair apparatus. The *pf15* strain carries a mutation in the p80 subunit of Katanin, a heterodimeric protein with microtubule-severing activity. The mechanism behind the action of katanin's effects on the central pair is the subject of the research of others, including Elisa Kannegaard in the Marshall Lab. While the *pf18* strain is used fairly frequently in the study of *Chlamydomonas* flagella, the genetic lesion that causes this phenotype has yet to be identified.

In this work, we compare the protein content of axonemes isolated from *pf15* and *pf18* cells to wild type axonemes, and identify two excellent candidates, FAP161 and FAP21 (also identified as BUG15 and MOT35), as new components of the central pair.

Materials and Methods

***Chlamydomonas* strains used in this study and culture conditions**

Strains cc125 (WT), cc1033 (*pf15*), and cc1036 (*pf18*) were used in the 2D-DIGE

analysis. Strains cc849 (*cw10*, cell wall-less 10) was used for transformation. All strains were obtained from the *Chlamydomonas* Center (www.chlamy.org). Strains were maintain on TAP plates then were grown in liquid TAP media in constant light at room temperature or 21C with agitation (5mL cultures in 18mm test tubes were grown on roller drums, 100-200mL cultures were grown on an orbital shaker running at 150rpm, and large 1L cultures were grown with gentle stirring and bubbling with house air).

Mid-scale flagellar isolation protocol

1-3 small cultures of 120mL were started with half a loop's worth of cells from TAP plates, then were grown for 3 days as described above. 100mL of each of these cultures were used to start a 1L TAP culture in a 2L flask which was grown for 5 to 7 days (this protocol works well for any starting culture volume from 1 to 3 liters). Cultures were checked visually for the presence of flagella. Each 1L culture was spun down in 1L bottles at 1500xg in a Beckman Coulter Avanti J-20XP centrifuge in a JLA 8.1000 rotor for 10 minutes (min) at 19-21C with a low brake. The cells were re-suspended in 150 to 200mL TAP media, transferred to a Corning 250mL centrifuge tube (430776) and then spun again at ~1000xg (2000rpm in a Beckman Coulter Allegra 6 with a GH3.8 rotor) for 10min at RT with no brake. Cells were re-suspending in 80mL TAP and transferred to a flask, where they were allowed to recover for 2 hours at RT in the light with gentle stirring and bubbling. These cultures were then pH shocked in the following way: a calibrated probe from a pH meter was inserted into the culture, at 0min 0.5M

acetic acid was added until the pH of the culture was between 4.5 to 4.6 typically within 30 seconds of first adding the solution. At 1.5min, 0.5M KOH was added until the culture reached a pH of between 7 and 7.2, again typically within 30 seconds, then 100 μ L of Sigma protease inhibitor cocktail (P8340) and 100 μ L of 100mM of EGTA, pH7.5 were added to the culture, which was then transferred to a 250mL tube and placed on ice. The efficiency of the pH shock was verified visually. The rest of the protocol was completed on ice. The culture was spun at \sim 1000xg (2000rpm GH3.8 rotor in an Allegra 6R centrifuge) for 10min at 4C with no brake. The supernatant was removed and transferred to a new tube, and the cell bodies were discarded. 50mL of 25% sucrose in TAP with red food coloring, to allowed it to be seen, was pipetted beneath the supernatant as an underlay, and the tube was spun at \sim 2500xg (3300rpm GH3.8 rotor) for 10min at 4C with no brake. The entire supernatant and the interface between the two layers was collected, transferred to a new tube, and the entire underlay process repeated. The entire supernatant and interface was again collected, transferred to a new tube, and placed on ice. 35mL of this supernatant at a time was transferred to a 50mL Nalgene polycarbonate centrifuge tube (3117-0500) and spun at \sim 16000xg (10000rpm in a HB-4 rotor in a Sorvall RC5C centrifuge) for 20min at 4C. The supernatant was discarded, and the next aliquot placed in the tube and spun. This was repeated until the entire sample was pelleted. The pellet was re-suspended in 1mL Applied Biomic's Cell Washing Buffer (10mM Tris-HCl, 5mM magnesium acetate, pH 8.0) and transferred to a 1.5mL microfuge tube. The quality of the isolation was assayed visually, checking for high concentrations of

flagella with low amounts of cell body debris. The isolated flagella were pelleted one final time at ~20000xg (14000rpm in an Eppendorf 5417C centrifuge) for 20min at 4C, the supernatant aspirated, and the pellet frozen in liquid nitrogen, then transferred to a -80C freezer.

2D DIGE and protein identification

Sample labeling, 2D DIGE, image analysis, spot analysis using DeCyder software, excision from gel, and identification using mass spectrometry were all performed by Applied Biomics, Hayward, CA (<http://www.appliedbiomics.com>).

Gene identification

Central pair candidate proteins in most species were identified using the NCBI protein BLAST resource, and the reciprocal best hits were retained as putative homologs. For Planaria, the *Schmidtea mediterranea* Genome Database was used (<http://smedgd.neuro.utah.edu>).

cDNA cloning

To obtain all FAP161 and FAP21 sequences, RT-PCR was performed on total RNA isolated using TRIzol (Invitrogen, 15596-026) according to the manufacturer's instructions. For the *Chlamydomonas* sequences, strain cc125 was used as source for RNA and the cDNAs were amplified using the primers listed below, then inserted into pKL3-HA+hyg and pKL3-GFP+hyg using NheI for FAP161 and SpeI for FAP21. The pKL3 vectors were all cut with NheI. All

enzymes are from NEB. These vectors were constructed by adding the hygromycin resistance cassette to two vectors, pKL3-HA and pKL3-GFP, which were derived originally from pKL3 (and were generous gifts from Karl-Ferdinand Lechtreck of the Witman Lab, Lechtreck and Witman, 2007), an expression vector that drives transcription of any gene with the *LC8* promoter and terminator regions. For Planaria, the RNA was isolated from the asexual strain, the cDNA sequences for our genes of interest amplified using the primers listed below, and the sequences were cloned into pPR-T4P, a modified pDONR-dT7 in which the gateway cloning site was replaced by a ligation-independent cloning site (kind gift from J. Rink).

Gene		Primer Sequence
Chlamy FAP161	F	GCTAGCCAGGGACACCACAAAATACAATG
	R	GCTAGCGCCCGCGCCCCCGCCGCGCTGCTGGCCGCCCGCAGGTC GTTTCGGAAG
Chlamy FAP21	F	ACTAGTCTCTTACTACGCAATCCCTCCGACGGACAAACTATG
	R	ACTAGTGCGAAGGTTGGTTCGATCTGCA
Smed FAP161.1	F	CATTACCATCCCGGCAACAAACGTACTTATAACTCATCA
	R	CCAATTCTACCCGGACATCCATTTCCGGCTTTGTG
Smed FAP161.2	F	CATTACCATCCCGTCATTGACAGCTGGTTTGACA
	R	CCAATTCTACCCGCCTTCGTGTTGAAGCCTTTTTTC
Smed FAP161.3	F	CATTACCATCCCGCAACGGCAAAACAATCTAAACATC
	R	oligo dT
Smed FAP21	F	CATTACCATCCCGGCCTAATCATGTGTTTGGAAC
	R	CCAATTCTACCCGGCCAGTTAAAGCTGTCAGTAAA

Note: The Smed FAP161.3 primer pair was non-productive.

RNAi via dsRNA injection

Sense and antisense DNA templates for *in vitro* transcription were obtained by amplifying sequences cloned into pPR-T4P using the following primer pairs:

Sense F: AACCCCTCAAGACCCGTTTAGA and R: GAATTGGGTACCGGGCCC;

Antisense F: CCACCGTTCCATGGCTAGC and R: GAGGCCCAAGGGGTTATGTG

dsRNA was synthesized using the T7 Ribomax Express RNAi system (Promega, Madison, WI). For standard RNAi experiments, 10 ~ 0.8-1cm long planarians were injected 3 consecutive days with 20-50ng dsRNA per injection using a Nanoject II injector (Drummond Scientific, Broomall, PA). The animals were then amputated from their head and tail at day 4. An additional injection was performed at day 11 and the flatworms were amputated again pre- and post-pharyngically at day 12. Phenotypes were assessed on regenerating heads, tails and trunks at day 21 (10 days after the second amputation). This protocol was modified slightly as described below to compensate for the unstable phenotype.

	experiment1	experiment2
Injection 1	day 1	day 1
Injection 2	day 2	day 2
Injection 3	day 3	day 3
Amputation 1	day 4	day 4
Injection 4	day 12	day 10
Injection 5	/	day 12
Amputation 2	day 13	day 14
Imaging	day 24	day 22

Imaging of Planaria

Live images were acquired using a Stemi 2000C stereomicroscope equipped with an AxioCam MRc digital microscope camera (Carl Zeiss MicroImaging, Thornwood, NY). Planarian locomotion speed was determined using ImageJ software, by measuring the distance covered by a single worm between frames separated by known time intervals.

Transformation of Chlamydomonas by glass beads

This protocol is modified slightly from Kindle, 1990. cc849 cells were grown in 200mL of TAP media at room temperature (RT) in constant light on an orbital shaker to a density of about 1×10^7 cells/mL. Cells were spun down in 50mL conical tubes at $\sim 1000 \times g$ (2000rpm in a Beckman Coulter Allegra 6 with a GH3.8 rotor) for 5min at RT, then re-suspended in M-N media in 1/2 the volume of the original culture. Cells were then returned to the same conditions above for between 3.5 to 4 hours. The cells were pelleted as before, and the supernatant dumped out from the tube, leaving traces of media. The cells were re-suspended in the remaining media, creating a very thick culture, and added to 13mm glass tubes containing roughly 300 μ L pre-autoclaved 780-1180 μ m glass beads, 1-2 μ g linearized DNA, and 100 μ L 20% PEG 8000 solution. The tubes were vortexed for 45 seconds on high, then the transformation was added to 10mL TAP in a culture tube. The cells were recovered for 24 to 48 hours at RT in constant light at 21C. The cells were spun down in 15mL conical tubes as described before and immediately decanted, then re-suspended in 200 μ L of untransformed culture, plated on selective TAP media, and gently spread onto the media. The plates were allowed to dry, then transferred to a clear, humid box and grown at RT in constant light. Colonies would typically appear in 5 to 7 days.

Results

Generating a list of candidate central pair proteins

In this work we make use of the rich history of mutational studies done in *Chlamydomonas*. Using the logic that proteins missing in flagella isolated from mutants lacking their central pair apparatus would likely be components of that structure, we compared the protein content of the flagella isolated from two central pair deficient mutants, *pf15* and *pf18*, to the protein content of wild type (WT) flagella.

We developed, based on previously published protocols, a mid-size procedure for isolating *Chlamydomonas* flagella, as detailed in the Materials and Methods section. *Chlamydomonas* cells were pH shocked, and their flagella were isolated using sucrose cushions to separate flagella from cell bodies (see Figure 1 for overview). The efficiency of the pH shock and enrichment of flagella in the final preparation were confirmed visually using DIC microscopy, which also allowed for the verification of low amounts of cell body contamination of the preparation.

Flagella from WT, *pf15*, and *pf18* *Chlamydomonas* strains were isolated and differentially labeled, then subjected to 2D DIGE. Briefly, the proteins of the isolated flagella were separated using 2-dimensional gel electrophoresis. The fold enrichment of individual spots on the gel was determined in pair-wise comparisons between the three different samples, and spots with a 1.5 fold change or more were excised from the gel and their identity determined using mass spectrometry.

This gave us a working list of central pair candidate proteins. We were disappointed that the few known central pair proteins, CPC1, Hydin,

PF20/SPAG16, and PF16/SPAG6, were not included in our list. However, the presence of phosphoglyceromutase suggested that this list did in fact include protein constituents of the central pair, as this enzyme acts immediately upstream of enolase, which has previously been identified as a central pair component (Mitchell et al., 2005). The list also included a number of protein components of the radial spoke complex which directly contacts the central pair. This provides some evidence that our list includes proteins associated with the central pair of *Chlamydomonas*.

In order to provide further evidence that this list of candidates might in fact be components of the central pair we looked for their presence in other species with motile cilia, and their absence in *Thalassiosira pseudonana*. *Thalassiosira* are well-studied marine diatoms, and this particular species was the first eukaryotic marine phytoplankton to be sequenced. Importantly, it has flagella that lack central pairs, along with the several other flagellar structures that are responsible for regulating waveform, including the radial spokes and inner arm dyneins (Heath and Darley, 1972; Manton et al., 1970). This absence of the central pair makes it ideal for this type of comparison - genes for proteins that are lacking in *Thalassiosira* flagella are more likely to be central pair components. Most of the proteins on our candidate list do have homologs in other ciliated organisms (data not shown), and among those candidates we failed to find homologs in *Thalassiosira* in only 4: IDA4, FAP21, RSP9, and FAP161. IDA4 and RSP9 have already been identified as inner arm dynein and radial spoke proteins, respectively, and therefore are clearly not the central pair candidates

we are interested in. FAP161 and FAP21, however, are two proteins of previously undescribed function, and are excellent candidates to be identified as new central pair components.

Further validation of FAP161 and FAP21 as central pair candidates

Importantly, both FAP161 and FAP21 are strongly represented in the axonemal fraction of the *Chlamydomonas* flagellar proteome (Pazour et al., 2005), and the transcripts of both are robustly up-regulated upon the initiation of flagellar regeneration (Stolc et al., 2005). This data is consistent with proteins that are an integral part of the structure of the axoneme itself.

To give us some hint towards their molecular function, we searched for conserved protein domains within FAP161 and FAP21 using various domain finding programs available online, including the NCBI Conserved Domain Search and the EMBL SMART site. Unfortunately, we were unable to find any homology to any known domains within these two sequences, leaving us with no further information about the role they play within flagella.

We searched in several other organisms for proteins with homology to FAP161 and FAP21, to confirm their importance in ciliated organisms. Promisingly, in nearly every organism with motile cilia in which we searched, we found homologs, while we found none in *C. elegans*, which contain no motile cilia at all (Figure 4). The protein Rib72, a component of the ribbon structure of the A-tubule of the outer doublets, is included as a control for axonemal proteins that are not part of the central pair. Its appearance in all organisms with cilia

indicates that the absence of FAP161 and FAP21 in organisms lacking motile cilia is significant. While we did not find homologs of FAP161 in either *Monosiga* (a choanoflagellate) or *Giardia*, we believe that this is likely due to the presence of gaps in the current versions of those genomes. The pattern of appearance of FAP161 and FAP21 in organisms with motile cilia containing central pairs, and their absence from *Thalassiosira* and *C. elegans*, which both lack the central pair structure, provides further support for the theory that these genes are an integral part of the central pair structure itself.

We next looked to the homologs of these genes in commonly studied organisms, such as mouse and zebrafish, to attempt to discover more about their patterns of expression and function. The gene that encodes the mouse homolog of FAP161, 1700026D08Rik, has been found to be most strongly expressed in ciliated tissues, and therefore was predicted to be important to cilia (McClintock et al., 2008), in a study that identified mRNAs which were selectively abundant in highly ciliated tissues: the olfactory epithelium, testes, vomeronasal organ, trachea, and lung. We note that several of these organs have high numbers of motile cilia, which certainly exhibit central pairs. In addition, *in situ* hybridization staining for 1700026D08Rik mRNA shows strong staining in the ventricles of the mouse brain, another location in the mouse that is rich in motile cilia (Allen Mouse Brain Atlas, Lein et al., 2007). In zebrafish, *in situ* hybridization on embryos at various developmental stages has been performed in high throughput manner, revealing that the transcript for the zebrafish FAP161 homolog, LOC550471 (gene name zgc:110373) is expressed in a number of ciliated

tissues including, importantly, in the Kupffer's vesicle (Thisse and Thisse, 2004). This structure is analogous to the mouse node discussed in the Introduction, where motile cilia are essential for the creation of a fluid flow that establishes the correct orientation of the left-right axis in the embryo. Interestingly, the cilia of the Kupffer's vesicle are known to contain central pairs, while the cilia of the mouse node are not thought to.

Homologs of FAP21 have been classified as members of an EF-hand domain containing family of proteins, with FAP21 corresponding member B, specifically (EF-hand domain family, member B, or EFHB). This is an intriguing categorization, as the EF-hand domain is a helix-loop-helix structural domain known to bind calcium; this is an extremely common motif in animal cells and family members perform a range of biochemical functions correlated with the way in which they respond to calcium binding (Nelson et al., 2002). As discussed above, many molecules thought to play a role in establishing the complex 3-D waveform typical of *Chlamydomonas* flagella are calcium binding proteins, and if such an activity were confirmed for FAP21 that would suggest it could also be involved in waveform regulation and perform its function in the central pair. In mouse, EFHB has been found to be expressed in a wide variety of tissues, implying that its function may go beyond simply playing a role in motile cilia (Mouse Genome Database). However, it has been shown to be especially strongly expressed in the testes (Finger et al., 2011) and robustly stains the cells lining the ventricles in the brain (Allen Mouse Brain Atlas, Lein et al., 2007),

indicating that playing a role in motile cilia still governs EFHB gene expression and suggesting that FAP21 remains a good candidate as a central pair protein.

RNAi of FAP21 in Planaria

No phenotype has previously been described for any mutant alleles in all of the organisms in which we found homologs for FAP161 and FAP21. Given knocking down the expression of genes using RNAi is typically fairly robust and easily accomplished in *Planaria* via injection of double-stranded RNA (dsRNA), and that the exterior of these flatworms are covered in thousands of motile cilia that are easily imaged (Rompolas et al., 2010), we opted to use the model organism *Schmidtea mediterranea* to identify any ciliary phenotype caused by the down-regulation of FAP161 and FAP21 homologs. In searching the genomic sequence of this Planarian, we found three homologs of FAP161 (encoded by genes mk4.000071.03.01/ mk4.000071.05.01 - two predicted portions of what we believe are the same gene; mk4.002433.01.01; and mk4.003299.00.01) and one of FAP21 (gene mk4.003874.01.01). Using two opposed PCR primers on mk4.000071.03.01/ mk4.000071.05.01, we were able to clone a large band that unifies both these sequences, indicating that they do in fact both form a single coding region. In addition, we were able to clone a significant portion of the FAP161 homolog mk4.002433.01.01, while unfortunately failing to amplify any of the third homolog. Because of the lack of the third FAP161 homolog and the potentially redundant nature of the three FAP161 genes, we have so far been unable to sufficiently knock-down expression of any of these proteins to elicit a

phenotype. We were able to clone only a fairly small region of the FAP21 homolog, mk4.003874.01.01, causing the RNAi affect to be less stable than is typical in Planaria, however, we had much better luck working with this single gene.

In Planaria injected with dsRNA corresponding to the homolog of FAP21, we were able to observe a significant motility defect (Figure 5). These worms had significantly reduced speed with respect to wild-type animals, indicating that their swimming behavior was negatively impacted by loss of this protein (Supplementary Table 1). Microscopic analysis indicates that at least the majority of the cilia on the ventral surface of the worms subjected to RNAi are still motile, and are not paralyzed (personal observation). This was expected due to the phenotype we saw - complete paralysis of the cilia would probably have resulted in an inching-worming behavior commonly seen in animals entirely lacking in cilia. However, the swimming behavior of Planaria requires the proper coordination of their thousands of cilia, along with the correct waveform executed by all of those cilia. It is entirely possible that removing FAP21 from the central pair in these cilia modifies, rather than prevents, ciliary beating or coordination, and therefore an altered waveform might result, causing the defect in swimming exhibited by the RNAi line. However, it is clear that the reduction of FAP21 homolog protein levels by RNAi results in a motility defect in Planaria.

Attempt to localize FAP161 and FAP21 in Chlamydomonas

To confirm the localization of FAP161 and FAP21 to the central pair structure, we cloned the cDNA from *Chlamydomonas* using the coding region predicted by the *Chlamydomonas* genome project of the Joint Genome Institute, JGI (Merchant et al., 2007) and added to these sequences both GFP and HA tags (Figure 6). We found no errors in our cloned sequences and confirmed that the splice sites predicted by JGI were correct, as the mRNA they predicted corresponded to the sequence we found (data not shown). The cloned genes were inserted upstream of the tag into two plasmids which contained the two different markers, pKL3-HA+hyg and pKL3-GFP+hyg.

All four constructs (FAP161-HA, FAP161-GFP, FAP21-HA, and FAP21-GFP) were transformed into *Chlamydomonas*, which randomly incorporates exogenous DNA into its genome, and colonies resistant to hygromycin were isolated from each transformation. As the resistance marker was located very close to the 5' end of the expression cassette, we needed to check for only the 3' end of the construct to confirm that the entire cloned gene was incorporated, and that no part was truncated. Hygromycin resistant strains carrying the entire cloned gene with its tag and regulatory regions were found for FAP161-HA, FAP21-HA, and FAP21-GFP. Unfortunately, we have yet to isolate a strain which expresses any of these constructs at high enough levels to detect the tag, a problem common in *Chlamydomonas* due to high levels of silencing of exogenous transgenes (Wu-Scharf et al., 2000). Perhaps in the future new strains which allow for consistently robust and stable expression (Neupert et al., 2009) could allow us to examine the sub-cellular location of these proteins, but

as of yet these strains are aflagellate, making examination of protein localization to the flagella impossible.

Conclusions

In this work we have presented a novel strategy for identifying proteins as components of the central pair of flagella. We compared the flagellar content of two mutants in *Chlamydomonas*, *pf15* and *pf18*, both strains that lack their central pairs, to the content of wild type flagella using 2-D DIGE. This generated a list of candidate proteins that may be integral components of the central pair apparatus. We chose to focus further on two members of this candidate list, FAP161 and FAP21, which were conserved exclusively in organisms that have motile cilia and lost from organisms that lack central pairs within their cilia. The patterns of expression of homologs to FAP161 and FAP21 in several well studied organisms reinforces that these two proteins are important in motile cilia. RNAi of the FAP21 homolog in *Planaria* confirms that this protein does in fact play a role in establishing effective ciliary beating. Together, this information leads us to conclude that we have established FAP161 and FAP21 as excellent candidates for central pair components, a designation to be confirmed by localization of the protein within the central pair structure.

It is worth noting that these studies were begun with the comparison of whole isolated flagella, and not isolated axonemes, which can be derived from detergent treating whole flagella. Previous studies have demonstrated that the flagella of *pf18* cells retain a large amount of electron dense material within their

center, where the central pair structure would typically be located (Adams et al., 1981). Additionally, they show that flagella which have been severed from the cell, by pH shock or other means, remain within their membrane and retain this material after they have been purified away from the cell body. It is possible that this material is composed of central pair proteins that have been transported to the correct sub-cellular location, however no longer have a structure on which to bind and anchor, and therefore remain in an unorganized state. The presence of this material in the isolated flagella, regardless of its organization, would result in little alteration in their levels when compared to wild type, and thus eliminate them from our study. It is therefore possible that the dearth of known central pair components on our candidate list is caused by the presence of the electron dense material in our samples. It would be interesting to compare the results of our list with that of a similar list generated from isolated axonemes, which would be free from this limitation.

Given the long history of *Chlamydomonas* genetics and the extensive study of their flagella, it is entirely possible that all the mutations that will completely destroy or freeze the ciliary waveform have been discovered, leaving only mutants with more subtle phenotypes to be described. The study of proteins that have mutations that alter, rather than completely terminate, ciliary beating are likely to be of interest in the future, given their potential importance to human health and disease. These mutations are likely to result in subtle pathologies that are as yet unexplained by medicine, and result in heritable syndromes that are passed down through generations. Because they would have graded effects

on the overall fitness of the parents, they are more likely to be maintained within the population, and therefore further research in this area may be of great practical use.

Figure 1

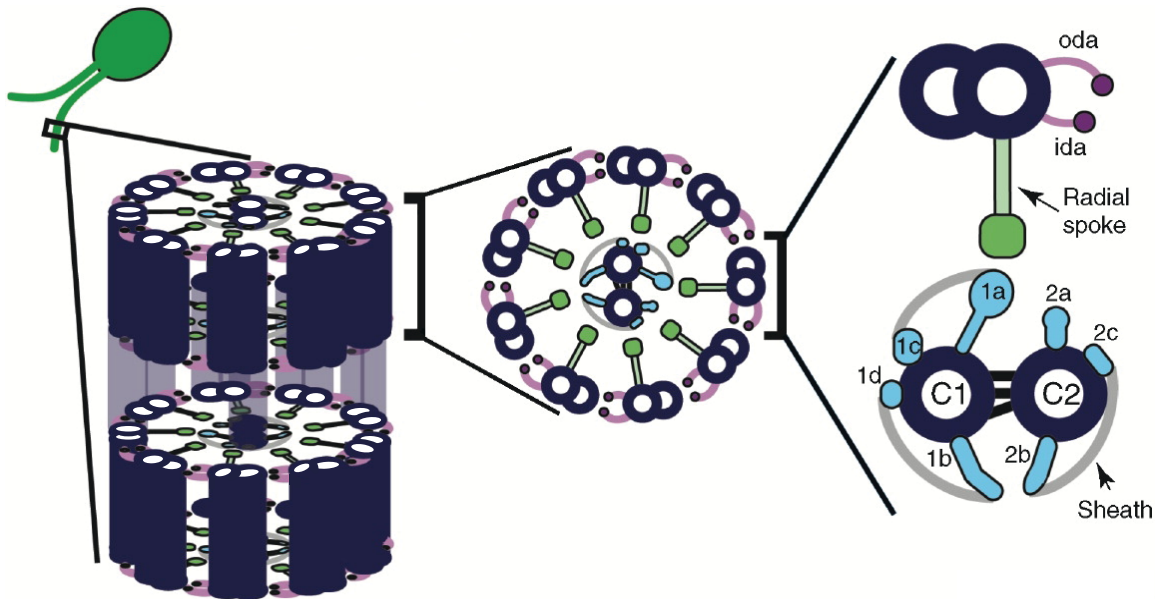


Figure 1. The structure of a flagellum.

This drawing depicts the structures within a flagellum. Microtubules (dark blue circles) make up the backbone of the structure. Middle: Cross section of a flagellum. Far right: the largest magnification, showing the central pair, consisting of the C1 and C2 tubules with their associated projections (1a-2c, light blue) and sheath (gray curves); and a single outer doublet with its radial spoke (green) and inner (ida) and outer (oda) dynein arms (pink).

Figure 2

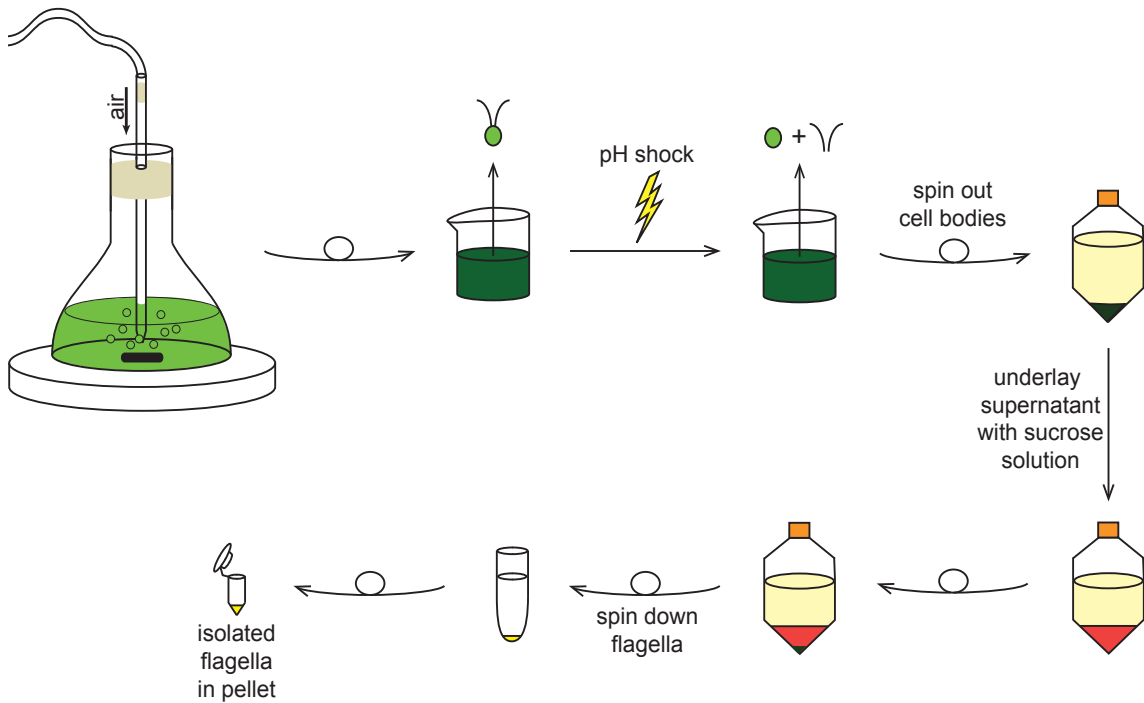
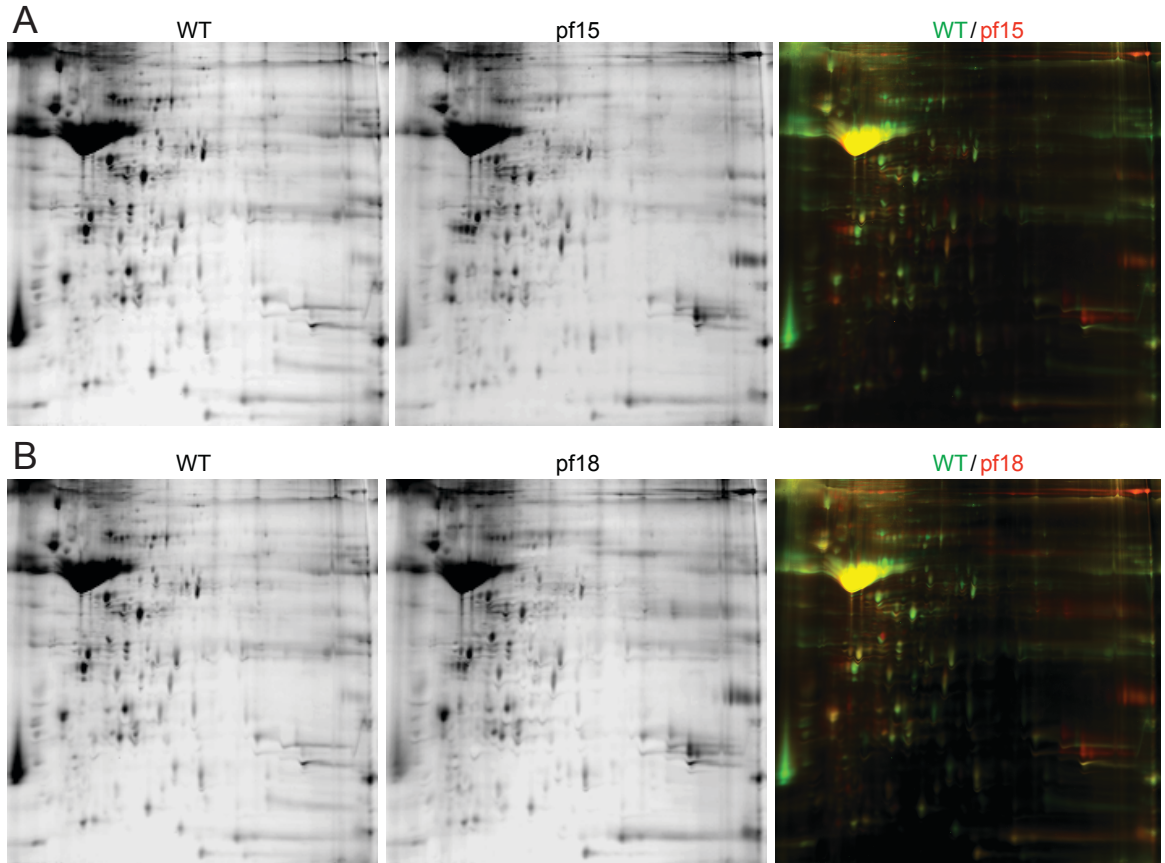


Figure 2. Overview of mid-scale flagellar preparation.

1L of culture is grown with gentle stirring and bubbling with house air in a 2L flask. The cells are spun down twice to remove debris, then are allowed to recover for 2 hours in fresh media. The cells are pH shocked to remove the flagella from the cell body. A slow spin removes the cells bodies, and a solution of 25% sucrose in media with food coloring is used to create an underlay to separate any remaining cell bodies from the flagella. The flagella, found in the upper layer and at the interface between the two layers, are collected by spinning at high speed. The flagella are re-suspended and washed, pelleted again, and finally stored as a pellet at -80C.

Figure 3



● enriched in WT ● depleted in WT ● at similar levels

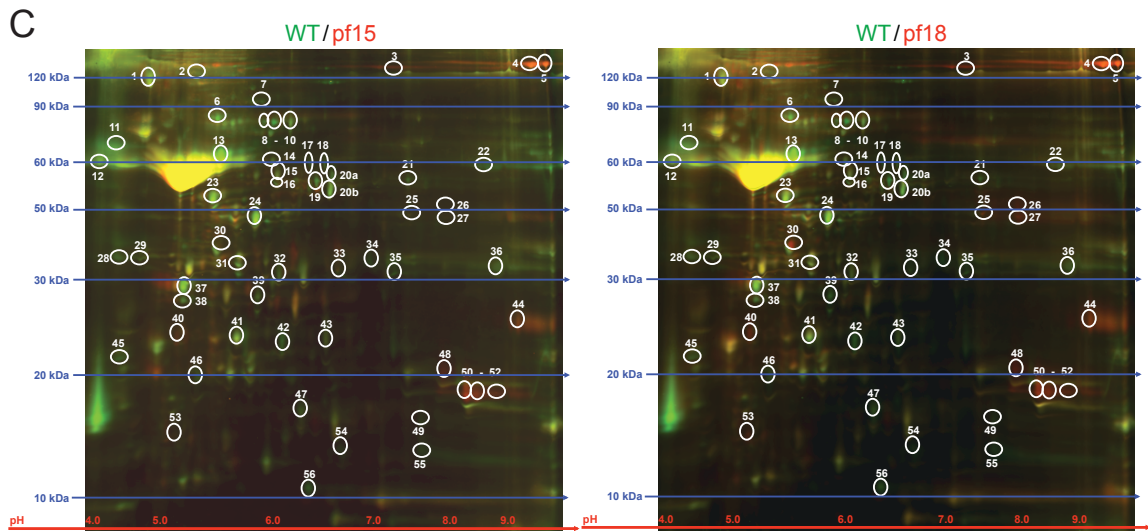


Figure 3. Gel images from 2D-DIGE experiment.

(A) Images of the individual channels of WT and *pf15*, as well as an image of the overlay of the two channels together. (B) Equivalent images to (A), but for WT and *pf18*. (C) Images showing the comparisons for WT:*pf15* and WT:*pf18*, with circles indicating the spots picked for analysis. Estimated molecular weights (kDa) are indicated by the blue lines on the gel, and the pH range for isoelectric focusing (pH) by a red line at the bottom of the gel.

Table 1 List of central pair candidates.

<i>pf15</i> / WT enrichment	<i>pf18</i> / WT enrichment	gene ID number (JGI version 2)	protein name
-5.77	-9.67	C_1100004	unknown
-13.19	-9.50	C_320189	DIP13
-7.31	-8.69	C_220018	Thioredoxin h1
-3.91	-7.35	fgenesh2_kg.C_scaffold_3000023	phosphoglyceromutase
-3.44	-5.93	C_90096	RIB43a
-2.00	-5.70	C_50316	superoxide dismutase
-2.11	-5.41	C_90096	RIB43a
-2.97	-5.26	C_200113	unknown
-2.44	-5.13	C_70115	unknown
-3.48	-5.05	C_260094	isocitrate lyase
-6.71	-4.69	Chlre2_kg.scaffold_24000235	RABB1
-2.79	-4.69	C_80235	BUG13
1.21	-4.54	C_140049	RAN1
-2.05	-4.40	C_860004	TUA2
-2.00	-4.37	C_390052	FAP103
-4.32	-4.11	C_640006	HSP70A
-4.18	-3.97	fgenesh2_kg.C_scaffold_3000023	phosphoglyceromutase
-2.66	-3.89	C_730010	FAP144
-4.00	-3.88	C_560011	IDA4
-2.74	-3.83	C_240190	Rab GDP dissociation inhibitor
-2.73	-3.57	C_820053	SIN3 component
-2.28	-3.49	C_720008	RSP10
-4.32	-3.17	C_740028	FAP162
-2.18	-3.13	C_230131	FAP106
-2.70	-3.03	C_230131	FAP106
-2.35	-2.97	C_40381	FAP252
-1.50	-2.92	C_260105	FAP85
-2.44	-2.90	C_440001	IDA5
-2.72	-2.88	C_240073	FAP12
-2.52	-2.81	C_140050	TUA1
-1.55	-2.78	C_250170	BUG15
-1.92	-2.70	C_200099	TUB1
-1.71	-2.63	C_90096	RIB43a
-2.19	-2.59	C_880042	FAP182
-1.33	-2.52	C_260094	isocitrate lyase
-2.31	-2.49	C_140050	TUA1
-1.92	-2.39	PYA_e_gwH.19.179.1	RSP1
-1.82	-2.25	C_550027	FAP115
-1.53	-2.09	C_70399	DLC1
-5.80	-2.08	C_30492	translation elongation factor
-1.75	-1.85	C_100107	RSP9
-1.50	-1.78	C_110201	FAP52
-1.27	-1.72	C_20049	FAP161

Figure 4

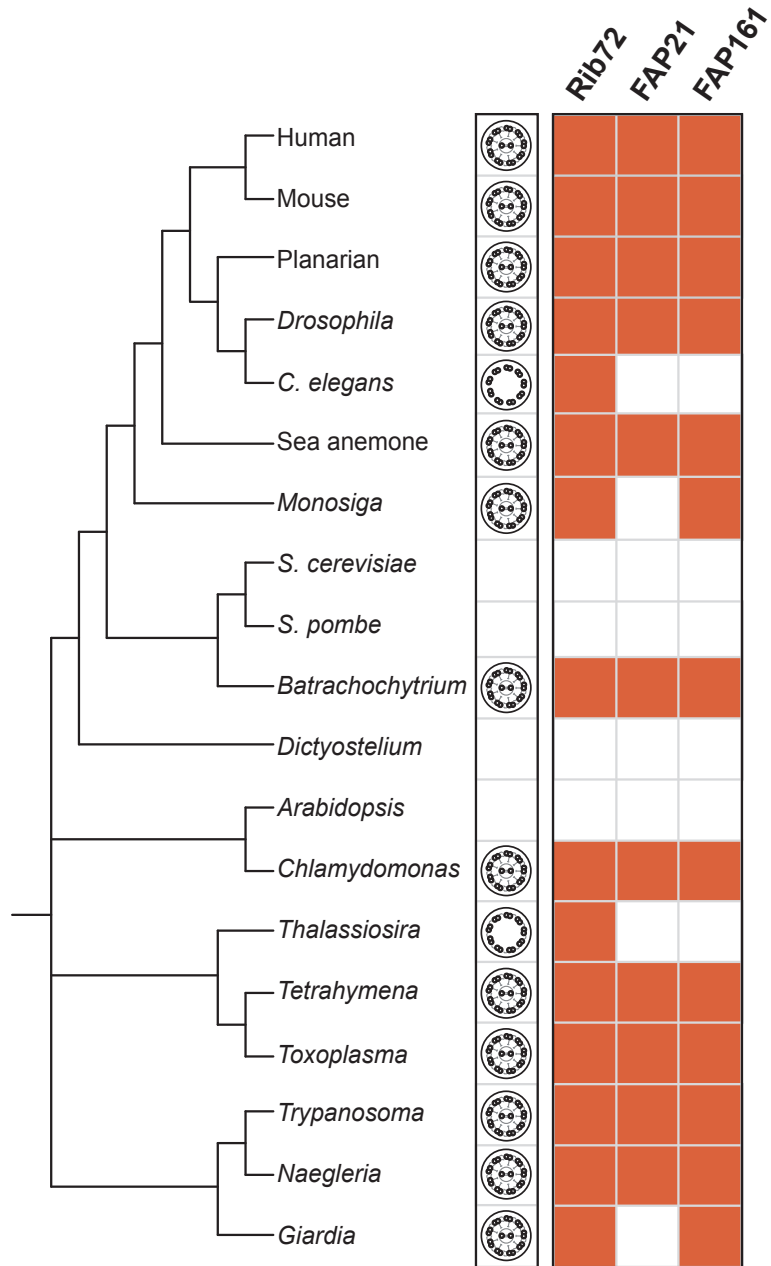


Figure 4. FAP 21 and FAP161 are present only in organisms which have motile cilia with central pairs.

This figure is adapted from the Tree of Life project, and is based on the relationships between the different species, not the FAP sequences. The presence or absence of the FAP homologs in each species is indicated with the presence or absence of an orange box. FAP161 and FAP21 appear only in organisms with motile cilia containing central pairs, and are absent in organisms lacking this structure. The absence of FAP21 in *Monosiga* and *Giardia* may be due to gaps in the genomes of those organisms. Rib72 is included as a control; it is a structural component of the A-tubule of the outer doublets. It therefore can be found in all organisms with cilia, but is absent from organisms that do not have cilia or flagella.

Figure 5

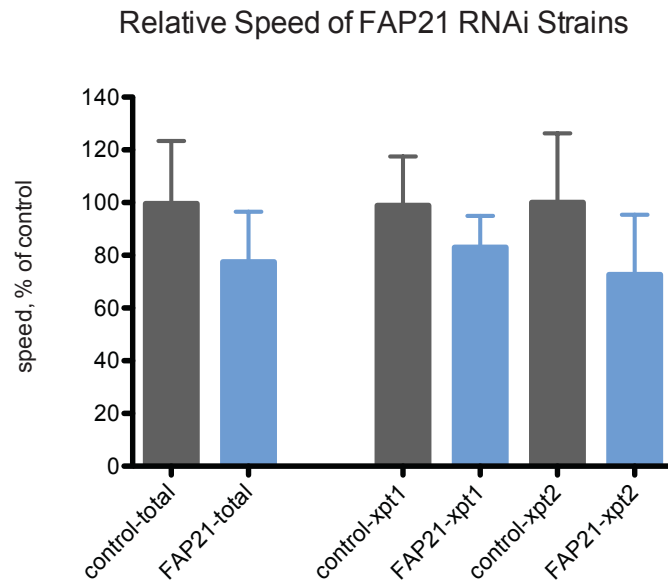


Figure 5. Knock-down of FAP21 with RNAi impairs swimming of Planaria.

RNAi knock-down of FAP21 in *S. mediterranea* results in impaired movement of the flatworm. Their motility is reduced by 20% when compared to control worms. This data represents the quantification of two separate experiments, xpt1 and xpt2, with the analysis of all collected data represented in the 'total' columns.

Figure 6

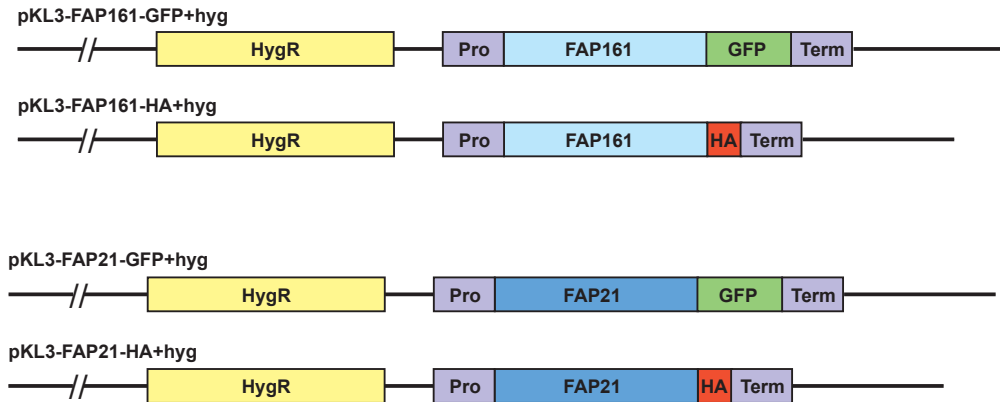


Figure 6. Constructs created to express FAP161 and FAP21 in *Chlamydomonas*.

Representations of constructs based on the pKL3 vectors created to express tagged versions of FAP161 and FAP21 in green algae. The HygR box represents the hygromycin resistance marker, which is actually constructed of: the $\beta 2$ -*Tubulin* promoter, the *aph7*⁺ hygromycin resistance gene from *S. hygroscopicus*, intron1 from *RbcS2* (Rubisco), and the 3' UTR of *RbcS2*. The regions labelled 'Pro' and 'Term' represent the promoter and terminator regions of the *LC8* gene. GFP and HA show the 3' location of the two tags.

Supplementary Table 1. Complete list of proteins identified by 2D-DIGE

Spot number	pf15/WT	pf18/WT	Top Ranked Protein Name
1	-1.92	-2.39	PYA_e_gwH.19.179.1 {RSP1} Radial spoke protein 1
2	-2.05	-4.40	estExt_fgensch2_kg.C_860004 {TUA2} alpha tubulin 2
3	9.24	12.08	estExt_fgensch2_pg.C_10745
4	7.13	7.26	estExt_fgensch2_pg.C_220120 {FAP233} Flagellar Associated Protein
5	6.71	6.52	estExt_fgensch2_pg.C_220120 {FAP233} Flagellar Associated Protein
6	-4.32	-4.11	estExt_fgensch2_kg.C_640006 {HSP70A} Heat shock protein 70A
7	-2.73	-3.57	estExt_gwp_1W.C_820053 {SNT3401} SIN3 component
8	-4.18	-3.97	MHS_fgensch2_kg.C_scaffold_3000023 {PGM1a} Phosphoglyceromutase
9	-3.91	-7.35	fgensch2_kg.C_scaffold_3000023 {PGM1b} Phosphoglycerate mutase, possible cytosolic form
10	-1.50	-1.78	estExt_gwp_1H.C_110201 {FAP52} Conserved Uncharacterized Flagellar Associated Protein
11	-2.72	-2.88	estExt_fgensch2_kg.C_240073 {FAP12} Flagellar Associated Protein
12	-1.92	-2.70	estExt_gwp_1H.C_200099 {TUB1}
13	-3.48	-5.05	estExt_fgensch2_pg.C_260094 {ICL1} isocitrate lyase
14	-1.55	-2.78	estExt_fgensch1_pg.C_250170 {BUG15} basal body protein of unknown function
15	-1.27	-1.72	estExt_fgensch2_pg.C_20049 {FAP161} Flagellar Associated Protein
16	-1.33	-2.52	estExt_fgensch2_pg.C_260094 {ICL1} isocitrate lyase
17	-2.74	-3.83	estExt_fgensch2_pg.C_240190 {GDIC1} Rab GDP dissociation inhibitor protein
18	-2.19	-2.59	estExt_fgensch2_pg.C_880042 {FAP182} Flagellar Associated Protein
19	-2.11	-5.41	estExt_GenewiseW_1.C_90096 {RIB43a} Coiled-coil
20a	-2.97	-5.26	estExt_fgensch2_pg.C_200113
20b	-1.71	-2.63	estExt_GenewiseW_1.C_90096 {RIB43a} Coiled-coil protein associated with protofilament ribbons
21	-3.44	-5.93	estExt_GenewiseW_1.C_90096 {RIB43a} Coiled-coil protein associated with protofilament ribbons
22	-5.80	-2.08	estExt_gwp_1W.C_30492 {EF1A1} eukaryotic translation elongation factor 1 alpha 1
23	-2.44	-2.90	estExt_fgensch1_pm.C_440001 {IDA5} Actin
24	-2.35	-2.97	estExt_fgensch2_pg.C_40381 {FAP252} Flagellar Associated Protein
25	1.06	3.73	estExt_fgensch2_pg.C_10669 {FAP155} Flagellar Associated Protein
26	1.39	9.34	estExt_gwp_1W.C_100141 {CSP41b} chloroplast stem-loop-binding protein
27	1.57	6.56	estExt_fgensch2_kg.C_240073 {FAP12} Flagellar Associated Protein
28	-2.70	-3.03	estExt_gwp_1W.C_230131 {FAP106} Conserved Uncharacterized Flagellar Associated Protein

Spot number	pf15/WT	pf18/WT	Top Ranked Protein Name
29	-2.18	-3.13	estExt_gwp_1W.C_230131 {FAP106} Conserved Uncharacterized Flagellar Associated Protein
30	1.26	5.04	estExt_fgenes2_pg.C_10438
31	-1.75	-1.85	estExt_fgenes2_kg.C_100107 {PF17} Radial spoke protein 9
32	-1.82	-2.25	estExt_fgenes2_pg.C_550027 {FAP115} Flagellar Associated Protein
33	1.21	-4.54	estExt_gwp_1H.C_140049 {RAN1} RAN1, Ran-like small GTPase
34	-2.44	-5.13	estExt_fgenes2_kg.C_70115
35	-4.00	-3.88	estExt_gwp_1H.C_560011 {IDA4} Flagellar inner arm dynein light chain p28
36	-2.79	-4.69	estExt_fgenes1_pg.C_80235 {BUG13} basal body protein of unknown function
37	-2.28	-3.49	estExt_fgenes2_kg.C_720008 {RSP10} Radial spoke protein 10
38	-2.31	-2.49	estExt_gwp_1H.C_140050 {TUA1}
39	-2.00	-5.70	estExt_GenewiseH_1.C_50316 {MSD1} superoxide dismutase [Mn], mitochondrial precursor
40	5.63	7.07	fgenes2_kg.C_scaffold_36000012 {PHC17} cell wall protein pferophorin-C17
41	-1.53	-2.09	estExt_fgenes2_pg.C_70399 {DLC1} Flagellar outer dynein arm light chain 1
42	-5.77	-9.67	estExt_fgenes2_pg.C_1100004
43	-1.50	-2.92	estExt_fgenes2_pg.C_260105 {FAP85} Flagellar Associated Protein
44	7.25	6.20	Chire2_kg.scaffold_22000171 {PHC15} cell wall protein pferophorin-C15
45	-4.32	-3.17	estExt_fgenes2_pg.C_740028 {FAP162} Flagellar
46	-2.52	-2.81	estExt_gwp_1H.C_140050 {TUA1}
47	-2.00	-4.37	estExt_GenewiseH_1.C_390052 {FAP103} Flagellar Associated Protein Similar to Nucleoside Diphosphate
48	19.97	13.54	HAL_fgenes2_pg.C_scaffold_97000001 {PHC7} cell wall protein pferophorin-C7
49	-2.66	-3.89	estExt_fgenes2_kg.C_730010 {FAP144} Flagellar Associated Protein
50	12.11	7.23	HAL_fgenes2_pg.C_scaffold_97000001 {PHC7} cell wall protein pferophorin-C7
51	16.42	14.89	HAL_fgenes2_pg.C_scaffold_97000001 {PHC7} cell wall protein pferophorin-C7
52	23.03	17.35	HAL_HAL_Chire2_kg.scaffold_1000873 {PHC2} cell wall protein pferophorin-C2
53	2.25	4.90	e_gwH.2.436.1 {PRPL7/L12} Plastid ribosomal protein L 12, imported to chloroplast, large ribosomal subunit
54	-6.71	-4.69	Chire2_kg.scaffold_24000235 {RABB1} RABB1, small Rab-related GTPase
55	-13.19	-9.50	estExt_gwp_1H.C_320189 {DIP13} Deflagellation inducible protein, 13 kD.
56	-7.31	-8.69	STE_estExt_gwp_1H.C_220018 {TRXh1} Thioredoxin h1, cytosolic

Supplementary Table 2. Data for FAP21 RNAi in Planaria

Worm	SPEED VALUES		AVERAGE SPEED		AVERAGE SPEED (%)	
	Control	<i>fap21(RNAi)</i>	Control	<i>fap21(RNAi)</i>	Control	<i>fap21(RNAi)</i>
1	0.259	0.304				
	0.269	0.287				
	0.270	0.275	0.266	0.289	102	111
2	0.335	0.224				
	0.334	0.215				
	0.337	0.204	0.335	0.214	129	83
3	0.184	0.183				
	0.177	0.169				
	0.187	0.183	0.183	0.178	70	69
4	0.213	0.211				
	0.195	0.216				
	0.200	0.200	0.203	0.209	78	81
5	0.262	0.265				
	0.253	0.251				
	0.237	0.276	0.251	0.264	97	102
6	0.274	0.158				
	0.288	0.170				
	0.270	0.161	0.277	0.163	107	63
7	0.154	0.187				
	0.146	0.205				
	0.153	0.226	0.151	0.206	58	79
8	0.228	0.198				
	0.215	0.217				
	0.219	0.184	0.221	0.200	85	77
9	0.300	0.213				
	0.300	0.219				
	0.310	0.213	0.303	0.215	117	83
10	0.282	0.242				
	0.274	0.228				
	0.277	0.256	0.278	0.242	107	93
11	0.274	0.175				
	0.275	0.210				
	0.286	0.197	0.278	0.194	107	75
12	0.270	0.158				
	0.267	0.201				
	0.261	0.187	0.266	0.182	102	70
13	0.276	0.241				
	0.258	0.227				
	0.265	0.253	0.266	0.240	103	93
14	0.321	0.212				
	0.307	0.212				
	0.320	0.222	0.316	0.215	122	83
15	0.278	0.289				
	0.261	0.262				

	SPEED VALUES		AVERAGE SPEED		AVERAGE SPEED (%)	
<i>Worm</i>	Control	<i>fap21(RNAi)</i>	Control	<i>fap21(RNAi)</i>	Control	<i>fap21(RNAi)</i>
	0.246	0.251	0.262	0.267	101	103
16	0.249	0.216				
	0.247	0.196				
	0.268	0.188	0.255	0.200	98	77
17	0.284	0.211				
	0.303	0.223				
	0.290	0.183		0.206		79
18	0.260	0.220				
	0.274	0.207				
	0.272	0.179		0.202		78
19		0.187				
		0.202				
		0.191		0.200		77
20		0.206				
		0.224				
		0.195		0.201		78
21		0.291				
		0.303				
		0.302		0.233		90
1	0.516	0.467				
	0.513	0.461				
	0.482	0.375	0.504	0.434	86	74
2	0.541	0.413				
	0.508	0.404				
	0.413	0.441	0.487	0.419	83	71
3	0.566	0.569				
	0.687	0.716				
	0.593	0.683	0.615	0.656	105	112
4	0.573	0.577				
	0.532	0.593				
	0.516	0.614	0.540	0.595	92	101
5	0.709	0.449				
	0.716	0.462				
	0.681	0.434	0.702	0.448	119	76
6	0.658	0.432				
	0.632	0.384				
	0.646	0.403	0.645	0.406	110	69
7	0.530	0.385				
	0.454	0.414				
	0.514	0.446	0.499	0.415	85	71
8	0.549	0.445				
	0.454	0.392				
	0.508	0.441	0.504	0.426	86	72
9	0.485	0.367				
	0.535	0.307				

Worm	SPEED VALUES		AVERAGE SPEED		AVERAGE SPEED (%)	
	Control	<i>fap21(RNAi)</i>	Control	<i>fap21(RNAi)</i>	Control	<i>fap21(RNAi)</i>
	0.503	0.312	0.508	0.329	86	56
10	0.568	0.245				
	0.614	0.287				
	0.578	0.276	0.587	0.269	100	46
11	0.754	0.364				
	0.796	0.384				
	0.756	0.385	0.769	0.378	131	64
12	0.703	0.325				
	0.716	0.287				
	0.694	0.337	0.704	0.316	120	54
13	0.548	0.613				
	0.636	0.586				
	0.547	0.583	0.577	0.594	98	101
14	0.782	0.213				
	0.774	0.239				
	0.752	0.215	0.769	0.222	131	38
15	0.489	0.611				
	0.471	0.600				
	0.523	0.651	0.494	0.621	84	106
16	0.446	0.320				
	0.391	0.362				
	0.439	0.367	0.425	0.350	72	59
17	0.426	0.486				
	0.344	0.507				
	0.358	0.529	0.376	0.507	64	86
18	0.640	0.705				
	0.684	0.723				
	0.658	0.756	0.661	0.728	112	124
19	0.795	0.487				
	0.781	0.473				
	0.749	0.410	0.775	0.457	132	78
20	0.760	0.340				
	0.822	0.337				
	0.800	0.347	0.794	0.341	135	58
21	0.862	0.441				
	0.812	0.456				
	0.855	0.415	0.843	0.437	143	74
22	0.619	0.398				
	0.633	0.342				
	0.598	0.356	0.617	0.365	105	62
23	0.600	0.381				
	0.631	0.348				
	0.572	0.273	0.601	0.334	102	57
24	0.601	0.240				
	0.634	0.214				

	SPEED VALUES		AVERAGE SPEED		AVERAGE SPEED (%)	
<i>Worm</i>	Control	<i>fap21(RNAi)</i>	Control	<i>fap21(RNAi)</i>	Control	<i>fap21(RNAi)</i>
	0.561	0.177	0.599	0.210	102	36
25	0.814					
	0.757					
	0.756		0.776		132	
26	0.404					
	0.277					
	0.278		0.320		54	
27	0.249					
	0.276					
	0.228		0.251		43	
28	0.754					
	0.728					
	0.608		0.697		118	
29	0.573					
	0.569					
	0.542		0.561		95	
30	0.754					
	0.768					
	0.720		0.747		127	
31	0.247					
	0.275					
	0.316		0.279		48	
			Total Avg (% Control)		100	77
			Total SD (% Control)		24	19
			P (Two-tailed) Mann-Whitney			0.000384

References

- Adams, G.M., B. Huang, G. Piperno, and D.J. Luck. 1981. Central-pair microtubular complex of *Chlamydomonas flagella*: polypeptide composition as revealed by analysis of mutants. *J Cell Biol.* **91**:69-76.
- Allen Brain Atlas Resources [Internet]. Seattle (WA): Allen Institute for Brain Science. ©2009. Available from: <http://www.brain-map.org>.
- Branche, C., L. Kohl, G. Toutirais, J. Buisson, J. Cosson, and P. Bastin. 2006. Conserved and specific functions of axoneme components in trypanosome motility. *J Cell Sci.* **119**:3443-3455.
- Dymek, E.E., P.A. Lefebvre, and E.F. Smith. 2004. PF15p is the *Chlamydomonas* homologue of the Katanin p80 subunit and is required for assembly of flagellar central microtubules. *Eukaryotic Cell.* **3**:870-879.
- Finger, J.H., C.M. Smith, T.F. Hayamizu, I.J. McCright, J.T. Eppig, J.A. Kadin, J.E. Richardson, and M. Ringwald. 2011. The Mouse Gene Expression Database (GXD): 2011 update. *Nucleic acids research.* **39**:D835-841.
- Fowkes, M.E., and D.R. Mitchell. 1998. The role of preassembled cytoplasmic complexes in assembly of flagellar dynein subunits. *Molecular biology of the cell.* **9**:2337-2347.
- Gene Expression Database (GXD), Mouse Genome Informatics website, The Jackson Laboratory, Bar Harbor, ME. <http://www.informatics.jax.org>. [August, 2011].
- Heath, I.B., and W.M. Darley. 1972. OBSERVATIONS ON THE ULTRASTRUCTURE OF THE MALE GAMETES OF *BIDDULPHIA LEVIS* EHR. *J. Phycol.* **8**:51-59.
- Heuser, T., M. Raytchev, J. Krell, M.E. Porter, and D. Nicastro. 2009. The dynein regulatory complex is the nexin link and a major regulatory node in cilia and flagella. *J Cell Biol.* **187**:921-933.
- Kawai, T., H. Abe, K. Wakabayashi, and Y. Oka. 2009. Calcium oscillations in the olfactory nonsensory cells of the goldfish, *Carassius auratus*. *Biochimica et biophysica acta.* **1790**:1681-1688.
- Kindle, K.L. 1990. High-frequency nuclear transformation of *Chlamydomonas reinhardtii*. *Proc Natl Acad Sci U S A.* **87**:1228-1232.
- Kohno, T., K. Wakabayashi, D.R. Diener, J.L. Rosenbaum, and R. Kamiya. 2011. Subunit interactions within the *Chlamydomonas* flagellar spokehead. *Cytoskeleton.* **68**:237-246.

Lehtreck, K.F., and G.B. Witman. 2007. *Chlamydomonas reinhardtii* hydin is a central pair protein required for flagellar motility. *J Cell Biol.* **176**:473-482.

Lee, L. 2011. Mechanisms of mammalian ciliary motility: Insights from primary ciliary dyskinesia genetics. *Gene.* **473**:57-66.

Lein, E.S., M.J. Hawrylycz, N. Ao, M. Ayres, A. Bensinger, A. Bernard, A.F. Boe, M.S. Boguski, K.S. Brockway, E.J. Byrnes, L. Chen, T.M. Chen, M.C. Chin, J. Chong, B.E. Crook, A. Czaplinska, C.N. Dang, S. Datta, N.R. Dee, A.L. Desaki, T. Desta, E. Diep, T.A. Dolbeare, M.J. Donelan, H.W. Dong, J.G. Dougherty, B.J. Duncan, A.J. Ebbert, G. Eichele, L.K. Estin, C. Faber, B.A. Facer, R. Fields, S.R. Fischer, T.P. Fliss, C. Frensley, S.N. Gates, K.J. Glattfelder, K.R. Halverson, M.R. Hart, J.G. Hohmann, M.P. Howell, D.P. Jeung, R.A. Johnson, P.T. Karr, R. Kawal, J.M. Kidney, R.H. Knapik, C.L. Kuan, J.H. Lake, A.R. Laramee, K.D. Larsen, C. Lau, T.A. Lemon, A.J. Liang, Y. Liu, L.T. Luong, J. Michaels, J.J. Morgan, R.J. Morgan, M.T. Mortrud, N.F. Mosqueda, L.L. Ng, R. Ng, G.J. Orta, C.C. Overly, T.H. Pak, S.E. Parry, S.D. Pathak, O.C. Pearson, R.B. Puchalski, Z.L. Riley, H.R. Rockett, S.A. Rowland, J.J. Royall, M.J. Ruiz, N.R. Sarno, K. Schaffnit, N.V. Shapovalova, T. Sivisay, C.R. Slaughterbeck, S.C. Smith, K.A. Smith, B.I. Smith, A.J. Sodt, N.N. Stewart, K.R. Stumpf, S.M. Sunkin, M. Sutram, A. Tam, C.D. Teemer, C. Thaller, C.L. Thompson, L.R. Varnam, A. Visel, R.M. Whitlock, P.E. Wohnoutka, C.K. Wolkey, V.Y. Wong, M. Wood, et al. 2007. Genome-wide atlas of gene expression in the adult mouse brain. *Nature.* **445**:168-176.

Maddison, D.R., and K.-S. Schulz. (eds.) 2007. The Tree of Life Web Project. <http://tolweb.org>.

Manton, I., K. Kowallik, and H.A. von Stosch. 1970. Observations on the fine structure and development of the spindle at mitosis and meiosis in a marine centric diatom (*Lithodesmium undulatum*). 3. The later stages of meiosis I in male gametogenesis. *J Cell Sci.* **6**:131-157.

Mastronarde, D.N., E.T. O'Toole, K.L. McDonald, J.R. McIntosh, and M.E. Porter. 1992. Arrangement of inner dynein arms in wild-type and mutant flagella of *Chlamydomonas*. *The Journal of cell biology.* **118**:1145-1162.

McClintock, T.S., C.E. Glasser, S.C. Bose, and D.A. Bergman. 2008. Tissue expression patterns identify mouse cilia genes. *Physiol Genomics.* **32**:198-206.

Merchant, S.S., S.E. Prochnik, O. Vallon, E.H. Harris, S.J. Karpowicz, G.B. Witman, A. Terry, A. Salamov, L.K. Fritz-Laylin, L. Maréchal-Drouard, W.F. Marshall, L.H. Qu, D.R. Nelson, A.A. Sanderfoot, M.H. Spalding, V.V. Kapitonov, Q. Ren, P. Ferris, E. Lindquist, H. Shapiro, S.M. Lucas, J. Grimwood, J. Schmutz, P. Cardol, H. Cerutti, G. Chanfreau, C.L. Chen, V. Cognat, M.T. Croft, R. Dent, S. Dutcher, E. Fernández, H. Fukuzawa, D. González-Ballester, D. González-Halphen, A. Hallmann, M. Hanikenne, M. Hippler, W. Inwood, K.

- Jabbari, M. Kalanon, R. Kuras, P.A. Lefebvre, S.D. Lemaire, A.V. Lobanov, M. Lohr, A. Manuell, I. Meier, L. Mets, M. Mittag, T. Mittelmeier, J.V. Moroney, J. Moseley, C. Napoli, A.M. Nedelcu, K. Niyogi, S.V. Novoselov, I.T. Paulsen, G. Pazour, S. Purton, J.P. Ral, D.M. Riaño-Pachón, W. Riekhof, L. Rymarquis, M. Schroda, D. Stern, J. Umen, R. Willows, N. Wilson, S.L. Zimmer, J. Allmer, J. Balk, K. Bisova, C.J. Chen, M. Elias, K. Gendler, C. Hauser, M.R. Lamb, H. Ledford, J.C. Long, J. Minagawa, M.D. Page, J. Pan, W. Pootakham, S. Roje, A. Rose, E. Stahlberg, A.M. Terauchi, P. Yang, S. Ball, C. Bowler, C.L. Dieckmann, V.N. Gladyshev, P. Green, R. Jorgensen, S. Mayfield, B. Mueller-Roeber, S. Rajamani, R.T. Sayre, P. Brokstein, et al. 2007. The *Chlamydomonas* genome reveals the evolution of key animal and plant functions. *Science*. **318**:245-250.
- Mitchell, B.F., L.B. Pedersen, M. Feely, J.L. Rosenbaum, and D.R. Mitchell. 2005. ATP production in *Chlamydomonas reinhardtii* flagella by glycolytic enzymes. *Mol Biol Cell*. **16**:4509-4518.
- Mitchell, D.R., and M. Nakatsugawa. 2004. Bend propagation drives central pair rotation in *Chlamydomonas reinhardtii* flagella. *J Cell Biol*. **166**:709-715.
- Mouse Genome Database (MGD) at the Mouse Genome Informatics website. <http://www.informatics.jax.org>. [August, 2011].
- Nakano, I., T. Kobayashi, M. Yoshimura, and C. Shingyoji. 2003. Central-pair-linked regulation of microtubule sliding by calcium in flagellar axonemes. *Journal of cell science*. **116**:1627-1636.
- Nelson, M.R., E. Thulin, P.A. Fagan, S. Forsen, and W.J. Chazin. 2002. The EF-hand domain: a globally cooperative structural unit. *Protein Sci*. **11**:198-205.
- Neupert, J., D. Karcher, and R. Bock. 2009. Generation of *Chlamydomonas* strains that efficiently express nuclear transgenes. *Plant J*. **57**:1140-1150.
- Omoto, C.K., and C.J. Brokaw. 1985. Bending patterns of *Chlamydomonas* flagella: II. Calcium effects on reactivated *Chlamydomonas* flagella. *Cell Motil*. **5**:53-60.
- Omoto, C.K., I.R. Gibbons, R. Kamiya, C. Shingyoji, K. Takahashi, and G.B. Witman. 1999. Rotation of the central pair microtubules in eukaryotic flagella. *Mol Biol Cell*. **10**:1-4.
- Pazour, G.J., N. Agrin, J. Leszyk, and G.B. Witman. 2005. Proteomic analysis of a eukaryotic cilium. *J Cell Biol*. **170**:103-113.
- Porter, M.E., J. Power, and S.K. Dutcher. 1992. Extragenic suppressors of paralyzed flagellar mutations in *Chlamydomonas reinhardtii* identify loci that alter the inner dynein arms. *J Cell Biol*. **118**:1163-1176.

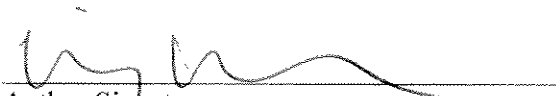
- Qin, H., D.R. Diener, S. Geimer, D.G. Cole, and J.L. Rosenbaum. 2004. Intraflagellar transport (IFT) cargo: IFT transports flagellar precursors to the tip and turnover products to the cell body. *The Journal of cell biology*. **164**:255-266.
- Rompolas, P., R.S. Patel-King, and S.M. King. 2010. An outer arm Dynein conformational switch is required for metachronal synchrony of motile cilia in planaria. *Mol Biol Cell*. **21**:3669-3679.
- Rubin, R.W., and P. Filner. 1973. Adenosine 3',5'-cyclic monophosphate in *Chlamydomonas reinhardtii*. Influence on flagellar function and regeneration. *The Journal of cell biology*. **56**:628-635.
- Smith, E.F. 2002. Regulation of flagellar dynein by calcium and a role for an axonemal calmodulin and calmodulin-dependent kinase. *Mol Biol Cell*. **13**:3303-3313.
- Stolc, V., M.P. Samanta, W. Tongprasit, and W.F. Marshall. 2005. Genome-wide transcriptional analysis of flagellar regeneration in *Chlamydomonas reinhardtii* identifies orthologs of ciliary disease genes. *Proc Natl Acad Sci USA*. **102**:3703-3707.
- Thisse, B., and C. Thisse. 2004. Fast Release Clones: A High Throughput Expression Analysis. ZFIN Direct Data Submission. <http://zfin.org>.
- Wargo, M.J., and E.F. Smith. 2003. Asymmetry of the central apparatus defines the location of active microtubule sliding in *Chlamydomonas* flagella. *Proc Natl Acad Sci USA*. **100**:137-142.
- Warr, J.R., A. McVittie, Sir J. Randall, and J.M. Hopkins. 1966. Genetic control of flagellar structure in *Chlamydomonas reinhardtii*. *Genet. Res.* **7**:335-351.
- Wilson, C.W., C.T. Nguyen, M.H. Chen, J.H. Yang, R. Gacayan, J. Huang, J.N. Chen, and P.T. Chuang. 2009. Fused has evolved divergent roles in vertebrate Hedgehog signalling and motile ciliogenesis. *Nature*. **459**:98-102.
- Wu-Scharf, D., B. Jeong, C. Zhang, and H. Cerutti. 2000. Transgene and transposon silencing in *Chlamydomonas reinhardtii* by a DEAH-box RNA helicase. *Science*. **290**:1159-1162.
- Yang, P., D.R. Diener, J.L. Rosenbaum, and W.S. Sale. 2001. Localization of calmodulin and dynein light chain LC8 in flagellar radial spokes. *J Cell Biol*. **153**:1315-1326.
- Yang, P., C. Yang, and W.S. Sale. 2004. Flagellar radial spoke protein 2 is a calmodulin binding protein required for motility in *Chlamydomonas reinhardtii*. *Eukaryotic Cell*. **3**:72-81.

Publishing Agreement

It is the policy of the University to encourage the distribution of all theses, dissertations, and manuscripts. Copies of all UCSF theses, dissertations, and manuscripts will be routed to the library via the Graduate Division. The library will make all theses, dissertations, and manuscripts accessible to the public and will preserve these to the best of their abilities, in perpetuity.

Please sign the following statement:

I hereby grant permission to the Graduate Division of the University of California, San Francisco to release copies of my thesis, dissertation, or manuscript to the Campus Library to provide access and preservation, in whole or in part, in perpetuity.



Author Signature



Date